Proceedings of the Indian Academy of Sciences
Earth and Planetary Sciences

Subscription Rates
(Effective from 1989)

All countries except India	1 year	3 years	5 years
(Price includes AIR MAIL charges)	US$75	$200	$300
India	1 year	10 years	
	Rs. 75	Rs. 400	

All correspondence regarding subscription should be addressed to **The Circulation Department** of the Academy

---

Editorial Office
Indian Academy of Sciences, C V Raman Avenue,
P.B. No. 8005, Bangalore 560080, India

Telephone: 342546
Telex: 0845-2178 ACAD IN

The "Notes on the preparation of papers" are printed in the last issue of every volume.

EDITORIAL

A perspective on seismology in India

Dr Vinod Gaur kindly asked me to be a guest editor for a special issue of the *Proceedings of the Indian Academy of Sciences* to be focussed on seismology in India. We selected a number of prospective topics and authors and I began negotiations for contributions. The result is the group of excellent papers in this volume. I made no effort toward a comprehensive coverage of seismology, but rather attempted to choose topics illustrative of a range of problems related to India. Thus many important topics (e.g. induced seismicity) are not represented. Some invited authors were unable to contribute, and probably others should have been invited to represent their topics, but the press of time and schedule, mostly on my part, made this impossible. I apologize to all those who could have made valuable contributions to this volume. The paper by Royer *et al* on the tectonic fabric of the Indian Ocean is not strictly seismological, but provides an important background for seismological interpretation, especially with regard to the structure in the Bay of Bengal. Many may feel that the authorship is too heavily weighted with scientists from outside India, and thus the overall perspective tends more to that of an outsider, and I would not disagree with this evaluation, but I am nevertheless hopeful that the volume will be stimulating to seismologists both inside and outside India. I would like to thank Dr Kailash Khattri for reviewing some of the contributions for me.

I began my career in seismology during the IGY (International Geophysical Year), an international programme which led to the installation of modern seismographs worldwide, and provided the data for my thesis. Thus I am very aware of the importance of international co-operative projects in seismology. The continuing benefit of such projects is illustrated by the strong motion data now being collected in India as a result of the Hawaii International Workshop on Strong Motion Arrays (1978), which stimulated arrays in India, Taiwan, Mexico, China, the U.S., and Turkey (see the article on strong motion seismology in this volume). The importance of such arrays is graphically emphasized by the recent damaging earthquake in the India-Nepal border region. Recognition of the importance of international co-operative projects is most recently illustrated by the plans for the International Decade of Natural Hazard Reduction, including an important meeting to be held in New Delhi in the summer of 1989. Of course national efforts in research will usually take priority over international efforts, however, most nations are realizing that international co-operative projects are crucial to their own national development.

The problems inherent in developing international co-operative projects illustrate some basic problems in research and I would like to share some of my views on these, based on my years of fruitful co-operative research in Mexico and my more recent visits to India.

As a scientific discipline seismology has developed from a young science to a mature science. The characteristics of the types of research programmes have changed, and

and purely national research. Many of us can remember when discoveries in seismology were simple and inexpensive, and contrast that situation with the current situation where much of the funding for seismology is for large multi-institutional projects.

When seismology was young, major discoveries, causing qualitatively great changes in our understanding, were made relatively simply by a few dedicated "basic" researchers and students, with minimal funding support. Research was carried out with individually constructed equipment and simple calculations using elementary first-order theory inspired by physical intuition. The individual scientist struggling to advance his own career, automatically helped other scientists advance their careers, and promoted the rapid advancement of science. Examples of discoveries during this stage include discoveries of the Mohorovicic discontinuity, the earth's core and general structure, surface wave dispersion, the double-couple earthquake mechanism, free oscillations of the earth, and of course, plate tectonics.

Seismology has now matured in many respects. Emphasis is on relatively small improvements in quantitative knowledge, and eliminating non-uniqueness in sophisticated theoretical models. These are brought about only with great difficulty by teams of scientists and technicians, many with an applied research and management orientation. There is a relatively great expenditure of money for small improvements in accuracy, with the research direction dictated by societal goals and relevance (e.g. nuclear test detection, and earthquake hazard reduction). The tools are standardized accurately calibrated commercial equipment, sophisticated higher order theoretical calculations requiring great mathematical skill and large computers, with relatively less reliance on intuition. If developing countries are to fully contribute they need to participate in multidisciplinary, multinational, mission-oriented projects, and need to be willing to invest the relatively large amounts of time and money required. Examples of such projects include large seismic arrays such as NORSAR and the Gauribidanur array, the worldwide seismograph network, strong motion arrays, multidisciplinary and multi-institutional ocean-going surveys, IRIS (Incorporated Research Institutions for Seismology) and PASSCAL (Program for Array Seismic Studies of the Continental Lithosphere). These projects usually result in papers with several co-authors.

As we are all aware, at this stage politics may play an important role. Large international or bi-national projects can impact a nation economically and militarily. Research can lead to unexpected results, and politicians are reluctant to commit national efforts and funds to projects which they do not understand and fear may affect them adversely. As a consequence, important research which could help a nation is not carried out. An excellent example might be the seismic hazard research in the Himalayas, which could obviously benefit millions of people, but which unfortunately is hampered by border security concerns. Because of the uniqueness of the Himalayan region, understanding the earth structure, tectonics, earthquake mechanism and wave propagation in that region could be of great importance to the international community, and in particular to the objectives of the International Decade of Natural Hazard Reduction.

There are strong incentives for government agencies to fund international co-operative projects e.g. national, economical and political advancement, national hazard reduction, increasing the national educational level, and, last but not least,

development of basic research capabilities. In the long run basic research will help all of the above objectives, but in the short run is often considered too costly a drain on resources for attacking more immediate social problems.

The career advancement of individual investigators, students, and technicians is one of the motivating factors behind co-operative research. Priorities must be balanced between, on the one hand, publishing results as soon as possible, and on the other hand allowing students and other apprentices to take the initiative on important problems in order to learn more effectively. There is the obvious scientific incentive of publishing as soon as possible. On the other hand, "hot" research projects are usually best for teaching students because they help develop enthusiasm and competence which will last into the future. Students and apprentices are less experienced and often take longer to work up data and finish research. A wise balance is required in these matters in order to maximize the short and long-term benefits to both the nation and the international community.

Of course military and economic interests often interfere with co-operative research. I will not discuss this obvious and much analysed problem except to observe that the United Nations has been much less effective in helping the situation than I and many others had hoped 20 years ago. We may hope that time will slowly improve the problem.

The problems discussed above have general relevance to India. As far as seismology in particular is concerned, the two problems I have had some experience with are study of the crustal structure in the Bay of Bengal, and attempting to share co-operative seismic source mechanism and hazard projects in the Himalayas. Both have been effected by such difficulties. Both the Himalayan tectonic belt and the Bengal sedimentary basin are unique and the largest examples of their type on our planet, and thus attract high interest. They are of obvious military and economic sensitivity. Naturally Indian researchers would like to have the funding support to attack these problems themselves. And, because of their uniqueness, they are also of great importance to the international community and consequently there is strong incentive to attempt to initiate co-operative field and sea-going operations. One would hope that some way would be found to overcome the difficulties involved with such co-operative research in such a way that all parties would benefit.

A specific problem in seismology is the lack of facilities and incentives to make data, especially early data, available to interested researchers. Again two incentives are at work. On the one hand there is the incentive to get the research done as soon as possible because it would provide answers to scientific problems important to the nation. From this point of view one would like to have the data made as widely available as possible, to both national and international researchers. On the other hand this policy would entail many of the real or perceived national and personal risks touched on above. To mention one, if other researchers use the data to make all of the exciting discoveries, this will deprive the students and personnel of the institution in charge of the data of the opportunity for making the discoveries themselves, and thus advancing their own careers. A wise balance would be to make sure that the institution in charge of the data has both an incentive for co-operation and adequate facilities and funding to co-operate with others on an equal basis.

As far as academic preparation for research is concerned, I feel that all the mechanisms for the high level training, required are potentially in place in India. What may be to a certain extent lacking is team organization and "critical mass" groups

necessary to be fully effective in the modern age of complex multidisciplinary rese
The isolated "ivory tower" scientist is obviously still important, however there
reason that such a person cannot be associated with an applied research group s
valuable cross-fertilization of ideas can occur. This cross-fertilization is difficult
scientist is the only one of his field at a spatially isolated university, even i
university is of high academic quality.

Government research groups are obviously critical in modern research, but
they could be more effective if there was a closer tie with nearby academic institu
Graduate student research and training, along with the natural energy
enthusiasm of students is important to stimulating fundamental research at
centers.

The future

As an old saying goes: "The future is upon us". This is certainly true in seism
with the advent of exploding computing power, rapid data transmission capab
greatly improved instruments, modern techniques of analysis of digital data
rapidly improving transportation and logistical facilities. I believe the way
future is toward standardized data collection techniques. A critical loss of effi
will result without this standardization. A recent publication of the U.S. Na
Academy Press (1988) "Geophysical data: Policy issues", graphically points o
fact that a tremendous amount of valuable data, collected at considerable cost,
actually available because of the lack of standardization of formats. This is natu
the early stages of development of a scientific field, but should be corrected as
develops. The report recommends that a series of guidelines and policies be ad
to correct the situation and to make future data more easily accessible and usef
for many of the issues discussed above, international co-operation will be crit
this regard. Formats should be standardized as soon as possible so that scient
developing countries will have easy access to the modern data, and to moder
analysis techniques. Data collected at considerable public expense cannot be "l
up" because only one or two scientists or technicians have the facilities and kno
to use it. especially when this data may relate to such issues as seismic safet
national economic development.

India currently has the capability of carrying out state-of-the-art resear
determination of earth structure, and the primary challenge of the future w
setting priorities in funding, based on the economic benefit of such st
Determination of earth structure can be of great importance to mineral explo
and seismic hazard reduction. Passive continental margins, the Bengal Fan, a
Indus Fan have great economic potential, and determination of regional and
crustal structure using seismic means may aid local exploration efforts. There m
some benefit to international co-operative studies in the deeper water parts of
structures.

It is obvious that India, with such a high population concentration i
Himalayan seismic region, will have to devote a major effort to seismic h
research in the next decade. The major thrust of this will have to be toward: (i) de
the actual seismic hazard in India (e.g. through seismicity studies, geologic stud
recent fault motion, refined estimates of probability, measurement of Fourier sp

and response spectra of earthquakes, determination of local ground motion amplification), and (ii) clarifying the various options for confronting these hazards (specifically involving cost-benefit analysis). The importance of such studies is highlighted by the controversy over the seismic hazard to Tehri Dam, a construction project of tremendous potential benefit to India, and at the same time of tremendous potential devastation if it should fail during the great earthquake expected in the region. In spite of such tremendous importance to India, knowledge of the tectonics and seismology of the region is only primitive, but could be greatly improved within a few years with modern instrumentation and geological studies.

Some specific critical decisions relating to seismology in India will probably need to be made in the next few years, or perhaps even in the next few months:

(i) Should a modern standardized national seismic system, both for strong and weak motion recording, be established?
(ii) How much effort should be made to integrate seismic data systems with those of the international community?
(iii) Should data transmission be primarily by satellite, with event recording, or should part of the national array have continuous recording, perhaps with microwave transmission?
(iv) How much emphasis should be placed on PC computer facilities for individual scientists, versus emphasis on large centralized facilities for data analysis and theoretical computations?
(v) How much emphasis should be placed on small research grants to individual investigators, versus support for large multidisciplinary, multi-institutional projects?
(vi) How much effort and expense should be put into earthquake resistant building design?
(vii) How much effort should be put into short-term earthquake prediction and earthquake warning systems?

Most of these issues are common to many other nations. In order to expedite the decision-making process, I would recommend that a high-level panel or commission be set up to make recommendations to the government on the above issues.

In conclusion, I feel that seismology in India is at the threshold of a most interesting and challenging period. The rewards for correct policy decisions can be great, but the consequences of error can be disastrous. India has the national capability to successfully attack these problems by itself, but the most cost-effective strategy would probably be to participate as fully as possible in future international co-operative projects such as the International Decade of Natural Hazard Reduction.

James N. Brune
Guest Editor

Department of Geological Sciences
Mackay School of Mines
University of Reno
Reno, Nevada 89557, USA

A preliminary tectonic fabric chart of the Indian Ocean

JEAN-YVES ROYER[1], JOHN G SCLATER[1,2]
and DAVID T SANDWELL[1]

[1]Institute for Geophysics, The University of Texas at Austin 8701 MOPAC Blvd, Austin, TX 78759-8345, USA
[2]Department of Geological Sciences, The University of Texas at Austin, Austin, TX 78713, USA

Abstract. We present a preliminary tectonic chart of the Indian Ocean based on a joint compilation of bathymetric data, magnetic anomaly data and Geosat altimetry data. Satellite altimeters such as Geosat map the topography of the equipotential sea surface or marine geoid. Our interpretation of the GEOSAT data is based on an analysis of the first derivative of the geoid profiles (i.e. deflection of the vertical profiles). Because of the high correlation between the vertical deflection (at wavelength <200 km) and the seafloor topography, the Geosat profiles can be used to delineate accurately numerous tectonic features of the ocean floor such as fracture zones, seamounts and spreading ridges. The lineations in the Geosat data are compared with bathymetric data and combined with magnetic anomaly identifications to produce a tectonic fabric chart of the Indian Ocean floor.

Keywords. Indian Ocean; GEOSAT altimeter; deflection of the vertical; tectonic fabric chart.

1. Introduction

During the past few years, as a result of development of remote sensing and data imaging techniques, better resolution and coverage have permitted the upgrading of the tectonic picture of the ocean floor. In the Indian Ocean, one may examine the development of this improved resolution by comparing the successive tectonic charts produced by Heezen and Tharp (1965) and Udintsev *et al* (1975), and the bathymetric charts of the GEBCO series (1975–1982) with the recent chart of the gravity field by Haxby (1985). Satellite altimeters (GEOS-3, SEASAT, GEOSAT) map the topography of the equipotential sea surface (marine geoid). Due to the uniform coverage of the satellite ground tracks and the excellent correlation between the short wavelengths (20–200 km) of the geoid signal with the topographic gradient of the ocean floor, the satellite altimeter data bring a wealth of rigorously comparable information bearing on the morphology of the seafloor, especially in the remote inhospitable and hence poorly charted southern oceans. There, in particular, previously unrecognized tectonic elements, specifically fracture zones and seamounts, have been delineated or verified (e.g. Lazarewicz and Schwank 1982; Sandwell 1984; Haxby 1985; Sandwell and McAdoo 1988).

Recently, Gahagan *et al* (1988) have used the anomalies and lineations in plots of the deflection of the vertical from SEASAT data to portray a preliminary fabric chart of the ocean floor. In this paper, we expand upon this approach by presenting first, plots of the actual deflection of the vertical data along tracks, second, identifying lineations in these plots and finally, comparing these lineations with bathymetric

features and magnetic anomaly identifications in order to construct a prelim tectonic fabric map of the ocean floor. This work is based primarily on the GEC data which we combine with the SEASAT data set. This analysis reveals new fea on the seafloor at the southerly latitudes that are related to the early phase evol of the Indian Ocean. Recently-refined portrayals of tectonic fabrics of the sea provide exceptionally good constraints for plate tectonic reconstructions far be those available to the pioneer modellers of the evolution of the Indian Ocean Fisher *et al* 1971; McKenzie and Sclater 1971; Sclater and Fisher 1974; Norton Sclater 1979; Partriat 1987). In fact, problems with previous reconstruction m have generally arisen in areas where either the fracture zone lineations or the mag lineations were poorly established through lack of shipborne coverage. Hence joint compilation of magnetic anomalies and fracture zone lineations from clo spaced altimetry traverses has proved to be a very powerful approach as it allow to revise and improve our understanding of the tectonic history of the ocean (e.g. Royer *et al* 1988; Royer and Sandwell 1989; Mayes *et al* 1989).

2. A tectonic history of the Indian Ocean

The Indian Ocean floor (figure 1) is characterized by a system of three active sprea ridges that now separates four major fragments of the former supercont Gondwana: Africa, India, Australia and Antarctica. The northern branch of this system rises in the Gulf of Aden, separating Africa from Arabia, and continues a the Carlsberg Ridge and the Central Indian Ridge which separates Africa from I At 25°S, 70°E, the Central Indian Ridge intersects the two other branches Southwest Indian Ridge that extends between Africa and Antarctica toward South Atlantic, and the Southeast Indian Ridge that extends towards the South P between Antarctica and India, and Antarctica and Australia. Numerous ridges plateaus of intermediate depth, which may be taken to characterize the Indian O appear on either sides of the spreading ridges. The size, number and distributi these elevations have raised many questions about their nature and origin as w their role in the continuing development of the Indian Ocean. From east to they are the South Tasman Rise, the plateaus off western Australia (Naturs Cuvier, Wallaby, Exmouth), Broken Ridge and the Kerguelen Plateau, Ninet Ridge, Chagos-Laccadive Ridge and the Mascarene Plateau, the Chain and M Ridges, Madagascar Plateau, Del Cano Rise, Crozet Plateau, Conrad Rise, Gun Ridge, Mozambique Ridge, Astrid Ridge, Agulhas Plateau and finally Maud (figure 1).

According to interpretations of the seafloor magnetic anomaly pattern as iden in the Indian Ocean, the major basins lying between the spreading ridges continental margins and the submarine ridges evolved during three main pe From the breakup of Gondwana in the Late Jurassic to the mid-Cretaceous, A separated from Madagascar and Antarctica, creating respectively the western Se Basin (Ségoufin and Patriat 1980; Rabinowitz *et al* 1983; Coffin and Rabinowitz

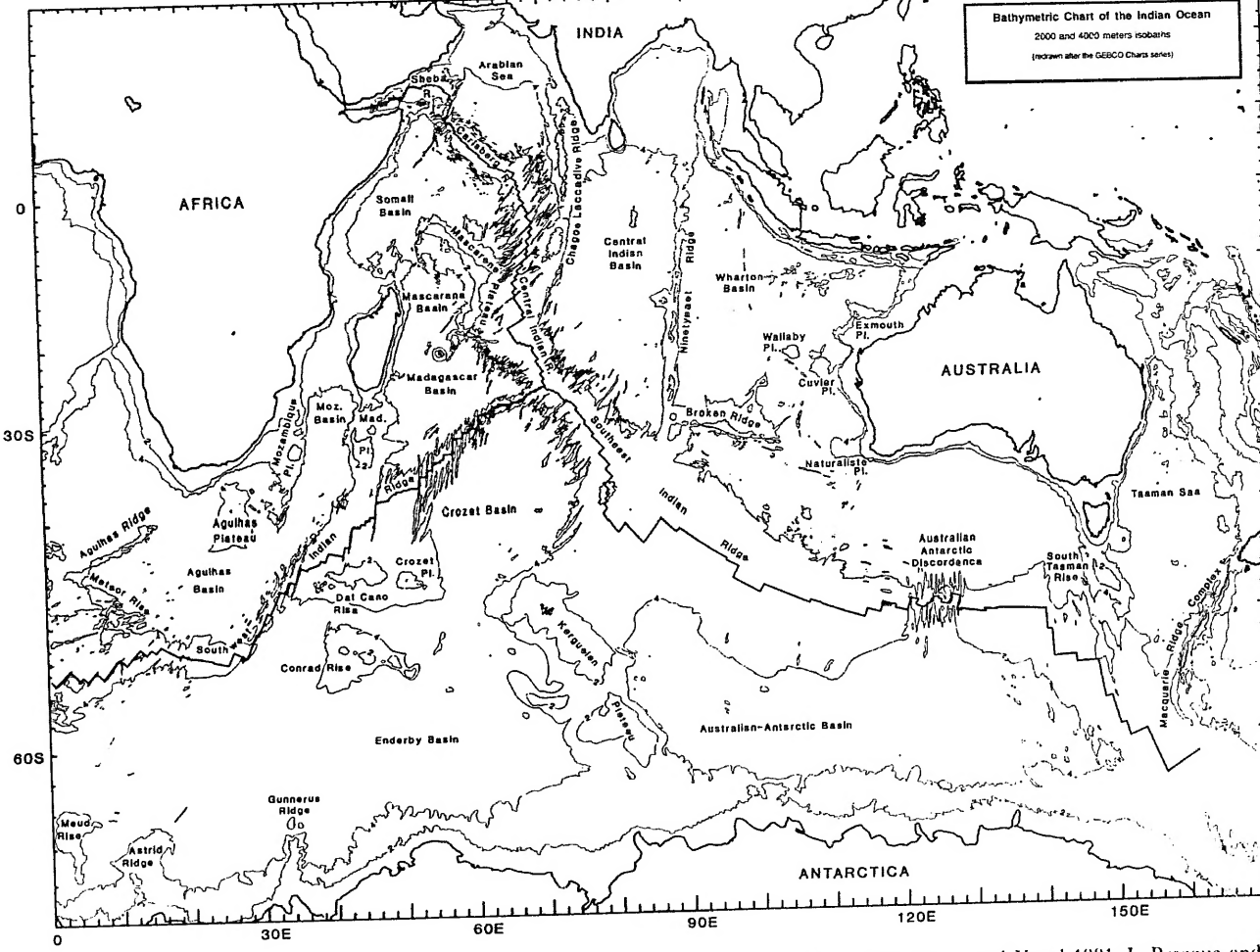

Figure 1. Chart index of geographical names of the Indian Ocean (redrawn from Laughton 1975; Hayes and Vogel 1981; LaBrecque and 1981; Falconer and Tharp 1982; Fisher *et al* 1982; Monahan *et al* 1982; Schlich *et al* 1987).

1978; Larson *et al* 1979; Veevers *et al* 1985). From the mid-Cretaceous to the Middle Eocene, the major motion resulted in the rapid northward drift of India towards Asia. Most of the floor of the Indian Ocean was created during this phase: the basins between Africa-Madagascar and Antarctica (Bergh and Norton 1976; Patriat 1979; LaBrecque and Hayes 1979; Sclater *et al* 1981; Fisher and Sclater 1983), the Madagascar and the Mascarene Basins, the eastern Somali Basin and the Arabian Sea between Africa-Madagascar and India (McKenzie and Sclater 1971; Whitmarsh 1974; Schlich 1975, 1982), the mirrored Central Indian Basin and Crozet Basin between India and Antarctica (McKenzie and Sclater 1971; Sclater and Fisher 1974; Schlich 1975, 1982) and the Wharton Basin between India and Australia (Sclater and Fisher 1974; Liu *et al* 1983). In addition, during this period, Australia and Antarctica commenced to separate (Cande and Mutter 1982). The latest period in the evolution of the Indian Ocean started with a major reorganisation of the spreading centres, consequent to the collision of India with Asia in the Middle Eocene. Seafloor spreading ceased in the Wharton Basin while major changes in the direction and rate of spreading occurred in the Central Indian Basin, the Crozet Basin, the Madagascar Basin, the eastern Somali Basin and the Arabian Sea. The new configuration of the spreading ridges corresponds to the present-day ridge system. During this phase, the Australian-Antarctic Basin (Weissel and Hayes 1972), the southern Central Indian Basin (Sclater *et al* 1976a) and the northern Crozet Basin (Schlich 1975) were created. Also, the Mascarene Plateau and the Chagos-Laccadive Ridge separated (Fisher *et al* 1971; McKenzie and Sclater 1971), and the Gulf of Aden opened (Laughton *et al* 1970). Because of the differential motion along the Central Indian Ridge and the Southeast Indian Ridge, the Southwest Indian Ridge propagated rapidly towards the east (Tapscott *et al* 1980; Sclater *et al* 1981; Patriat 1987).

3. Analysis of the altimetry data: Lineations in the deflection of the vertical charts

The SEASAT satellite, launched by NASA in 1978, used a radar altimeter to make precise measurements (Tapley *et al* 1982) of the sea-surface or geoid height ($\sim$ 1·0 m) over most of the world's oceans. Unfortunately, the SEASAT mission failed after a few months, and almost no data were recovered from the areas south of 62°S because of the ice-coverage around Antarctica at the time that SEASAT operated. In March 1985, the US Navy launched the GEOSAT altimeter in order to map the marine geoid to a high spatial resolution on a global basis. Only the data from the Exact Repeat Mission, started in November 1987, which duplicated the 17 days SEASAT repeat orbits, have yet been unclassified. However, because the ground track spacing ($\sim$164 km at the Equator) decreases at the high latitudes, and because GEOSAT operated during the Austral ice-free summer, the information from the high southerly latitudes, between 60°S and 72°S, is exceptionally good. In this study, we use mainly the GEOSAT data. The accuracy is about 3 times better than for the SEASAT (Sandwell and McAdoo 1988) and we improve this accuracy and data recovery along tracks by stacking 22 GEOSAT repeat cycles. For wavelengths greater than 20 km, the rms noise level of the GEOSAT data is about 1 to 2 mGals. However, in order to take advantage of the better density of the SEASAT data north of 60°S, we combine both SEASAT and GEOSAT data sets when the amplitudes of the SEASAT signal were above the noise level.

To enhance the short wavelengths of the marine geoid signal, it is more appropriate to use the deflection of the vertical which is the first derivative of the geoid along the track. Deflection of the vertical, expressed in microradians, measures the variation of the horizontal gravity field. One microradian (μrad) is roughly equivalent to a horizontal variation in gravity of one milligal (mGal). Figures 2 and 3 display the deflection of the vertical plotted along respectively the descending and ascending satellite ground tracks. Vertical bars along tracks are spaced every 4 data points ($\sim$14 km apart). Amplitudes are positive to the north. The scale of amplitude is 20 μrad/degree of longitude; however when greater than 30 μrad, the amplitudes are reduced through an arctangent function. Long wavelength (>4000 km) and short wavelength noise (<20 km) have been removed from each pass using the procedure described by Sandwell and McAdoo (1988).

Figure 4A through 4J display a series of different interpretations of the deflection of the vertical signal. In a tectonic fabric chart, we are mostly interested in the lineated features such as fracture zones, spreading ridges, linear troughs, ridges or plateaus, and trenches. Depending on their extension, most of these features have a reproducible signature on a set of parallel profiles, which make them easy to identify. The signature of a fracture zone will vary according to the spreading rate and the age offset (figures 4A and 4B). Depending on the direction of the satellite and the orientation of the tectonic feature relative to the satellite ground track, the signature of a tectonic feature can be identical or reversed on the ascending or descending data sets. As a rule of thumb, topographic features oriented north-south will have same signatures; in the case of a fracture zone (figure 4C), both the ascending and descending profiles cross the topographic (age) offset from the same side. East-west oriented features will have reversed signatures; in figure 4D, ascending and descending profiles approach the fracture zone from opposite sides. Because the age offset reverses at the midpoint of the transform segment of a fracture zone, the signature of a fracture zone is symmetric relative to the fracture zone axis and of opposite sign on either side of this point (figure 4E). Finally, the spacing of parallel fracture zones is also an important factor; the combined effects of parallel topographic (age) offsets may produce a large signal where the signal produced by each individual fracture zone cannot be identified (e.g. Prince Edward FZ area along the Southwest Indian Ridge). The signature of a spreading ridge axis depends on the spreading rates as does the topography (figures 4F and 4G). Seamounts have a typical signature (figure 4H) recognizable at isolated, sharp and narrow positive and negative picks of equal amplitude. Trenches (figure 4I) are characterized by a succession of positive and negative picks related to the flexure of the lithosphere ahead of the trench and to the trench itself. Continental rise (figure 4J) and linear offsets in the oceanic basement are also clearly identifiable. Finally, aseismic ridges and plateaus are clearly visible, but, depending on their width and height relative to the adjacent basins, they are difficult to chart. The deflection of the vertical charts of the Indian Ocean (figures 2 and 3) provides examples for each type of feature. We have traced lineations in these charts by correlating respectively peaks and troughs (i.e. steepest horizontal gradient of the gravity) in the deflection of the vertical plots, on both the ascending and descending passes. Figure 5 summarizes our interpretation of the lineations in the deflection of the vertical plots. We have abbreviated the name of this chart to deflection of the vertical lineations. Symbols show the actual location of the data points and lines, the lineations. We deliberately have not represented the peaks and troughs associated with large topographic features

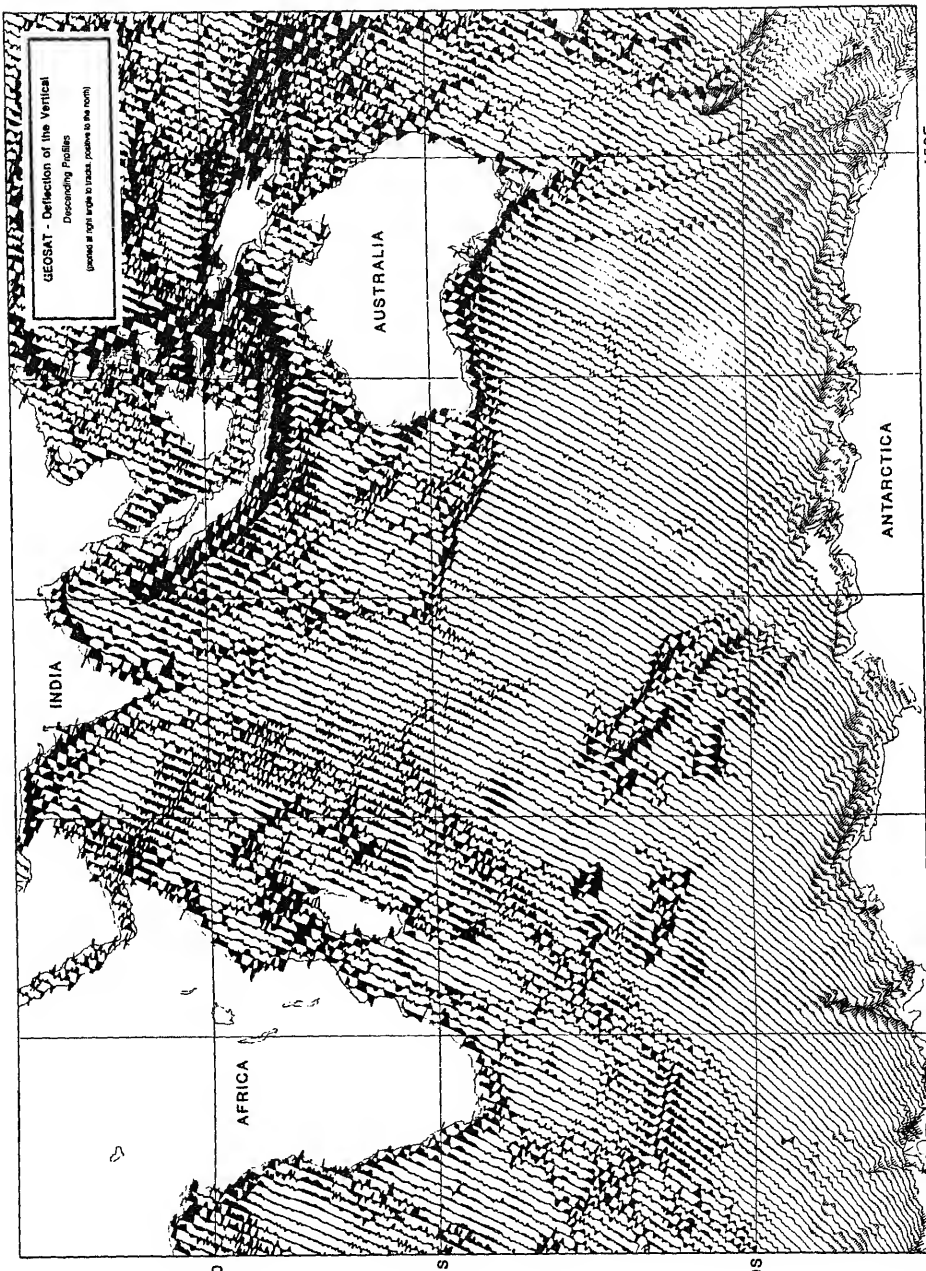
GEOSAT - Deflection of the Vertical
Descending Profiles
(grades at right angle to tracks, positive to the north)
INDIA
AUSTRALIA
ANTARCTICA
AFRICA
0
30S
60S

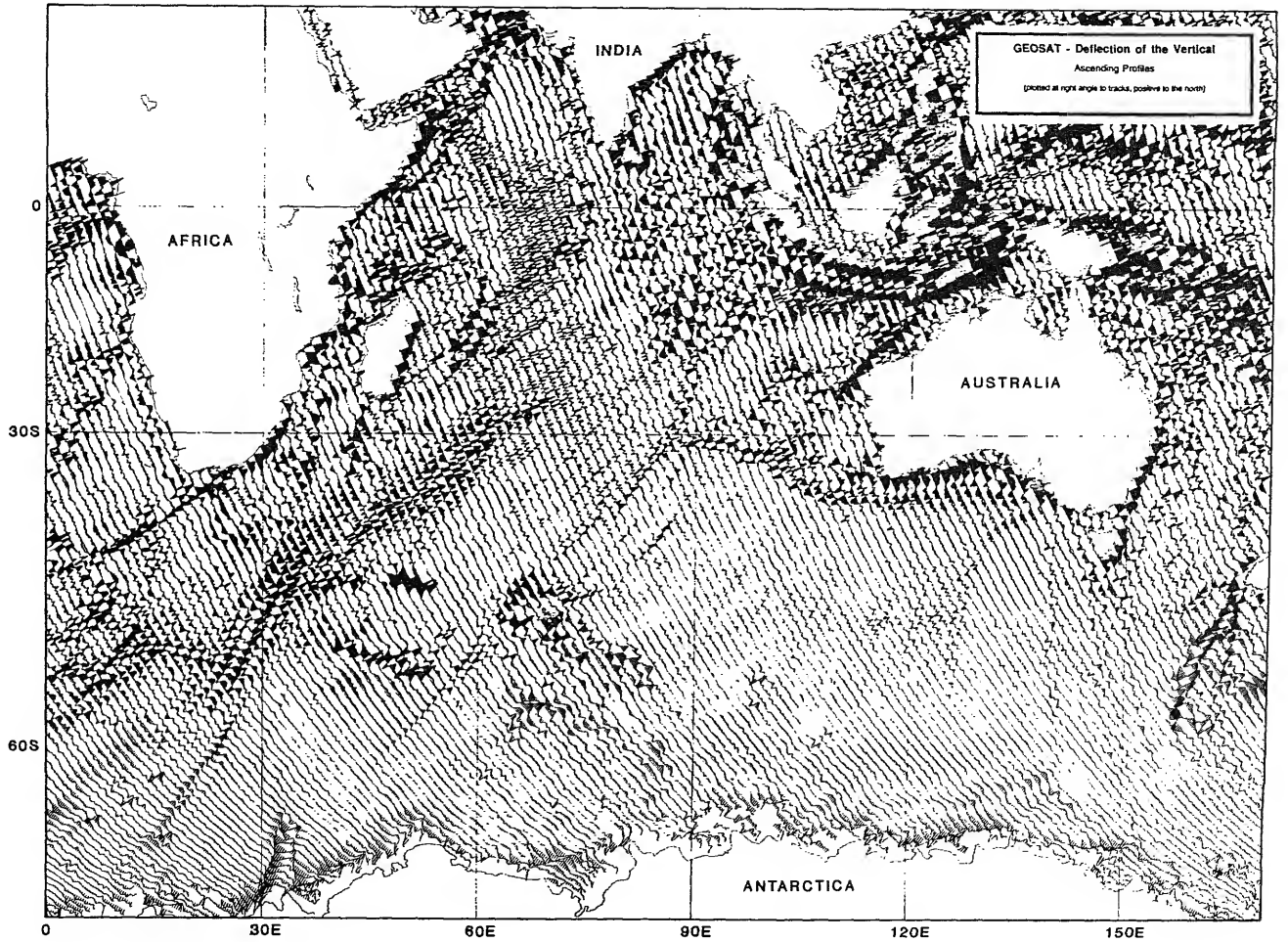

Figure 3. GEOSAT ascending profiles of the deflection of the vertical plotted along the satellite ground tracks. Positive is the north.

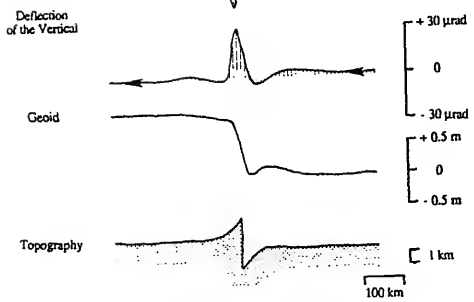

A

Fracture Zone (fast spreading)

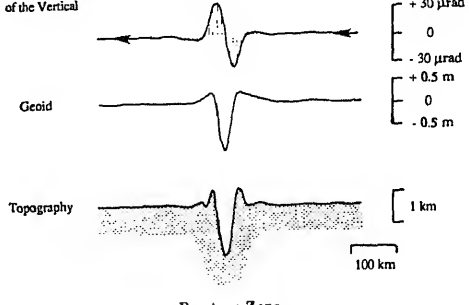

B

Fracture Zone (slow spreading)

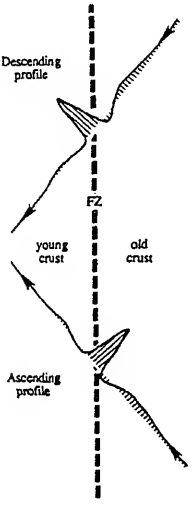

C

North-South Fracture Zone

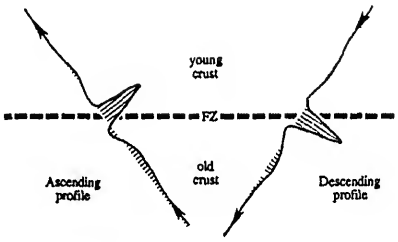

D

East-West Fracture Zone

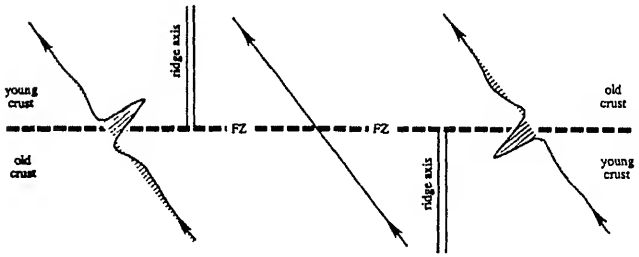

E

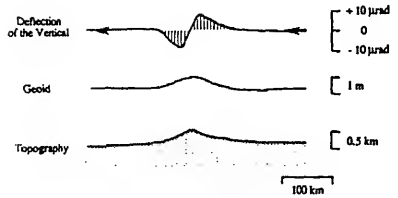

F

Spreading Ridge (fast spreading)

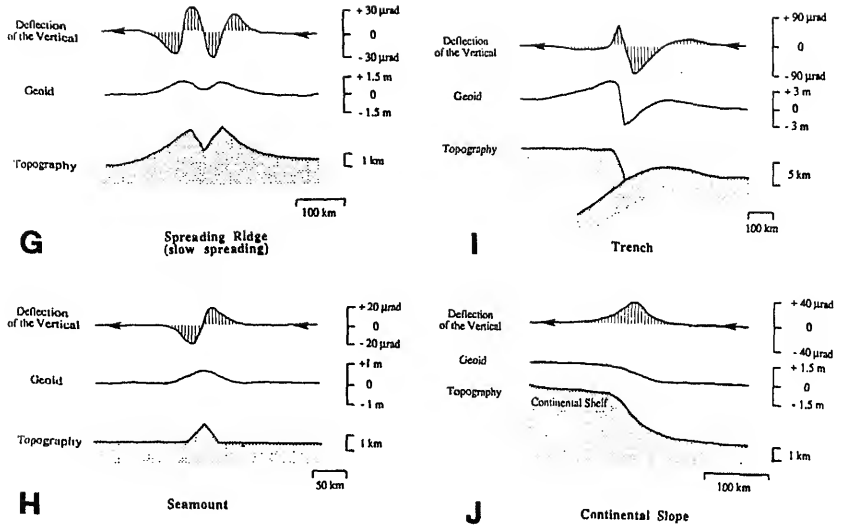

Figure 4. Schematic signatures of the geoid and the deflection of the vertical (horizontal derivative of the gravity field) across some tectonic features of the ocean floor: (A), (B) Fracture zones. Since the deflection of the vertical is the horizontal derivative of the geoid along the satellite ground track, the sign of the signal changes with the direction of the satellite. (C), (D) Deflection of the vertical plotted at right angle of the subsatellite tracks. Positive is to the north (top of page). Descending and ascending profiles will have an identical signature across a north-south oriented fracture zone while they will show an opposite signature across an east-west oriented fracture zone. (E) Variation of the deflection of the vertical signal along a fracture zone (same convention as for C and D). The signal reverses at the midpoint of the transform segment of the fracture zone as does the age offset. (F), (G) Deflection of the vertical signature above spreading ridge axes. (H) Seamount signatures generally show two sharp positive and negative picks of equal amplitude. (H) Trench (J) Continental rise.

of the ocean floor, outlined in figure 5 by bathymetric contours. Such features are better represented by direct contouring of the gravity field (e.g. Haxby 1985).

4. Tectonic fabric chart of the Indian Ocean

The deflection of the vertical plots amplify the short wavelengths of the geoid. Lineations in these charts are in general related to high amplitude short wavelength topographic features such as transform faults, fracture zones, seamounts and other discrete entities on the seafloor. By combining the lineations of the deflection of the vertical charts with transform faults and fracture zones known from topographic and magnetic surveys, it is possible to create an improved tectonic chart of the sea floor. Because of the greater coverage of the satellite data and the ability of the presentation to amplify and extend lineated features both above and below sediment, the resultant signal presents a fabric chart of the igneous basement of the seafloor. We have abbreviated the name of these combined charts to "tectonic fabric charts".

The lineations in the deflection of the vertical charts (figure 5) are documented to varying degrees depending on the characteristics of seafloor spreading in the oceanic basins: spreading rate, paleo-direction of spreading relative to the satellite ground

tracks and the age offsets across the fracture zones. The interpretation of the deflection of the vertical charts brings new information mainly on the southerly latitudes around Antarctica regarding the early phase of seafloor spreading between Africa and Antarctica during the Late Jurassic up to the Late Cretaceous, and between Antarctica and Australia during the Middle Eocene. In addition, due to the uniform coverage of the satellite profiles, the fracture zones are generally better sampled and their pattern better defined on the deflection of the vertical charts than on tectonic charts based on shipborne data. This is for instance the case along the Central Indian Ridge, or between Broken Ridge and the Kerguelen Plateau, or between Tasmania and Antarctica. Except for this latter area, most of the fracture zones in the Indian Ocean are oblique or perpendicular to the ascending satellite tracks and parallel or sub-parallel to the descending tracks. Therefore, they are more visible on the ascending passes (figure 3) than on the descending passes (figure 2), while the opposite occurs for the Indian Ocean spreading ridges. However, in some areas such as the Australian-Antarctic Discordance where the fracture zones are oriented north-south and the ridge axes east-west, both data sets are complementary.

In regard to the evolution of the Indian Ocean, the best documented period corresponds to the latest and most recent phase of seafloor spreading that started after the general reorganization of the plate boundaries in the Middle Eocene. Along the Sheba, Carlsberg and Central Indian Ridges, the fracture zones strike N50°E to N60°E. From the northwest to the southeast, the main fracture zones are the Alula-Fartak FZ (13°N, 51°E) at the mouth of the Gulf of Aden, the Owen FZ (12°N, 56°E) separating the Sheba Ridge from the Carlsberg Ridge, the fracture zone at 3°N, the Mahabiss FZ (3°S), the Sealark FZ (4°S), the Vitiaz FZ (8°S), the Vema FZ (11°S), the Argo FZ (14°S), the Marie Celeste FZ (17°S) and the Egeria FZ (20°S) which lies east of the Rodrigues Ridge. Except for the Alula-Fartak FZ and the fracture zone at 3°N, all the transform offsets are left-lateral. The largest transform offsets are located along the Alula-Fartak FZ (200 km), the Owen FZ (300 km), the Vema FZ (200 km) and the Marie Celeste FZ (220 km). Along the Southwest Indian Ridge, the orientation of the fracture zones varies progressively from N45°E in the vicinity of the Bouvet Triple Junction (55°S, 1°W) to north-south, west of the Indian Ocean triple junction (25°S, 70°E). From west to east, they are Bouvet FZ (2°E), Moshesh FZ (5°E), Islas Orcadas FZ (6°E), Shaka FZ associated with the Shaka Ridge (8°E), Dingaan FZ (12°E), Mandela FZ (15°E), Du Toit FZ (26°E), the Andrew Bain FZ complex (28°E), Prince Edward FZ (35°E), Discovery II FZ (43°E), Indomed FZ (46°E), Gallieni FZ (52°E), the Atlantis II FZ (58°E) and the Melville FZ (61°E). The transform offsets are right-lateral and generally important (100 to 200 km) for all these fracture zones; the major offset (800 km) along the Southwest Indian Ridge axis occurs between Bain FZ and Prince Edward FZ (28°E to 35°E). Finally, along the Southeast Indian Ridge, the fracture zone trends, oriented N45°E in the vicinity of the Indian Ocean triple junction, shift progressively to N15°E-N10°E between Australia and Antarctica, and reach N15°W in the vicinity of the Macquarie triple junction (61°S, 162°E). The major offsets are located along the Amsterdam and St Paul FZ (78°E) and along the George V, Tasman and Balleny FZ. The fracture zone pattern between Australia and Antarctica, particularly the prominent fracture zones

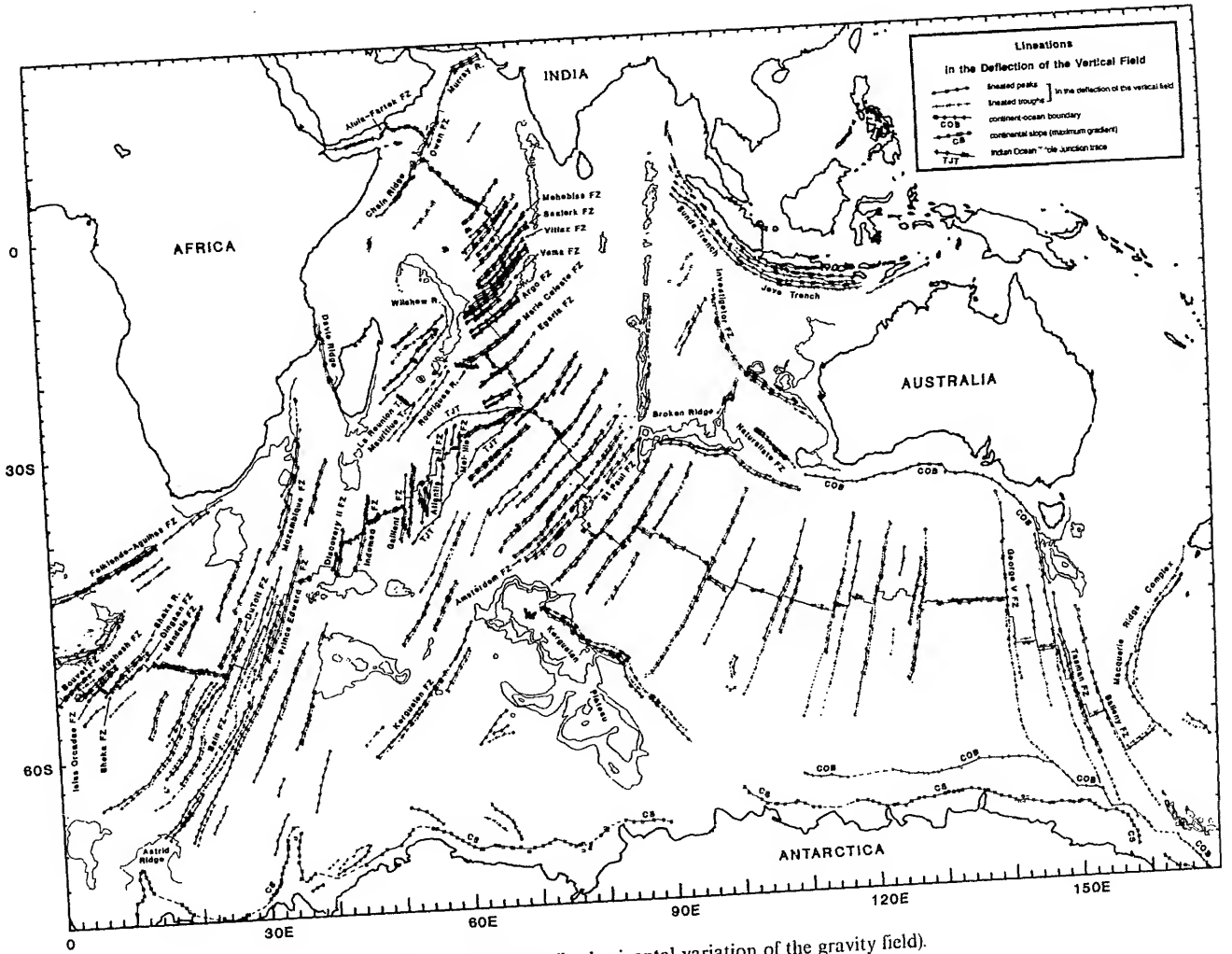

Figure 5. Lineations in the deflection of the vertical profiles (i.e. horizontal variation of the gravity field).

and Antarctic margins.

The spacing between satellite profiles is generally too large (160–80 km) to allow an accurate mapping of the mid-oceanic ridge axes. However in several areas, the deflection of the vertical data shows an excellent correlation with the location of the ridge axes deduced from bathymetric and magnetic data. The Sheba Ridge is characterized by a slow spreading rate (1 cm/a, Laughton *et al* 1970) and an axial valley that deepens towards the east. The ridge axis produces a clear signature on the deflection of the vertical signal, as illustrated in figure 4G, that defines two continuous ridge segments separated by the Alula-Fartak FZ. The Carlsberg Ridge has similar characteristics as the Sheba Ridge with spreading rate ranging from 1·2 to 1·3 cm/a (Le Pichon and Heirtzler 1968; McKenzie and Sclater 1971) and shows a linear and nearly continuous ridge axis from the Owen FZ to the Equator. The Central Indian Ridge, which runs between the Mascarene Plateau and the Chagos-Laccadive Ridge, is extremely segmented by closely spaced fracture zones. The first ridge segments clearly identifiable out of the geoid signal caused by the fracture zones are located southeast of the Rodrigues Ridge. The spreading rates for this mid-oceanic ridge range from north to south between 1·8 and 2·4 cm/a (Fisher *et al* 1971; Patriat 1987). The Southwest Indian Ridge has a very slow spreading rate (less than 1 cm/a; Schlich and Patriat 1971a; Sclater *et al* 1976b, 1981; Patriat 1987) and is expressed by a deep and pronounced inner valley. Several extensive ridge segments are well delineated by the deflection of the vertical data between the Mandela and Du Toit FZ which is the longest segment, east of the Prince Edward FZ, between the Discovery II, Indomed, and Gallieni FZ, and between the Melville FZ and the Indian Ocean triple junction. The Southeast Indian Ridge is the most active of the three Indian mid-oceanic ridges with medium spreading rates increasing from west to east from 3·0 to 3·5 cm/a (Schlich and Patriat 1971b; Weissel and Hayes 1972; Schlich 1975; Patriat 1987). Between the Indian Ocean triple junction and the Amsterdam and St Paul FZ, the ridge axis is segmented by several fracture zones and is generally well expressed by an axial valley, while east of the St Paul FZ the ridge segments are long and continuous and expressed by a central rise typical for medium or fast spreading ridges (Weissel and Hayes 1972; Royer and Schlich 1988). The area of the Australian-Antarctic Discordance presents an anomalous topography and fracture zone pattern (Vogt *et al* 1983). The deflection of the vertical signal along the Southeast Indian Ridge varies from that of figures 4a and 4b. The trenches along the Java and Sumatra Islands and south of New Zealand are the second type of present-day plate boundaries that clearly show on the deflection of the vertical data.

The altimetry data add little information on the fabric of the oceanic basins related to the second phase of opening of the Indian Ocean, from the mid-Cretaceous to the Middle Eocene. Only the Murray Ridge and the Chain Ridge, on either sides of the Owen Fracture Zone, document in the Arabian Sea and eastern Somali Basin the drift of India away from the Seychelles and East Africa. Structural directions in the Central Indian Basin and the Wharton Basin (McKenzie and Sclater 1971; Sclater and Fisher 1974), which record the fast northward drift of India relative to Antarctica and Australia, do not show well on the deflection of the vertical data. Their north-south orientation is too close from those of the satellite profiles. In the Wharton Basin, in addition to the Investigator FZ and the eastern scarp of the Ninety east Ridge, a cross grain is apparent, while intraplate deformation within the Central Indian Basin cause

east-west undulation of the lithosphere that obliterate and obscure the tectonic fabrics (e.g. Weissel *et al* 1980; Geller *et al* 1983; Haxby 1985; McAdoo and Sandwell 1985). However, in the conjugate basins, the Madagascar and Crozet Basins, the fracture zone pattern is well recognizable. The most important feature is the Kerguelen Fracture Zone that offset the magnetic lineations 32, 33 and 34 (Schlich 1982; Patriat 1987) by more than 800 km. With the GEOSAT data, it becomes clear that this feature does not extend further south than 62°S, and therefore post-dates the plate boundary reorganization in the mid-Cretaceous. In the Mascarene Basin, part of the extinct spreading system is visible. This system initiated at the time of the break-up between India and Madagascar in the mid-Cretaceous and died in the Paleocene/Early Eocene (chron 31 to 27; Schlich 1982) when the spreading ridge jumped to the north to form the Carlsberg Ridge and subsequently separated India from the Seychelles and the northern Mascarene Plateau. Remnant of the fossil spreading axis can be identified southwest of La Réunion Island (La Réunion Trench), north of the Mauritius Trench extension that forms the limit of the extinct spreading system with the Madagascar Basin. The fossil spreading ridge is offset 400 km to the north by the Mahanoro FZ and Wilshaw Ridge complex. Further north, the fracture zone pattern becomes unclear. Finally, the most interesting information related to mid-Cretaceous/Middle-Eocene time span concerns the relative motion of Africa and Antarctica. A clear set of parallel fracture zones can be defined between the Agulhas Plateau and the Maud Rise and Astrid Ridge, off Antarctica. At 48°S on the northern flank, and at 58°S, on the southern flank, there is a clear disruption of the fracture zone pattern which is shifted, by 50 to 100 km, to the east or to the west, respectively. This demonstrates the change of motion that occurred in the Paleocene (anomaly 31 to 24; Larson *et al* 1985; Patriat *et al* 1985; Royer *et al* 1988). This change of motion is particularly well recorded by the large offset northeast of Astrid Ridge (~40 Ma age offset). Such a change of motion will also match perfectly the extremities of the fracture zones lying immediately west of the Madagascar Plateau (northern flank) and Conrad Rise (southern flank). The Prince Edward FZ is therefore a recent feature (Middle Eocene, chron 20) and is not the continuation of the fracture zone running from Astrid Ridge.

Finally, new evidence about the early phase of opening of the Indian Ocean, from the Late Jurassic to the mid-Cretaceous, are found in the western part of the Enderby Basin. East of the fracture zone near Astrid Ridge, several parallel fracture zones are delineated in the deflection of the vertical charts. It shows that the direction of motion between Africa and Antarctica remained the same for 34 Ma, from chron M0 (118 Ma) identified east of the Astrid Ridge (Bergh 1977, 1987) to chron 34 (84 Ma) located west of Conrad Rise (Bergh and Norton 1976; Patriat *et al* 1985). To the north, except for the Davie Ridge that records the relative motion between Africa and Madagascar, no fracture zone shows on the deflection of the vertical data: neither in the Mozambique Basin (Ségouffin 1978; Simpson *et al* 1979), nor in the western Somali Basin (Ségoufin and Patriat 1981; Rabinowitz *et al* 1983) or off the east African margin (Bunce and Molnar 1977; Cochran 1988). This is duc to their north south orientation and to the very important thickness of sediments in these old basins. Along the western Australian margins, only the large offset Investigator FZ, the scarps of the Wallaby

produce a typical signature on the horizontal gravity field. Among the most spectacular are the conjugate escarpments of Broken Ridge and the Kerguelen Plateau. These lines correspond to an offset of the basement along the Kerguelen Plateau (Coffin *et al* 1986) and to a deep linear trough along Broken Ridge (Fisher *et al* 1982). According to Mammerickx and Sandwell (1986), these topographic features are related to the demise of seafloor spreading in the Wharton Basin (Liu *et al* 1983; Geller *et al* 1983) and the initiation of spreading between the two plateaus (Mutter and Cande 1983) at chron 18–19 (~45 Ma). The match of these two curves provides a tight constraint upon the relative position of the Kerguelen Plateau and Broken Ridge prior to their break-up. The continent/ocean boundary mapped along the southern margin of Australia from magnetic and seismic evidence (Talwani *et al* 1979; Konig 1980; Veevers 1986) has a distinct and characteristic deflection of the vertical signature. We have used this criterion to identify the conjugate boundary along the Antarctic margin where the data are very limited. The deflection of the vertical signature also clearly outlines the limit of the continental shelf break (steepest gradient of the horizontal gravity field). Generally, this structural limit is well mapped from bathymetric data; however, around Antarctica where the data are sparse and scattered because of the remoteness and the ice-coverage, the altimery data now permit accurate delineation of the limit of the continental plateau. Another clearly visible feature is the change of topographic grain between the crust created along the Southwest Indian Ridge (at a slow spreading rate) and the crust created along the Southeast Indian Ridge and the Central Indian Ridge (at medium spreading rates). Actually, the age of this limit decreases towards the east, demonstrating the eastward propagation of the Southwest Indian Ridge (Patriat 1979; Tapscott *et al* 1980; Sclater *et al* 1981). Patriat (1987) mapped independently these two limits as the traces of the Indian Ocean triple junction respectively on the African and Antarctic plates.

5. Conclusion: a revised tectonic summary diagram for the Indian Ocean

Comparison of bathymetric data, deflection of the vertical lineations, and magnetic anomaly data permits the construction of a revised tectonic fabric chart for the Indian Ocean (figure 6). This chart is of significant value especially in the far southern ocean where new fracture zones have been identified and previously charted fracture zones extended. However, it is still only preliminary in nature as we have neither integrated the deflection of the vertical data with the actual topographic data to produce improved topographic charts (e.g. Driscoll *et al.*, unpublished manuscript 1986) or repicked any magnetic anomalies. In addition, the geoid or gravity field of the oceans (Haxby 1985) contains very valuable information on the origin and structure of broad basic features of the ocean floor. The present study is the first step towards an international attempt to integrate all the above information, to provide some useful preliminary constraints for studies of the Indian Ocean tectonic history, and to show what can be accomplished by such integrated approach.

For the sake of clarity, we did not represent in figure 6 all the magnetic lineations that have been identified in the Indian Ocean; in particular for the Cenozoic, we have

satellite altimetry data. In *Mesozoic and Cenozoic plate reconstructions* (eds) C R Scote W W Sager; *Tectonophysics*, **155** 1–26

Geller C A, Weissel J K and Anderson R N 1983 Heat transfer and intraplate deformation in the Indian Ocean; *J. Geophys. Res.* **88** 1018–1032

Haxby W F 1985 *Gravity field of World's oceans* (color map). Lamont Doherty Geological Obse of Columbia University, Palisades, NY

Hayes D E and Vogel M 1981 General Bathymetric Chart of the Oceans (GEBCO), sheet 5.13. Ca Hydrographic Service, Ottawa, Canada

Heezen B C and Tharp M 1965 Physiographic diagram of the Indian Ocean (with descriptive sheet *Soc. Am. Inc.* New York, NY

König M 1980 Geophysical investigations of the southern continental margin of Australia a conjugate sector of East Antarctica. PhD. Thesis, Columbia University, New York, NY, 337 p

LaBrecque J L and Hayes D E 1979 Seafloor spreading history of the Agulhas Basin; *Earth Pla Lett.* **45** 411–428

LaBrecque J L and Rabinowitz P D 1981 General Bathymetric Chart of the Ocean (GEBCO), she Canadian Hydrographic Service, Ottawa, Canada

Larson R L, Mutter J C, Diebold J B and Carpenter G B 1979 Cuvier Basin: a product of ocea formation by Early Cretaceous rifting off Western Australia. *Earth. Planet. Sci. Lett.* **45** 105–1

Larson R L, Pitman W C, Golovchenko X, Cande S C, Dewey J F, Haxby W F and LaBrecque J The Bedrock Geology of the World (color map), Freeman and Co, New York, NY

Laughton A S, Whitmarsh R B and Jones M T 1970 The evolution of the Gulf of Aden; *Philos. R. Soc. London* A267 227–266

Laughton A S 1975 General Bathymetric Chart of the Oceans (GEBCO), sheet 5.5. Canadian Hydro Service, Ottawa, Canada

Lazarewicz A R and Schwank D C 1982 Detection of uncharted seamounts using satellite alt *Geophys. Res. Lett.* **9** 385–388

Le Pichon X and Heirtzler J R 1968 Magnetic anomalies in the Indian Ocean and sea-floor spr *J. Geophys. Res.* **73** 2101–2117

Liu C S, Curray J R and McDonald J M 1983 New constraints on the tectonic evolution of the Indian Ocean; *Earth Planet. Sci. Lett.* **65** 331–342

McAdoo D C and Sandwell D T 1985 Folding of the oceanic lithosphere; *J. Geophys. Res.* **90** 85

McKenzie D P and Sclater J G 1971 The evolution of the Indian Ocean since the Late Cret *Geophys. J. R. Astron. Soc.* **25** 437–528

Mammerickx J and Sandwell D T 1986 Rifting of old oceanic lithosphere; *J. Geophys. Res.* **91** 19

Markl R G 1974 Evidence for the breakup of Eastern Gondwanaland by the Early Cretaceous; *(London)* **251** 196–200

Markl R G 1978 Further evidence for the Early Cretaceous breakup of Gondwanaland off South Australia; *Marine Geol.* **26** 41–48

Mayes C M, Sandwell D T and Lawver L A 1989 Tectonic history and new isochron chart of the Pacific; *J. Geophys. Res.* in press

Monahan D, Falconer R H and Tharp M 1982 General Bathymetric Chart of the Oceans (GI sheet 5.10. Canadian Hydrographic Service, Ottawa, Canada

Mutter J C and Cande S C 1983 The early opening between Broken Ridge and Kerguelen Plateau *Planet. Sci. Lett.* **65** 369–376

Norton I O and Sclater J G 1979 A model for the evolution of the Indian Ocean and the brea Gondwanaland; *J. Geophys. Res.* **84** 6803–6830

Patriat P 1979 L'océan Indien occidental: la dorsale ouest-indienne; *Mém. Mus. Nat. Hist. Nat.* **4**

Patriat P 1987 Reconstitution de l'évolution du systeme de dorsales de l'océan Indien par les m de la cinématique des plaques. Publ. by Territoire des Terres Australes et Antarctiques Fra Paris, 308 p

Patriat P, Ségoufin J, Goslin J and Beuzart P 1985 Relative positions of Africa and Antarctica Upper Cretaceous: evidence for a non-stationary behaviour of fracture zones; *Earth Planet. Sci.* 204–214

Rabinowitz P D, Coffin M F and Falvey D 1983 The separation of Madagascar and Africa; *Scie* 67–69

Royer J-Y and Schlich R 1988 The Southeast Indian Ridge between the Rodriguez Triple Junction and the Amsterdam and Saint-Paul Islands: detailed kinematics for the past 20 Ma; *J. Geophys. Res.* **93** 13524–13550

Royer J Y and Sandwell D T 1989 Evolution of the eastern Indian Ocean since the Late Cretaceous: Constraints from GEOSAT altimetry; *J. Geophys. Res.* (in press)

Sandwell D T 1984 A detailed view of the South Pacific geoid from satellite altimetry; *J. Geophys. Res.* **89** 1089–1104

Sandwell D T and Mc Adoo D C 1988 Marine gravity of the Southern Ocean and Antarctic Margin from GEOSAT: tectonic implications; *J. Geophys. Res.* **93** 10389–10396

Schlich R 1975 Structure et âge de l'océan Indien occidental; *Mém. hors série Soc. Géol. France.* **6** 103 p

Schlich R 1982 The Indian Ocean: aseismic ridges, spreading centres and basins. In *The Ocean Basins and Margins: the Indian Ocean* (eds) A E Nairn and F G Stheli (New York: Plenum Press) **6** 51–147

Schlich R and Patriat P 1971a Mise en évidence d'anomalies magnétiques axiales sur la banche ouest de la dorsale médio-indienne; *C. R. Acad. Paris* **B272** 700–703

Schlich R and Patriat P 1971b Anomalies magnétiques de la branche est de la dorsale médio-indienne entre les îles Amsterdam et Kerguelen; *C. R. Acad. Sci. Paris* **B272** 773–776

Schlich R, Coffin M F, Munschy M, Stagg H M J, Li Z G and Revill K 1987 Bathymetric chart of the Kerguelen Plateau. Joint publication of the Bureau of Mineral Resource, Canberra, Australia, and the Institut de Physique du Globe, Strasbourg, France.

Sclater J G and Fisher R L 1974 Evolution of the east-central Indian Ocean, with emphasis on the tectonic setting of the Ninetyeast Ridge; *Geol. Soc. Am. Bull.* **85** 683–702

Sclater J G, Luyendyk B P and Meinke L 1976a Magnetic lineations in the Southern part of the Central Indian Basin; *Geol. Soc. Am. Bull.* **87** 371–378

Sclater, J G, Bowin C, Hey R, Hoskins H, Peirce J, Phillips J and Tapscott C 1976b The Bouvet triple junction; *J. Geophys. Res.* **81** 1857–1869

Sclater J G, Fisher R L, Patriat P, Tapscott C and Parsons B 1981 Eocene to recent development of the Southwest Indian Ridge, a consequence of the evolution of the Indian Ocean triple junction; *Geophys. J. R. Astron. Soc.* **64** 587–604

Ségoufin J 1978 Anomalies magnétiques mesozoiques dans le bassin de Mozambique; *C. R. Ac. Sci. Paris* **B287** 109–112

Ségoufin J and Patriat P 1980 Existence d'anomalies mésozoiques dans le bassin de Somalie. Implications pour les relations Afrique-Antarctique-Madagascar; *C. R. Acad. Sci. Paris*, **B291** 85–88

Ségoufin J and Patriat P 1981 Reconstructionns de l'océan Indien occidental pour les époques des anomalies M21, M2 et 34. Paléoposition de Madagascar; *Bull. Soc. Géol. France*, **23** 693–707

Simpson E S W, Sclater J G, Parsons B, Norton I O and Meinke L 1979 Mesozoic magnetic lineations in the Mozambique Basin; *Earth Planet. Sci. Lett.* **43** 260–264

Talwani M, Mutter J, Houtz R and König M 1979 The crustal structure and evolution of the area underlying the magnetic quiet zone on the margin south of Australia. In Geological and geophysical investigations of the continental margins; *Am. Assoc. Pet. Geol. Mem.* (eds) Watkins, Montadert and Dickerson **29** 151–175

Taplcy B D, Born G H and Park M E 1982 The SEASAT alimeter data and its accuracy assessment; *J. Geophys. Res.* **87** 3179–3188

Tapscott C, Patriat P, Fisher R L, Sclater J G, Hoskins H, and Parsons B, 1980 The Indian Ocean triple junction; *J. Geophys. Res.* **85** 4723–4739

Udintsev G B, Fisher R L, Kanaev V F, Laughton A S, Simpson E S W and Zhiv D I, 1975 Geological-geophysical atlas of the Indian Ocean. Academy of Sciences of the U.S.S.R., Moscow, 151 p

Veevers J J 1986 Breakup of Australia and Antarctica estimated as mid-Cretaceous (95 ± 5 Ma) from magnetic and seismic data at the continental margin; *Earth Planet. Sci. Lett.* 77 91–99

Veevers J J, Tayton J W, Johnson B D and Hansen L 1985 Magnetic expression of the continent-ocean boundary between the western margin of Australia and the Eastern Indian Ocean; *J. Geophys.* **56** 106–120

Vogt P R, Cherkis N Z and Morgan G A 1983 Project Investigator I: evolution of the Australia-Antarctic disordance deduced from a detailed aeromagnetic survey. In Antarctic Earth Science, Proceeding of the IV International Symposium on Antarctic Earth Science (eds) R L Oliver, P R James and J B Logo (Canberra: Australian Academy Press) 608–613

Weissel J K and Hayes D E 1972 Magnetic anomalies in the Southeast Indian Ocean. In Antarctic Oceanology II: The Australian-New Zealand sector *Am. Geophys. Un. Ant. Res. Ser.* (ed.) D E Hayes **19** 165–196

Weissel J K, Anderson R N and Geller C A 1980 Deformation of the Indo-Australian plate; *Nat (London)* **287** 284–291

Whitmarsh R B 1974 Some aspects of the plate tectonics in the Arabian Sea. In Initial reports of Deep Sea Drilling Project **23** 527–535

Anomalous crustal structure beneath the Bay of Bengal and passive oceanic sedimentary basins

JAMES N BRUNE and KEITH PRIESTLEY

Seismological Laboratory, Department of Geological Sciences, Mackay School of Mines, University of Reno, Reno, Nevada 89557, USA

Abstract. Recently Brune and Singh (1986) reported evidence for anomalous continent-like crustal structure beneath the Bay of Bengal, possibly caused by perturbation in the temperature-pressure regime and consequent phase chage, partial melting, or mass transport (e.g. convection or underplating). Recent refraction results indicate the existence of an anomalous lower crustal or subcrustal layer of *P*-wave velocity about 7·3 km per second along the eastern North America passive margin, possibly a result of underplating of the oceanic crust just after initial rifting. We have searched for other evidence of anomalous crustal structure. The data suggest some mechanism may cause a general increase in the anomalous thickness of the crust with increasing thickness of the accumulated sediments, up to a thickness of about 6–7 km. On the other hand, anamolous crustal structure may in fact be transitional between oceanic and continental, or may have been modified by aseismic ridges, thus requiring no sediment related structure modification mechanism. The explanation for all the data may require more than one mechanism, all probably involving severe temperature perturbations. The general tendency is for perturbations of normal oceanic crust to make it more continent-like, suggesting that normal oceanic crust is an unstable end-member in crustal states.

Keywords. Anomalous crust; underplating; Bay of Bengal; sedimentary basin.

1. Introduction

Recently Brune and Singh (1986) reported evidence for anomalous continent-like crustal structure beneath the Bay of Bengal. Surface wave dispersion data could not be fit by a simple model of oceanic crust with overlying sediments—the model expected from current understanding of the tectonic evolution of the Bay of Bengal (Curray *et al* 1982; Royer *et al* this volume). The data required a progressively more continent-like crustal structure as the sediment load increased northward. This suggested that either the sediment deposition had altered the crustal structure, or that the structure had not been a simple oceanic type before deposition. If the anomalous structure were a result of modification by the sedimentary load it might be caused by the perturbation in the temperature-pressure regime and consequent phase change, partial melting or mass transport (e.g. convection or underplating), and this might have important implications not only for the Bay of Bengal, but also for the classical geodynamic problem of basin formation.

Recent results of Trehu *et al* (1988) have increased interest in the problem. Using ocean bottom seismometers they were able to show the existence of an anomalous lower crustal or subcrustal layer of *P*-wave velocity about 7·3 km per second. They suggested that this could be the result of underplating of the oceanic crust just after the initial rifting of the North American plate from the African Plate. These results are discussed in more detail below.

what might have been expected to be normal oceanic crust is so similar to the
for the Bay of Bengal that it suggests a common causal factor. The fact that for th
of Bengal the perturbation in structure correlates with sediment thickness (incr
from south to north) suggests that some sediment load effect should be consider
the Carolina Trough results. On the other hand, whatever mechanism is estab
for the Carolina Trough results should be considered as a possible explanation f
Bay of Bengal results.

If the original structure beneath the Bay of Bengal was not oceanic, then
modifications of the current plate tectonic model for the Indian Ocean mig
suggested. However the excellent fit between the coast of India and the co
Antarctica (Lawver and Scotese 1987) argues against any other structure thai
oceanic in the majority of the Bay of Bengal.

An alternate explanation of the anomalous dispersion might be a combinat
structural perturbations, including effects of a marginal rifting event
perturbations by the 90 deg east ridge and the 85 deg east ridge (e.g. th
underplating).

2. Evidence from other areas

Brune and Singh (1986) mentioned evidence that anomalous structure unde
thick sediments on oceanic structure might not be unique to the Bay of Beng
some anomalous surface wave dispersion evident in figure 8 of Sykes and Oli
Part II (1964) for the Argentine sedimentary basin. We have searched for
evidence of the phenomenon, and report the results here. Most of the evidence is
published studies. A paper documenting anomalous crustal structure in small
basins was published by Menard (1967). Although his results may be related
data considered here, we have not placed heavy emphasis on it because in most
it is not clear that the original structure before sedimentation was oceanic.

We have not included results from active tectonic areas such as the Bering Se
Mediterranean, and the Sea of Okotsk, which, although they have consid
thicknesses of sediments, have not been stable tectonically in the same mani
passive margins and the Bay of Bengal, and in some cases seem to have n
oceanic crust underlying the sediments, possibly a result of creation of new cr
back-arc spreading or some other type of active tectonism.

3. Data

Selected data correlating the sediment thickness to the thickness of the anon
crust is plotted in figure 1, and is discussed below.

3.1 *The Bengal Fan*

The data for the Bengal Fan are taken from Brune and Singh (1986). For a disc
of that data the reader is referred to the publication. The main conclusion fro
data is that there is an apparent correlation between sediment thickness and thi

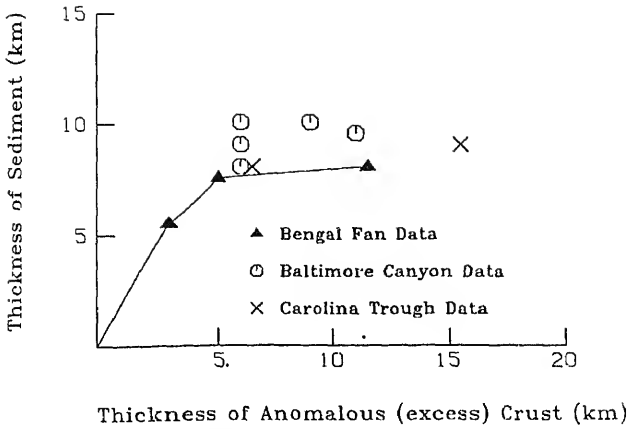

Figure 1. Plot of selected data for thickness of sediments versus thickness of anomalous crust, i.e. crustal thickness in excess of 6 km.

of anomalous lower crust (figure 1). This apparent correlation suggests that some causal mechanism increases in effect from south to north, rather than parallel to the coast as might be expected from a remanent continental margin effect or the initial rifting event or from effects of the 85 East and 90 East ridges. However since the width of the Bay of Bengal decreases from south to north it would take less of a contaminating structure to influence the apparent average crustal thickness.

3.2 *The Arabian Sea*

Singh (1988) has recently published results on surface wave dispersion across the Arabian Sea. The Indus Fan sedimentary basin in not as large as the Bengal Fan and the location of seismic stations and earthquake sources is not as favourable, with no good paths crossing the thick part of the fan. Many of the paths are contaminated by the Maldive and Laccadive ridges. The dispersion results suggest the existence of anomalous crust for much of the Arabian Sea area studied by Singh (1988).

3.3 *Anomalous crustal structure at passive continental margins*

Recently Trehu *et al* (submitted 1989) reported new results for the crustal structure underlying the sedimentary basin of the Carolina trough. These results were obtained using new ocean bottom seismographs which recorded clear deep crust and mantle arrivals, arrivals not reliably recorded in earlier studies using surface sonobouys. The data provided evidence for a thick (up to 15 km) high-velocity (7·2–7·6 km/s) lower crustal or upper mantle layer extending beneath the Carolina trough and the adjacent ocean basin. This layer was either very thin or absent landward of the hinge zone (continental broader). Trehu *et al*, following similar results from the Baltimore Canyon Trough (LASE Study Group 1986), interpreted this anomalous crust to represent material that was underplated to the crust during the late stage of continental drifting and early seafloor spreading.

Both the Carolina Trough and The Baltimore Canyon have very thick sedimentary accumulations, similar to the thicknesses of sediments in the Bengal Fan, and thus fit

the correlation of anomalous crust with sediment thickness. However results fro Hatton Bank, a sediment starved margin, also indicate the presence of an anom layer which Trehu *et al* (1989) label as "underplated", but it is more localized the continental border.

3.4 *Gravity*

A detailed study of gravity using data collected in recent cruises has not been c out in the Bay of Bengal. Liu *et al* (1982) presented a free-air gravity map of the B Fan. The free-air anomalies tend to be 20 to 30 milligals negative over the w part, and near zero close to the eastern margin near the Ninety-East Ridge. If m sediments were flooded onto a perfectly rigid oceanic crust-mantle system the fr anomaly would be positive since more dense sediments would replace less water. However in a non-rigid system isostatic compensation will cause the an to move more or less rapidly toward zero. Liu *et al* (1982) showed that the eff flooding sediments around a ridge, in this case the buried Eighty-Five East ridge create a local gravity low over the ridge, but we know of no mechanism which give a broad low over a region where turbidity currents are rapidly depo sediments. The negative values are probably related to more global factors, e. assumed shape of the geoid. We do not believe that at this stage gravity provi reliable constraint on the crust-mantle structure, or on the interpretation surface wave data.

Rao and Rao (1986) made an approximate gravity interpretation assumin sedimentary layers of density 2·3 and 2·5 g/cc, respectively, and a basement dens 2·84 g/cc overlying a mantle with density 3·4 g/cc. Their interpretation indica slight crustal thinning northward in the Bay of Bengal; however the interpret depends on unverified density contrasts, does not consider a possible lower c layer, and does not deal with the question of local and regional compensatio thus cannot resolve the questions being dealt with in this paper.

4. Discussion

Figure 1 is a plot of sediment thickness versus thickness of the anomalous crustal (crustal thickness remaining after subtracting out a "normal" crustal thickn 6 km). The Bengal Fan data are connected by a line, starting at the origin (means no sediments and no excess crustal thickness). The data are consistent some mechanism causing a general increase in the thickness of the crust increasing thickness of the accumulated sediments, but there is considerable scat the data and the correlation does not establish any particular mechanism to ex the data. If there is a causal mechanism relating anomalous crustal thickne sediment thickness, figure 1 suggests that it is not linear but has a "corner" sediment thickness of about 6–7 km, possibly suggesting a saturation effect s beyond this thickness, further sediments have less of an effect in modifyin structure.

Possible general interpretations of the data include:

by a mechanism yet to be established e.g. thermal blanketing, phase change, underplating; etc. (causal sedimentary effect).
(ii) Since all the data are from oceanic areas near continental margins, or areas with aseismic ridges, the actual underlying crust may not have been (before sedimentation) originally normal oceanic as assumed, but in fact transitional between oceanic and continental, or may have been modified by aseismic ridges, and thus no sediment related structure modification mechanism is required.

There is no established mechanism for a causal connection between sediment load and crustal thickness. The data suggest that the modification in structure occurs near the Moho, but there is strong evidence from our recently developed understanding of the evolution of oceanic crust that the oceanic Moho is a compositional boundary, not a phase change or pressure-temperature boundary. Thus it is difficult to see how sediment load could lead to large structural changes near the Moho. Furthermore the most obvious candidate for a pressure effect, the basalt-eclogite phase change would work the opposite direction and cause the Moho to shallow. This suggests that if there is a large structure modification near the Moho, it must involve either temperature or mass transport, or both. One such mechanism might be reactivated basalt underplating brought about by an increased geothermal gradient, possibly from the sedimentary blanketing effect and/or reactivated shallow convection in the mantle. Neither of these mechanisms has been quantitatively evaluated.

Since great sedimentary basins are of necessity near continents (to provide a supply of sediment), there is usually some question as to where the exact continent-ocean boundary is, and whether or not the structure of the crust underneath the basin is truly oceanic. An exact knowledge of plate tectonic history may be required to establish the original type of structure unambiguously. In the case of the Bengal Fan the location of the remnant boundary between the Antarctic and Indian plates is well established from the deflection of the vertical data (Royer *et al* this volume), and the most recent plate reconstructions (Lawver and Scotese 1987), and thus we expect the Bengal Fan to be underlain by oceanic crust.

Even if it is accepted that the Bay of Bengal is underlain by oceanic crust, there is the possibility of structural perturbations not only by continental margin effects but also by anomalous structures such as aseismic oceanic ridges. The nature of the Ninety-East Ridge is not known for certain, and conceivably could exert some influence on the surrounding structure. The same is true for the buried Eighty-Five Degree East Ridge.

5. Conclusion

Evidence for anomalously thick crust in areas expected from plate tectonic reconstructions to have normal oceanic crust suggest that various factors may be acting to perturb the crust-mantle structure. Evidence from the Bay of Bengal suggests a strong correlation with sediment thickness. Evidence from eastern U.S. passive continental margin sedimentary basins suggests a similar anomalous crustal structure related to the original rifting event. If there is a strong effect related to sediment blanketing it could result from temperature perturbations and related mass transport phenomena, e.g. underplating. The explanation for all the data may require more than one mechanism, e.g. mechanical mechanisms related to stretching and rifting,

mechanisms related to thermal effects of sedimentary blanketing, and mec
related to emplacement of aseismic ridges. All of these probably involv
temperature perturbations. Whatever mechanisms are operating, the general t
for perturbations of normal oceanic crust is to alter the structure in such a w
make it more continent-like. Perhaps this indicates that normal oceanic cr
unstable initial crustal state, and various mechanisms can restructure it toward
continental structure.

References

Brune J N and Singh D D 1986 Continent-like crustal thickness beneath the Bay of Bengal sedim
Seismol. Soc. Am. **76** 191–203

Curray J R, Emmel F J, Moore D G and Raitt R W 1982 Structure, tectonics, and geological his
northeastern Indian Ocean. In *The Oceans basins and margins* (eds) Alan E M Nairn and
Stehli (Plenum Publishing Corporation) Vol. 6

Lase Study Group 1986 Deep structure of the U.S. East Coast passive margin from large apertu
experiments (LASE); *Mar. Petrol. Geol.* 3 234–242

Lawver L A and Scotese C R 1987 In *Gondwana six, structure, tectonics and geophysics* (ed) G D
AGU Geophys. Monograph, Vol. 40 pp. 17–23

Liu C S, Sandwell D T and Curray J R 1982 The negative gravity field over the 85°E ridge; *J. Geo*
87 7673–7686

Menard H W 1967 Transitional types of crust under small ocean basins; *J. Geophys. Res.* **72**

Rao T C S and Rao B B 1985 Some structural features of the Bay of Bengal; *Tectonophysics* **12**

Royer J-Y, Sclater J G and Sandwell D T 1989 *Proc. Indian Acad. Sci. (Earth Planet. Sci.)* **98**

Singh D D 1988 Quasi-continental oceanic structure beneath the Arabian fan sediments from
surface-wave dispersion studies; *Bull. Seismol. Soc. Am.* **78** 1510–1521

Sykes L R and Oliver J 1964 The propagation of short-period seismic surface waves across ocean
Part I and Part II; *Bull. Seismol. Soc. Am.* **54** 1341–1416

Trehu A M, Klitgord K D, Sawyer D S and Buffler R T *The geophysical framework of the C*
United States (eds) L Pakiser and W D Mooney (GSA memoir)

High velocity anomaly beneath the Deccan volcanic province: Evidence from seismic tomography

H M IYER[#], V K GAUR, S S RAI, D S RAMESH, C V R RAO, D SRINAGESH and K SURYAPRAKASAM

National Geophysical Research Institute, Hyderabad 500 007, India
[#]US Geological Survey, Menlo Park CA, USA

Abstract. Analysis of teleseismic *P*-wave residuals observed at 15 seismograph stations operated in the Deccan volcanic province (DVP) in west central India points to the existence of a large, deep anomalous region in the upper mantle where the velocity is a few per cent higher than in the surrounding region. The seismic stations were operated in three deployments together with a reference station on precambrian granite at Hyderabad and another common station at Poona. The first group of stations lay along a west-northwesterly profile from Hyderabad through Poona to Bhatsa. The second group roughly formed an L-shaped profile from Poona to Hyderabad through Dharwar and Hospet. The third group of stations lay along a northwesterly profile from Hyderabad to Dhule through Aurangabad and Latur. Relative residuals computed with respect to Hyderabad at all the stations showed two basic features: a large almost linear variation from approximately + 1 s for telseisms from the north to − 1 s for those from the southeast at the western stations, and persistance of the pattern with diminishing magnitudes towards the east. Preliminary ray-plotting and three-dimensional inversion of the *P*-wave residual data delineate the presence of a 600 km long approximately N-S trending anomalous region of high velocity (1–4% contrast) from a depth of about 100 km in the upper mantle encompassing almost the whole width of the DVP. Inversion of *P*-wave relative residuals reveal the existence of two prominent features beneath the DVP. The first is a thick high velocity zone (1–4% faster) extending from a depth of about 100 km directly beneath most of the DVP. The second feature is a prominent low velocity region which coincides with the westernmost part of the DVP. A possible explanation for the observed coherent high velocity anomaly is that it forms the root of the lithosphere which coherently translates with the continents during plate motions, an architecture characteristic of precambrian shields. The low velocity zone appears to be related to the rift systems (anomaly 28, 65 Ma) which provided the channel for the outpouring of Deccan basalts at the close of the Cretaceous period.

Keywords. Deccan volcanic province; seismic tomography; deep structure; high velocity anomaly; teleseismic residuals; three-dimensional inversion.

1. Introduction

The Deccan volcanic province (DVP) encompasses an area of about a half million km^2 in west-central India with a possible extension of an additional 1 million km^2 beneath the Arabian Sea to the west. The Deccan basalts are primarily of tholeiitic composition with a few pockets of acidic volcanism. The volcanic flows occur as a relatively thin veneer at the surface with a thickness of 1–1·5 km in the western third of the province, thinning to about 0·4 km in the middle section and to a few meters in the eastern section (Kaila 1982). The bulk of the Deccan volcanism is now known to have occurred around·65 Ma (Mahoney 1988). About 200 Ma ago, India was wedged in the southern latitudes between Africa and Antarctica as part of the

migrating northwards as an independent continent eventually colliding with E about 45 Ma ago. Morgan (1972) proposed that the Deccan basalts erupted c this northward migration as the sub-continent traversed over a mantle associated with the Reunion hot spot.

1.1 *Gravity*

The Deccan Traps lie in a broad gravity low which encompasses the whole south Indian shield. Within this broad low are shorter wavelength "lows" and "h A few of these short wavelength features have been interpreted variously: upli subsidence due to cycles of volcanic activity (Kailasam 1975); crustal intrusi mafic rock (Takin 1966) and linear channels of magma flow (Qureshy 1981). W show later that preliminary two-dimensional modelling of the gravity data ind a lower-than-normal density in the upper mantle beneath the central part of the

1.2 *Deep seismic sounding*

Deep seismic sounding was carried out along two profiles over the Koyna reg the Deccan Traps and several others in the Saurashtra Peninsula and acro Narmada-Son lineament (Kaila *et al* 1981, 1985; Kaila 1982). Though the ve models obtained from these profiles reflect the thickness of the surficial basa to 2 km, the crustal structure beneath the DVP is not significantly different fror of the precambrian south Indian shield model elsewhere as revealed by data the Kavali-Udipi profile (Kaila 1982). Moho depth is found to vary from 39– west of Koyna to 36–38 km eastwards. There is no evidence of drastic changes depth of major discontinuities like the Conrad discontinuity across the profi is there evidence of unusually high upper or lower crustal velocities whic characteristic of rift zones.

1.3 *Heat-flow*

Except for the Cambay graben where the heat-flow is somewhat higher-than-nc other parts of the Deccan Traps show normal heat flow typical of stable conti regions (Gupta and Gaur 1984). Except for implying that the volcanic ep responsible for the Deccan volcanic flows did not leave a detectable thermal rema in the lithosphere, the heat-flow data do not provide any information on the structure beneath the DVP.

In summary, the available geophysical data are inadequate to constrain a s model for the Deccan volcanism. For example, if the magmatism was caused mantle plume, extensive melting, differentiation and variations in physica chemical properties of the deep structure of the lithosphere might have taken But the available heat-flow and deep seismic sounding data are inadequate to the structure of the lithosphere and asthenosphere beneath the DVP which expose alterations in structure associated with that volcanism. With this ground, we designed a tomographic experiment to model in three dimensio compressional wave velocity structure of the upper mantle beneath the DVP. R from this experiment reveal a vast anomalous region in the upper mantle

DVP where the *P*-wave velocity is a few per cent higher than in the surrounding region. This is the first effort to map the deep structure beneath the DVP.

2. Tomography using teleseismic residuals

Teleseismic residuals provide an excellent approach to model the two- and three-dimensional velocity structures of the earth's crust and mantle. Numerous publications describe the use of the technique to delineate heterogeneous earth structure from global and continental scales to local scale. Recent introduction of inversion methods for teleseismic residuals (also called seismic tomography) has considerably enhanced the power of the teleseismic residual technique (Aki *et al* 1977; Humphreys and Clayton 1988). Tomographic modelling of small and large heterogeneities in the earth's crust and mantle have been carried out in diverse geologic settings (Thurber and Aki 1987; Iyer and Hitchcock 1988). The present study is the first application of this technique in India.

3. Estimation of teleseismic residuals

Teleseisms (earthquakes occurring at distances greater than approximately 20 degrees from the recording station) are recorded by a dense array of seismic stations sited over the region of interest to provide the data for tomography. The average instrument spacing in the array limits the smallest size of the velocity anomaly that can be resolved. Two-dimensional arrays yield three-dimensional models, while linear arrays yield two-dimensional models. Arrival times of the first seismic phases (P or PKIKP, PKP) are read from the seismograms and travel time from the source to the recording stations are estimated from a knowledge of the earthquake origin times. Knowing the hypocentral location of the earthquake, theoretical travel times are computed using a standard seismological table. In the present study, we used the *P*-wave travel time tables of Herrin (1968a). The travel-time residuals are simply the differences between the observed and theoretical travel times. In the mathematical notation we write,

$$R_{ij} = T^{o}_{ij} - T^{th}_{ij}$$

where, R_{ij} is the absolute residual in seconds, and T^{o}_{ij} and T^{th}_{ij} are the observed and theoretical travel times respectively at station i for event j. In addition to the information on the deep structure beneath the seismic array, R_{ij} contains effects due to errors associated with the location and origin times of the earthquakes travel-time tables, and anomalous structure at the source and along the seismic wave paths. In order to isolate the local structures from extraneous effects, relative residuals are computed independently for each event by subtracting the residual at a reference station which hopefully is located outside the anomaly under investigation from the absolute residuals at each station. Alternatively, a weighted mean of absolute residuals for each event can be used as the reference residual. Thus, the relative residual RR_{ij} for event j can be defined as,

$$RR_{ij} = R_{ij} - R_{rj},$$

where the subscript r represents the reference station, or as

$$RR_{ij} = R_{ij} - R_j,$$

where R_j represents the weighted mean of R_{ij} using all readings available for the event j. In this study all weights were chosen to be equal to unity. Consequently, R_j is a simple average of absolute residuals for the whole array.

RR_{ij} contains the information needed to model the three-dimensional relative-velocity structure beneath the seismic array. The magnitudes of the relative residuals indicate the change in velocity within the anomaly; the sign of the residuals being negative for high-velocity anomalies and vice versa. The azimuthal pattern of RR_{ij} gives an idea of the depth of the anomaly. As a rule of thumb, it may be remembered that a 10-km long anomalous ray-path in which the seismic velocity differs from the normal by 10% produces a residual of about 0·2 s.

4. Three-dimensional inversion

We have used the three-dimensional inversion technique developed by Aki *et al* (1977) (now popularly referred to as the ACH technique) to model the teleseismic residuals. Since the ACH technique is described in detail in various papers (Aki *et al* 1977; Ellsworth and Koyanagi 1977; Iyer *et al* 1981; Achauer *et al* 1986) and also its application (Aki 1982; Thurber and Aki 1987; Iyer and Hitchcock 1988), only a brief outline of the theory will be given here along the lines presented by Achauer *et al* (1986). In this technique, the volume under the array is divided into layers and each layer into a grid of rectangular blocks. An initial P-wave velocity from a known or assumed model is assigned to each layer for ray-tracing purposes. It turns out that the final results are not very sensitive to the choice of this initial velocity model. The incident wave at the bottom of the deepest layer is assumed to be plane. As it travels to the seismograph, it encounters an unknown velocity perturbation in each block. The resultant travel time delays and advances accumulated along the ray path equal the observed residual at the surface. In this treatment, the refraction of the seismic ray due to the velocity perturbation is assumed to be negligible. Thus for each ray, the following linear equation can be generated in a matrix form.

$$Am = d,$$

where A is a matrix with calculated unperturbed travel times of ray segments, m is a vector containing the unknown fractional slowness perturbations (slowness is the reciprocal of velocity), and d is a vector containing the travel time residuals. Since A^TA is near singular, Aki *et al* (1977) used the damped least-squares method to obtain the model estimate $\hat{m}$ as,

$$m = (A^TA + \theta^2 I)^{-1} A^T d,$$

where $\theta^2 = \sigma_d^2/\sigma_m^2$ is the damping parameter and σ_d^2 and σ_m^2 are the estimated variances of the data and the (unknown) true model m (Achauer *et al* 1986). It should be remembered that the estimated model contains only relative velocities, as the inputs are relative residuals.

The main drawback with the block inversion described above (resulting from coefficients

t it provides only a 'fuzzy' picture of the real model. The degree of 'fuzziness' n the density of instruments deployed in the seismic network, the number thal distribution of teleseisms used and the block size. Fortunately, the ast-squares inversion also produces a resolution matrix and standard errors ble one to estimate the figure of merit for a computed model. The 'true' s related to the 'fuzzy' model $\hat{m}$ by the relation

$$m = R\hat{m},$$

s the resolution matrix. Each element of the symmetric singular matrix R ie between -1 and $+1$ with positive values on the diagonal. Therefore, of the matrix can be considered as an average kernel relating all of m, the l, to one block of the estimated 'fuzzy' model. Thus large diagonal elements olution matrix imply that $\hat{m}$ is a good representation of m. In general, is good towards the middle of each layer and is rather poor near the edges. ly related to the number of ray-hits in the block. The standard errors, om the diagonal of the covariance matrix, are indicators of the accuracy elocity perturbation. As a rule of thumb, the accuracy of individual on estimates are about ($\pm$) 2 times the standard error for 0·8 resolution —4 times for 0·6 resolution (Evans 1982). When small blocks are used, the of the inversion can be assessed by looking at the whole resolution matrix c blocks.

periment

ted fifteen vertical-component seismic stations (Teledyne protacorders with z, seismometers) in and around the southern half of the DVP (figure 1, n three consecutive deployments with Hyderabad (HYB) and Poona (POO) mon to the whole experiment. A total of 168 teleseisms mainly from north, east and southeast, and in the distance range of 19 to 95 degrees were by this network (table 2). The recorders were operated at their maximum ed of 240 mm/min and internal clocks synchronized with radio time oadcast by the National Physical Laboratory, New Delhi. Considerable taken in reading the arrival times of the first phases, thereby achieving a racy of 0·05 s. Visual correlation of seismic waveforms and multiple readings k, peak, zero-crossing, trough etc) were used to ensure a high relative of picks (figure 2). Despite these precautions substantial signal changes e array led us to discard about 10% of the readings (figure 3). This as well amplitudes of the signals also contributed to the scatter in data. Even so, magnitude of the observed relative-residuals permits us to draw significant ns.

nalysis

tion *of residuals with azimuth and distance*

—7 show the relative residuals, with respect to HYB at 13 stations plotted

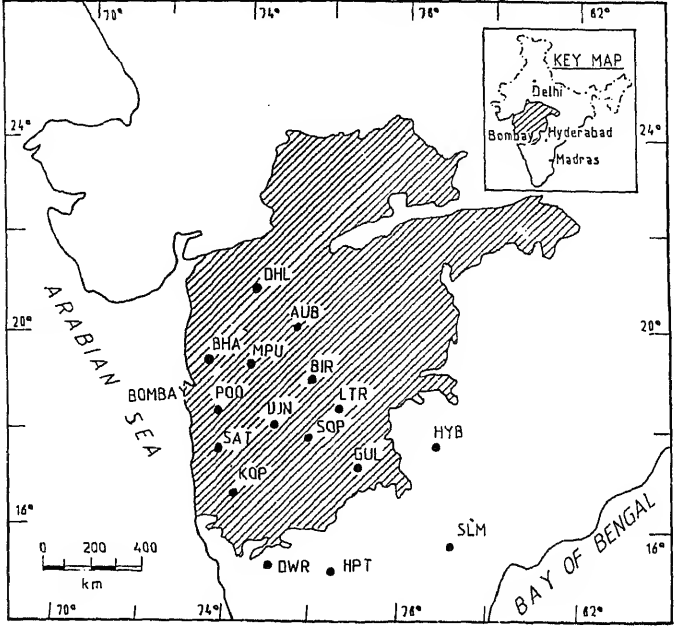

Figure 1. Map of west-central India showing the locations of seismic stations (three-letter names) used in this study. The approximate outline demarking the extension of the DVP.

Table 1. Coordinates of seismic stations.

Station name	Latitude (N)	Longitude (E)	Elevation (meters)	Duration of operation
Hyderabad (HYB)	17°25·03′	78°33·18′	510·0	Sept. 1985–Dec. 1987
Poona (POO)	18°32·84′	73°49·07′	579·3	Sept. 1985–Dec. 1987
Bhatsa (BHA)	19°31·12′	73°24·06′	185·9	Dec. 1985–Apr. 1986
Ujani (UJN)	18°04·00′	75°06·87′	496·9	Jan. 1986–Apr. 1986
Solapur (SOP)	17°38·90′	75°54·93′	475·6	Jan. 1986–May. 1986
Gulbarga (GUL)	17°19·57′	76°53·25′	470·0	Jan. 1986–Apr. 1986
Satara (SAT)	17°40·17′	74°00·19′	670·5	Jun. 1986–Feb. 1987
Kolhapur (KOP)	16°40·20′	74°15·10′	563·8	Jun. 1986–Feb. 1987
Dharwar (DWR)	15°25·27′	74°55·79′	731·5	Jun. 1986–Jan. 1987
Hospet (HPT)	15°15·31′	76°20·58′	478·5	Jun. 1986–Jan. 1987
Srisailam (SLM)	16°06·00′	78°53·50′	438·9	Jan. 1987–Mar. 1987
Aurangabad (AUB)	19°54·38′	75°18·66′	569·0	May. 1987–Dec. 1987
Bir(BIR)	18°58·37′	75°46·28′	560·0	May. 1987–Dec. 1987
Latur (LTR)	18°21·25′	76°33·75′	610·0	May. 1987–Dec. 1987
Dhule (DHL)	20°55·49′	74°47·01′	265·0	Jun. 1987–Dec. 1987

Table 2. List of teleseisms used in this study which provided readings in at least 3 stations.

Sl. No.	Source region	Origin time	Depth (km)	Coordinates	
1.	MOLUCAzc(01/03/86)	09·43·28·6	39	00:58·32S	126:52·08E
2.	AFGHAN(01/14/86)	03·03·37·4	245	36:20·46N	71:01·44E
3.	HONSHUzc(01/16/86)	08·34·43·7	436	29:48·12N	138:39·72E

(*continued*)

Table 2. (*continued*)

Sl. No.	Source region	Origin time	Depth (km)	Coordinates	
4.	MINDROzc(01/16/86)	15·45·06·7	223	13:41·10N	120:49·32E
5.	ALUTINtr(01/18/86)	01·59·01·6	33	51:33·18N	173:06·54W
6.	MOLUCAtr(01/22/86)	14·57·13·0	59	00:28·02S	124:21·96E
7.	HOKADOtr(01/31/86)	17·48·04·4	69	42:13·68N	142:59·76E
8.	CELBEStr(02/01/86)	15·00·35·8	392	02:54·36N	124:04·50E
9.	VANATUzc(02/02/86)	01·44·05·4	31	13:37·56S	166:41·58E
10.	BONINtr(02/03/86)	20·47·35·3	508	27:47·46N	139:33·12E
11.	HINDKUzc(02/04/86)	19·43·56·6	203	36:25·56N	70:41·76E
12.	AFGHANpk(02/11/86)	07·14·24·2	119	36:22·32N	70:54·60E
13.	HONSHUpk(02/12/86)	02·59·30·4	30	36:23·04N	141:07·68E
14.	PAPNGUzc(02/12/86)	11·27·45·4	34	06:32·16S	147:25·98E
15.	HALMHApk(02/12/86)	23·02·12·8	135	01:36·24N	127:18·30E
16.	CARSBRzc(02/15/86)	19·56·35·9	10	04:24·72N	62:42·24E
17.	KURILEpk(02/19/86)	10·54·46·2	115	48:34·74N	153:24·90E
18.	PHLPNEzc(02/19/86)	11·40·27·5	77	18:56·70N	121:18·24E
19.	AUSTLAzc(02/24/86)	01·26·58·2	32	12:45·24S	114:36·54E
20.	HALMHApk(02/24/86)	02·31·26·7	118	01:43·74N	127:21·24E
21.	BANDCApk(03/01/86)	16·41·40·6	80	06:18·00S	130:56·94E
22.	KAMCHK(03/02/86)	03·14·41·8	118	51:40·68N	156:56·16E
23.	SOLMONzc(03/06/86)	12·31·24·0	72	07:00·00S	155:46·86E
24.	NEWBRTfb(03/07/86)	02·46·52·0	116	04:59·40S	151:42·60E
25.	HANDUKzc(03/11/86)	23·07·38·2	206	36:28·92N	70:39·60E
26.	BONINzc(03/17/86)	09·18·25·2	476	27:25·26N	139:51·96E
27.	FLOREStr(03/21/86)	21·35·35·8	614	07:27·30S	120:38·76E
28.	HONSHUtr(03/25/86)	04·00·43·3	144	37:15·72N	139:25·38E
29.	BRAZILzc(03/26/86)	22·06·57·6	609	07:07·50S	71:38·28W
30.	NBRTANzc(04/03/86)	07·39·53·9	30	06:20·40S	151:42·90E
31.	KURILEzc(04/05/86)	22·59·09·4	80	44·27·96N	147:51·42E
32.	MINDNOtr(04/09/86)	21·56·19·6	56	09:58·14N	126:09·24E
33.	MOLUCAzc(04/10/86)	02·21·13·3	33	00:58·14S	126:50·28E
34.	MARANAzc(04/13/86)	03·00·20·9	304	17:11·28N	145:37·26E
35.	VANATUzc(04/14/86)	00·25·12·4	33	13:56·76S	166:58·62E
36.	KURILEzc(04/16/86)	12·52·19·7	52	43:52·98N	147:33·96E
37.	TANMBRzc(04/18/86)	08·08·39·2	44	06:00·42S	131:32·82E
38.	WIRIANzc(04/20/86)	07·03·30·8	33	02:22·50S	139:19·08E
39.	CRETE tr(04/27/86)	09·27·02·3	10	34:38·46N	23:24·42E
40.	SUMTRAzc(04/29/86)	13·59·21·8	47	04:24·00N	95:00·24E
41.	RYUKYUtr(04/30/86)	23·14·43·7	44	28:42·66N	130:02·82E
42.	PAPUAGzc(06/24/86)	03·11·30·9	102	04:26·88S	143:56·58E
43.	FLOREStr(06/27/86)	03·09·50·8	229	07:56·82S	122:47·46E
44.	FLORESpk(06/27/86)	03·09·50·8	229	07:56·82S	122:47·46E
45.	TAGYKApk(06/29/86)	21·47·59·6	20	05:20·16S	20:32·34E
46.	MEXICOpk(07/05/86)	22·09·36·9	112	15:28·02N	92:34·92W
47.	CARBRGfb(07/07/86)	16·26·56·6	8	10:23·34N	56:49·92E
48.	MINAHAzc(07/08/86)	04·27·34·6	245	01:59·82N	124:18·30E
49.	MOLUCApk(07/09/86)	23·10·53·1	28	01:54·24N	126:31·50E
50.	SIRANfb(07/12/86)	07·54·26·8	10	29:57·72N	51:34·92E

Table 2. (*continued*)

Sl. No.	Source region	Origin time	Depth (km)	Coordinates	
51.	AFUSSRzc(07/17/86)	15·46·37·0	47	36:40·08N	71:14·82E
52.	FOXIS zc(07/19/86)	04·31·55·9	33	53:21·12N	165:52·92W
53.	KURILEzc(07/19/86)	05·59·36·2	141	47:15·84N	151:07·62E
54.	BURMAtr(07/26/86)	20·24·47·8	27	23:45·18N	94:10·62E
55.	EUSSRpk(07/26/86)	14·46·18·9	310	45:25·32N	137:04·20E
56.	CHINApk(08/06/86)	19·55·15·6	34	29:20·64N	100:54·90W
57.	PHILPNzc(08/09/86)	00·53·12·6	80	14:05·94N	120:20·10E
58.	HALMRAzc(08/10/86)	04·40·49·7	104	01:59·10N	128:16·26E
59.	MOLUCAtr(08/17/86)	15·27·41·2	31	02:16·56N	126:57·54E
60.	BANDASzc(08/19/86)	12·52·41·1	33	04:07:32S	129:19·44E
61.	PHILPNzc(08/19/86)	22·41·35·8	98	12:30·84N	124:28·68E
62.	SIOCENtr(08/20/86)	21·15·46·4	10	01:58·38S	87:05·28E
63.	ROMANAzc(08/30/86)	21·28·35·4	132	45:32.82N	26:18·86E
64.	VOLCNOpk(08/31/86)	09·23·04·7	46	23:02·52N	144:07·20E
65.	KURILEtr(09/01/86)	21·47·35·0	148	46:37·86N	150:00·60E
66.	HALMRAzc(09/09/86)	15·58·22·5	33	00:55·62N	127:56·64E
67.	NBRTANtr(09/11/86)	00·18·25·5	51	05:11·22S	152:26·52E
68.	MOLUCAtr(09/11/86)	17·54·03·0	33	00:28·44N	125:51·72E
69.	HINDKUtr(09/13/86)	14·14·54·3	200	36:26·52N	70:45·96E
70.	SOLMONzc(09/14/86)	20·58·23·1	59	06:28·20S	154:54·96E
71.	ANDREOtr(09/15/86)	06·29·35·8	33	51:33·66N	177:05·10W
72.	MARINAtr(09/16/86)	18·20·17·7	48	19:22·56N	146:18·06E
73.	AFUSSRzc(09/17/86)	12·08·09·4	120	37:17·40N	71:43·80E
74.	AFUSSRtr(09/17/86)	12·08·09·4	120	37:17·40N	71:43·80E
75.	CARBRGfb(09/17/86)	21·25·15·0	10	10:29·82N	56:59·98E
76.	HONSHUzc(09/20/86)	03·04·58·7	75	36:27·24N	140:31·20E
77.	BANDAzc(09/22/86)	16·15·05·8	123	06:42·96S	130:25·62E
78.	BONINzc(09/27/86)	19·38·42·1	30	27:52·02N	142:46·62E
79.	BANDASzc(10/01/86)	13·00·06·3	343	05:34·74S	128:37·02E
80.	MEDRNSpk(10/02/86)	10·12·45·6	46	34:50·76N	28:18·84W
81.	HALMRAtr(10/04/86)	02·00·08·0	106	02:58·92N	128:02·16E
82.	ANDREOzc(10/06/86)	04·21·46·7	43	51:51·78N	176:15·42W
83.	SHONSUtr(10/07/86)	11·40·55·0	400	31:54·42N	137:40·56E
84.	JAVARzc(10/10/86)	17·48·24·6	82	07:29·88S	107:13·98E
85.	HINDKUtr(10/13/86)	16·11·40·4	117	36:04·02N	70:50·88E
86.	HINDKUzc(10/13/86)	16·11·40·4	117	36:04·02N	70:50·88E
87.	HONSHUtr(10/13/86)	21·17·50·9	65	37:06·12N	141:00·66E
88.	BANDASzc(10/17/86)	07·32·51·3	67	05:16·32S	131:25·92E
89.	ANDREOpk(10/18/86)	01·02·52·1	33	51:43·80N	175:17·10W
90.	JAVAzc(10/18/86)	22·09·31·7	643	05:37·86S	109:59·82E
91.	HALMRApk(10/21/86)	21·57·59·4	142	01:32·46N	127:25·44E
92.	SACRUZtr(10/22/86)	08·59·28·8	165	10:34·14S	166:02·40E
93.	EPGNEAzc(10/23/86)	03·54·20·8	127	06:05·82S	146:18·36E
94.	NCHILEpk(10/24/86)	02·42·51·6	51	25:19·14S	70:10·56W
95.	NCHILEzc(10/24/86)	02·42·51·6	51	25:19·14S	70:10·56W
96.	AIRISEpk(10/28/86)	15·11·23·3	10	30:28·26S	60:10·92E
97.	MINDNOfb(10/29/86)	20·11·39·7	72	05:43·32N	125:19·86E

Table 2. (*continued*)

Sl. No.	Source region	Origin time	Depth (km)	Coordinates	
98.	MINDNOzc(10/29/86)	20·11·39·7	72	05:43·32N	125:19·86E
99.	BURMAzc(11/01/86)	05·02·42·4	26	26:54·12N	96:25·50E
100.	MINDNOzc(11/06/86)	02·48·23·6	62	09:00·42N	126:14·40E
101.	ANDREOzc(11/06/86)	18·27·00·1	33	51:28·14N	176:41·04W
102.	MOLUCAfb(11/11/86)	00·02·32·0	79	02:24·84N	126:48·66E
103.	MOLUCAzc(11/11/86)	00·02·32·0	79	02:24·84N	126:48·66E
104.	TAKXJGfb(11/12/86)	10·06·15·3	115	38:27·30N	73:16·68E
105.	TAKXJGzc(11/12/86)	10·06·15·3	115	38:27·30N	73:16·68E
106.	TAIWANtr(11/14/86)	21·20·10·5	34	23:54·06N	121:34·44E
107.	TAIWANzc(11/14/86)	23·04·37·0	33	23:51·96N	121:42·66E
108.	PRUECQfb(11/23/86)	01·39·23·9	106	03:20·52S	77:24·66W
109.	PRUECQzc(11/23/86)	01·39·23·9	106	03:20·52S	77:24·66W
110.	HJAPANzc(11/28/86)	22·29·35·1	41	36:20·70N	141:10·44E
111.	HPAJANpk(11/30/86)	20·15·30·3	37	38:51·18N	141:56·88E
112.	NIBRISpk(12/07/86)	05·40·39·2	215	06:46·98N	95:07·20E
113.	SOLMISfb(12/11/86)	19·56·12·5	61	10:29·28S	160:42·90E
114.	HJAPANfb(12/14/86)	00·11·31·2	352	32:43·62N	137:43·38E
115.	AFUSSRzc(12/17/86)	08·31·30·3	225	36:32·34N	71:07·50E
116.	AFUSSRzc(12/18/86)	07·23·30·0	182	36:34·08N	71:21·18E
117.	ANDREOfb(12/19/86)	13·50·10·3	33	51:31·02N	176:58·62W
118.	ANDREOtr(12/19/86)	13·50·10·3	33	51:31·02N	176:58·62W
119.	TAIWANzc(12/21/86)	02·42·49·0	275	25:31·02N	121:30·42E
120.	MARINAtr(01/01/87)	16·25·34·1	74	02:42·90S	138:21·78E
121.	MARINAzc(01/01/87)	16·25·34·1	74	02:42·90S	138:21·78E
122.	CHINAzc(01/05/87)	22·52·46·5	17	41:57·84N	81:19·14E
123.	TAIWANfb(01/06/87)	05·07·48·1	38	23:58·56N	121:43·74E
124.	TAIWANzc(01/06/87)	05·07·48·1	38	23:58·56N	121:43·74E
125.	NIRELRfb(01/08/87)	19·48·55·4	44	04:44·16S	153:06·30E
126.	NIRELRzc(01/08/87)	19·48·55·4	44	04:44·16S	153:06·30E
127.	HONSHUzc(01/09/87)	06·14·44·8	68	39:53·70N	141:40·62E
128.	HOKKAIzc(01/14/87)	11·03·48·7	102	42:33·90N	142:51·00E
129.	KAMCHTzc(01/19/87)	06·47·43·0	42	54:44·64N	163:16·62E
130.	NEPALzc(01/19/87)	07·46·24·4	33	28:23·10N	83:40·92E
131.	NEPALzc(01/19/87)	08·12·05·8	33	28:14·58N	83:34·32E
132.	MARINAzc(01/21/87)	11·26·36·6	118	20:36·48N	144:53·10E
133.	MOLUCAfb(01/23/87)	17·51·09·2	72	01:38·76N	126:31·86E
134.	MOLUCAzc(01/23/87)	17·51·09·2	72	01:38·76N	126:31·86E
135.	HINDKUtr(05/05/87)	15·40·47·5	208	36:28·80N	70:40·38E
136.	KAZAKHzc(05/06/87)	04·02·05·6	1	49:49·80N	78:07·50E
137.	ANDREOzc(05/06/87)	04·06·14·1	20	51:16·32N	179:53·88W
138.	NBRITNzc(05/06/87)	12·39·49·1	20	05:42·90S	152:39·36E
139.	EUSSRzc(05/07/87)	03·05·49·1	430	46:44·16N	139:13·92E
140.	BALIStr(05/10/87)	00·37·10·0	42	07:44·22S	115:59·82E
141.	TALAUDzc(05/11/87)	09·59·34·1	94	04:28·20N	127:42·54E
142.	MINDNOzc(05/12/87)	01·30·25·0	25	07:05·40N	126:42·06E
143.	ICELNDzc(05/25/87)	11·31·54·3	8	63:51·00N	19:43·68W
144.	BANDASzc(05/30/87)	16·54·04·7	138	06:03·84S	130:31·08E

Table 2. (*continued*)

Sl. No.	Source region	Origin time	Depth (km)	Coordinates	
145.	KURILEzc(05/30/87)	17·19·00·1	53	44:40·14N	150:17·34E
146.	MINHSAzc(05/31/87)	18·32·17·0	79	00:44·88N	121:56·46E
147.	ANDREOzc(06/01/87)	00·15·14·3	33	51:32·40N	177:30·54W
148.	CHINAzc(06/05/87)	04·59·58·3	1	41:35·04N	88:44·22E
149.	PHILIPtr(06/05/87)	21·25·11·2	45	05:22·86N	127:32·04E
150.	PHILIPtr(06/05/87)	22·00·03·1	47	05:15·90N	127:30.78E
151.	PHILIPzc(06/07/87)	05·49·43·6	15	20:25·74N	121:21·96E
152.	KURILEfb(06/13/87)	14·00·39·3	42	44:40·26N	150:23·52E
153.	TALAUDtr(06/15/87)	06·31·44·7	136	03:54·94N	125:56·94E
154.	KAZAKHzc(06/20/87)	00·53·04·8	1	49:54·78N	78:44·10E
155.	IRIANtr(06/27/87)	00·17·04·6	21	02:09·84S	138:10·20E
156.	KYUSHUzc(07/03/87)	10·10·43·7	168	31:11·76N	130:19·32E
157.	CHAGOStr(07/03/87)	18·03·59·7	26	06:47·16S	72:14·82E
158.	ALEUTNpk(07/05/87)	09·23·00·0	33	51:29·16N	174:39·60E
159.	ALEUTNpk(07/06/87)	00·03·25·6	33	51:30·48N	174:43·26E
160.	TALAUDpk(07/07/87)	10·36·03·7	70	05:24·18N	125:01·68E
161.	KURILEzc(07/08/87)	22·56·02·7	152	46:26·22N	149:33·48E
162.	TALAUDzc(07/14/87)	04·31·23·0	33	03:50·04N	126:32·52E
163.	OKHTSKzc(07/14/87)	23·46·03·5	591	49:37·86N	147:49·68E
164.	HONSHUtr(07/16/87)	05·46·29·5	310	33:03·54N	138:05·76E
165.	KAZAKHpk(07/17/87)	01·17·07·0	1	49:47·94N	78:06·60E
166.	TALAUDtr(07/22/87)	08·03·17·2	51	04:03·06N	125:34·92E
167.	MINHASfb(07/31/87)	00·27·32·0	167	00:10·50N	123:36·30E
168.	KAZAKHzc(08/02/87)	00·58·06·8	1	49:52·80N	78:55·02E

Note: Code after event name indicates pick: fb, first break; zc, zero crossing; pk pea
tr, trough. There are a few multiple readings in the data set.

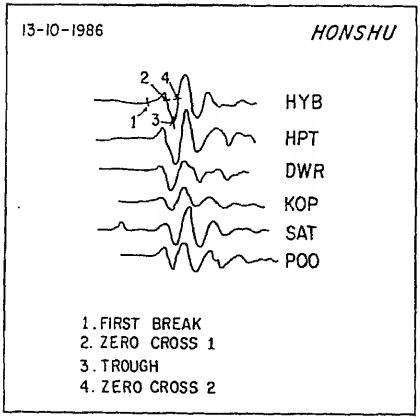

Figure 2. Seismograms showing how arrival-time are made.

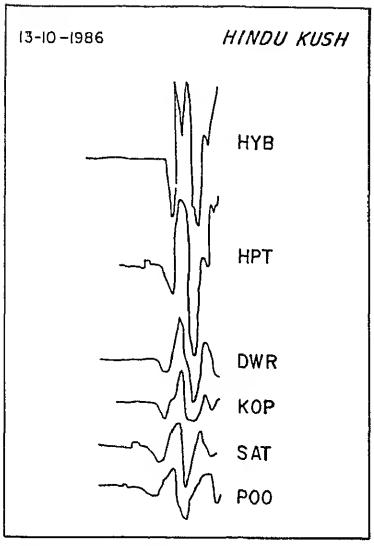

Figure 3. Signal attenuation and signal-shape changes observed at some of the stations.

station because of its location on Precambrian granite outside the DVP. A comparison of residuals at HYB with those at Srisailam—a station also on Precambrian granite about 150 km south-southeast of HYB—supports our assumptions that stations on the Precambrian granite are "normal" compared to those over the Deccan basalts.

For each station, the data were grouped into four categories according to epicentral distances: all distances, closer than 30°, 30° to 70° and beyond 70°. We first examine the data from Poona (POO) where the largest data set is available (figure 4). Note that the range of variation of residuals is about 2 s varying from 1 s in the north to -1 s in the east (figure 4a). The relative residuals also depend on the epicentral distance and which determines the angle of emergence at the seismic station. Observe that for distances $<30°$ the relative residuals are mostly positive (about $+1$ s) for all azimuths (figure 4b), with strong azimuthal variation occurring in the 30° to 70° range (figure 4c) and a less pronounced but still clear variation occurring for distances $>70°$ (figure 4d). Comparison of the relative residuals along the east-southeasterly profile from BHA, the westernmost station, to GUL on the eastern margin of DVP shows the pattern of residuals at BHA to be quite similar to that at POO but with larger variations from $+1{\cdot}5$ s to $-1{\cdot}8$ s (figure 5). Relative residuals at UJN, SOP and GUL show a similar azimuthal variation, but with a progressive decrease in magnitude towards HYB (figure 5). GUL, closest to HYB, shows the smallest residuals and is a key station to substantiate our argument that the strong azimuthal variation observed at other stations are associated with some anomaly in the deep structure beneath the DVP. The relative residuals along the southeasterly profile from DHL to AUB, BIR and LTR (figure 6) also show a decreasing azimuthal variation towards the eastern margin of the DVP, though LTR has five strong negative residuals in the 40–100° azimuth range and 30–70° distance range, cautioning against simplified inferences. Note that the residuals at these stations for distances $<30°$ are generally negative,

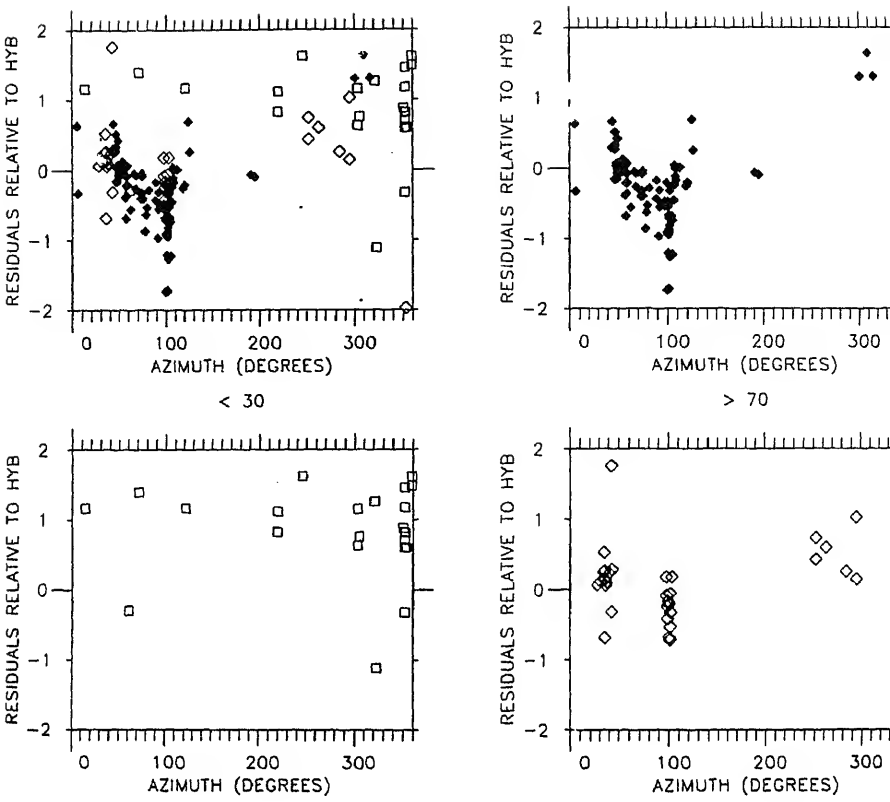

Figure 4. Relative residuals at POO with respect to HYB plotted as a function of azi of arrival. **(a)** All distances; hollow squares represent events at distances $<30°$; solid diam represent events in the distance range of 30–70°; hollow diamonds represent even distances $>70°$. **(b)** Events at distances $<30°$. (c) Events in the distance range 30 (d) Events at distances $>70°$.

unlike those observed at other stations. The southerly profile, comprised of stat SAT, KOP and DWR (figure 7) shows a behaviour similar to BHA and POO (fig 4 and 5). One surprise is at the southernmost station HPT (figure 7), south of C (figure 5) but outside the DVP. This station behaves similar to the western stat implying that the velocity anomaly responsible for the observed azimuthal variat extends even outside the DVP to the southeast.

Note the abrupt transition of residuals from negative values to positive near 100° azimuth range observed at all stations in the experimental area. In order to whether this feature in the azimuthal pattern of residuals could be due to a pos residual bias at HYB, we examined the relative residual patterns using the ave event residual as reference and found that no such bias exists. The relative resid thus calculated retained this feature at all these stations including Hyderabad, impl that it could not have arisen from any fortuitous cause related to the choic Hyderabad as a reference station. We feel that this sharp transition in the resi patterns reflects a sharp velocity transition in the upper mantle outside the re being modelled.

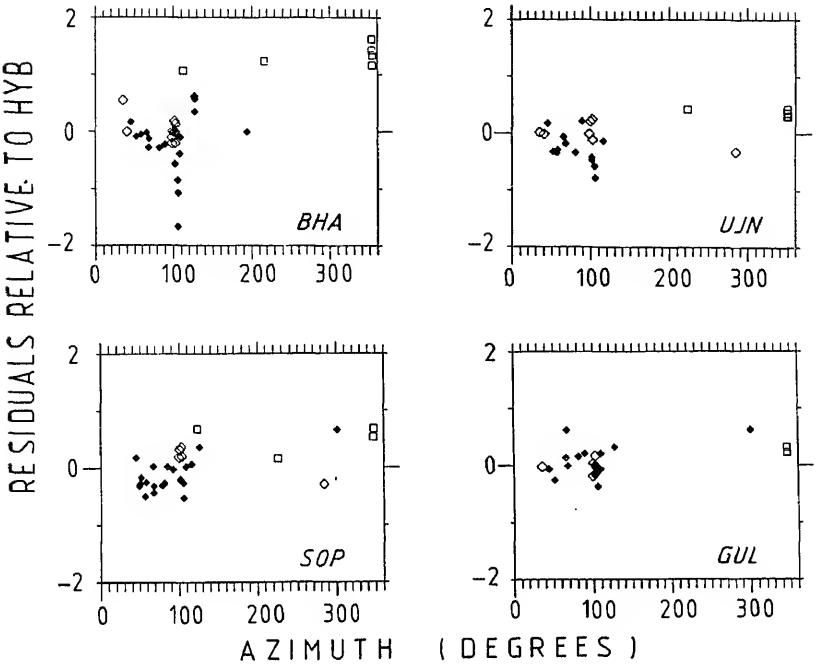

Figure 5. Relative residuals at BHA, UJN, SOP and GUL.

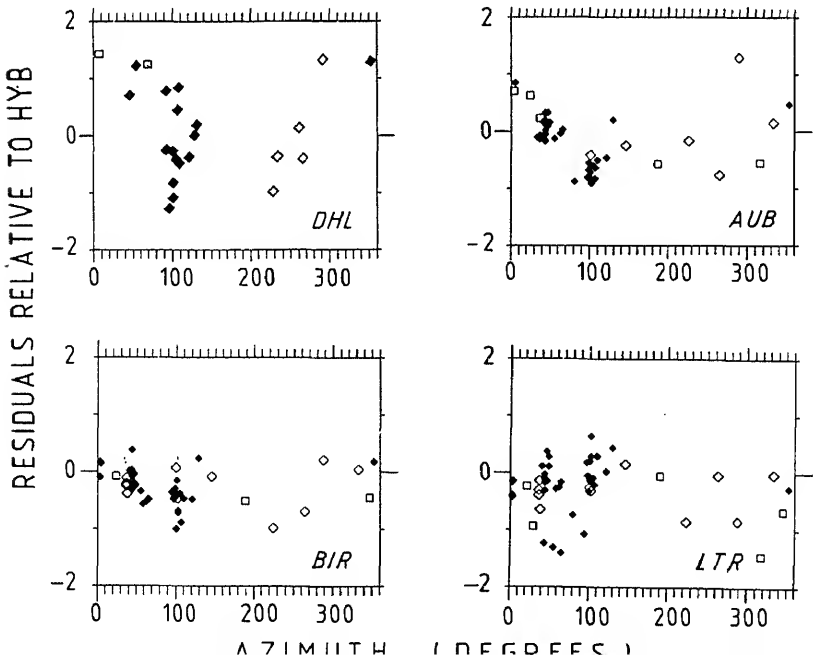

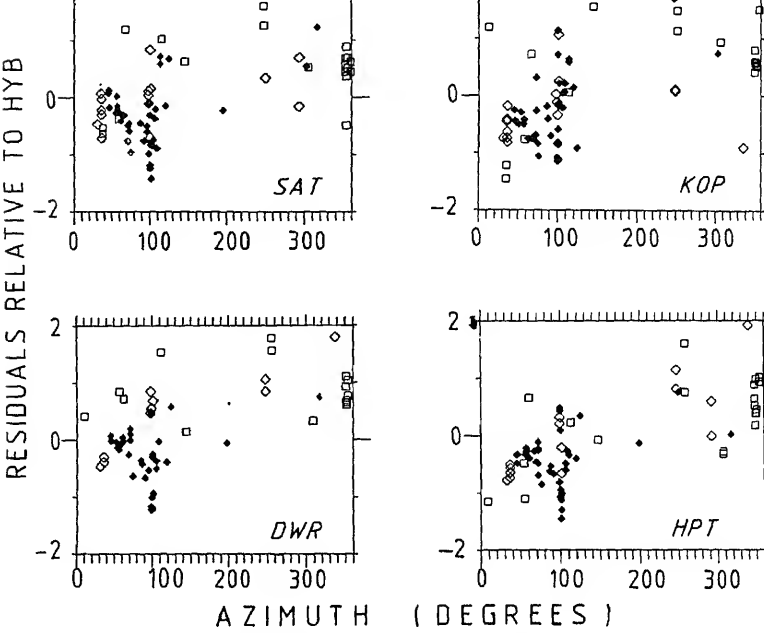

Figure 7. Relative residuals at SAT, KOP, DWR and HPT.

7. Analysis using the simple ray plotting technique

In this section we use simple ray-plotting techniques to show that the azimutha spatial variation of the relative residuals discussed above can be explained o terms of velocity perturbations in the upper mantle of the DVP region. But fi evaluate the possible contributions that surficial and crustal layers can make residuals.

Variation in the thickness of basalt cover which attains a maximum of about in the western part, can given rise to a maximum relative residual of +0·04 s assu the *P*-wave velocity of the Deccan basalts and the basement rock to be 4·8 and 6·0 km/s respectively (Kaila 1981; Kaila 1982). Further, even a 1·0 km low-velocity sedimentary layer with a velocity of 4·0 km/s underlying the D Traps, such as that found by Kaila *et al* (1981) in the Saurashtra Peninsul contribute a residual of less than 0·1 s. This is even lower than the noise level i experiment.

7.1 *Effect of the variation of crustal thickness*

The sub-trappean crustal model in the Koyna area of Deccan basalts has approximated by three layers of 10, 15 and 15 km thickness with average velo of 5·7, 6·5 and 7·0 km/s respectively (Kaila *et al* 1982). Variation in the thickn any of these layers by as much as 5 km will give rise to a total residual of only 0·1 s. Crustal models of the Koyna region show that its thickness varies from 3 near the coast to 39 km near Koyna (Kaila 1982). Even if we take the velocity co

across the Moho to be about 1·0 km/s this order of variation in crustal thickness will only cause the arrivals to be 0·2 s earlier at the western stations compared with those at the eastern stations. The effect is approximately the same if the thinning of the crust is distributed over all the three layers.

It is thus clear that possible variations in the thicknesses of basalts, and sub-trappean sedimentary layers, if present, as well as those of the upper or of the whole crust can at the most account for only +0·2 s of the observed spatial variation of the relative residuals. The azimuthal variation cannot be accounted for by such shallow features at all. We therefore conclude that most of the observed residual pattern can only be accounted for by deep upper mantle features.

7.2 *Ray plotting analysis*

To delineate qualitatively the zones of anomalous velocity structure responsible for the large azimuthally varying observed residuals, we first used a simple ray-tracing procedure similar to that used by Iyer *et al* (1981). From a knowledge of the emergent angles of seismic rays at various stations, inferred from the depth and epicentral distances of the respective teleseisms, rays are projected backwards from the various stations for each teleseism. The corresponding relative residuals are then projected on flat layers at three different depths (100, 200 and 300 km). If the observed residuals are due to the presence of an anomalous body rather than a random velocity perturbation, the whole set of projected residuals would be expected to show coherent signs and magnitudes so that they can be contoured when the depth chosen for the projection is correct. After considerable experimentation using data corresponding to $\Delta > 30°$, we found that the maximum coherence was achieved for projection at a depth of 200 km. Also, some form of subjective averaging was needed to reduce too many overlapping numbers. Figure 8 shows the result of this projection to 200 km depth using the above constraints. The main inference from this figure is that it outlines, albeit broadly, a 200-km wide north-south trending region of negative residuals of magnitude >0·5 s extending from AUB in the north and probably continuing south beyond HPT. Since better constraints on the region of anomalous high velocity is provided by inversion of residuals which is presented below, we do not want to overinterpret this rather crude modelling of our data. However, we would like to state that this analysis, though not providing adequate constraints to delineate the anomalous structure beneath the Deccan Traps, suggests that the observed residuals are best interpreted in terms of a heterogeneous structure in the upper mantle consisting of higher-than-normal velocities beneath the south-central part of the DVP and lower-than-normal velocities in the west-central part.

8. Tomographic results

Ideally, to obtain well-constrained tomographic models, we need a set of teleseismic arrivals from events that are fairly well-distributed in various azimuths and distance ranges. Further, the arrival-time readings should be of high quality with minimal scatter, and the data set should be homogeneous and simultaneous at all stations in the seismic network. Though our experiment does not satisfy any of these criteria strictly, the similarity of inverted models for varying block and layer configurations,

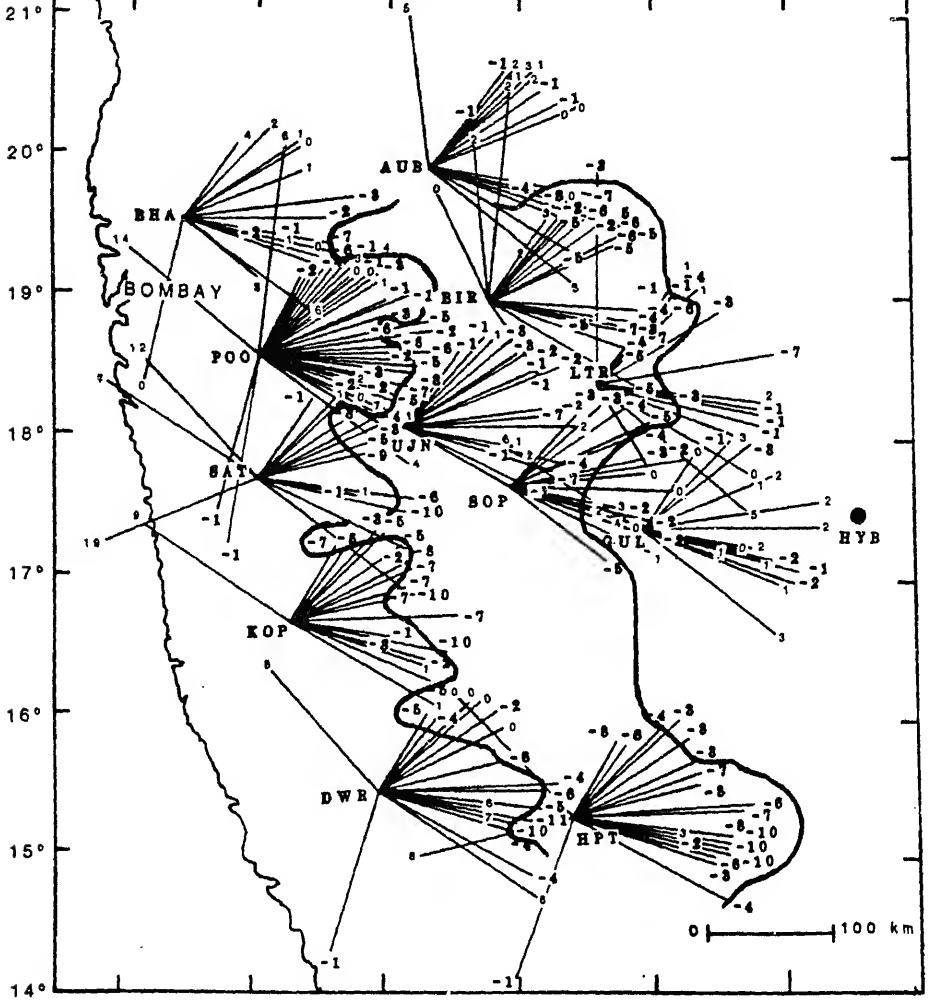

Figure 8. Selected averaged relative residuals projected at 200-km depth.

suggests that they correctly resolve first-order features of the anomalous three-dimensional *P*-velocity structure beneath the DVP. Also, these models agree with the qualitative inference derived from the azimuthal patterns of residuals using the ray-plotting approach discussed above. We performed numerous ACH inversions for a variety of layered models. The dimensions of the block were 200 km in the east-west direction and 150 km in the north-south direction. We use mantle velocities from Herrin's (1968b) earth model and the crustal velocity of 6·45 km/s (Kaila 1982). For each inversion the respective resolution matrix and standard errors were studied with a view to assessing the figure of merit of the solution. Note that ACH inversions use relative residuals based on the average of all available readings over the network for each event. Hence no specific reference stations were used.

9. Models

Although a large number of models were used for inversion, description of a few of these models together with the corresponding data variance improvements are given in table 3. The main feature of the models, that is an anomalous high-velocity zone, appears to be significant only at sub-crustal depths. In order to constrain the upper boundary of the anomalous zone, we first analyse a series of two-layer models using all available data. These are shown in figure 9. The numbers indicate velocity perturbations, positive numbers denoting higher-than-normal velocities and negative numbers

Table 3. Description of models.

No. of Layers	Layer thicknesses (km)	Variance improvement (%)
2	40, 60	16·0
2	40, 160	27·0
2	40 260	30·0
2	40, 360	31·0
3	100, 300, 200	53·0
3	150, 250, 200	63·0
4	40, 160, 200, 200	46·0

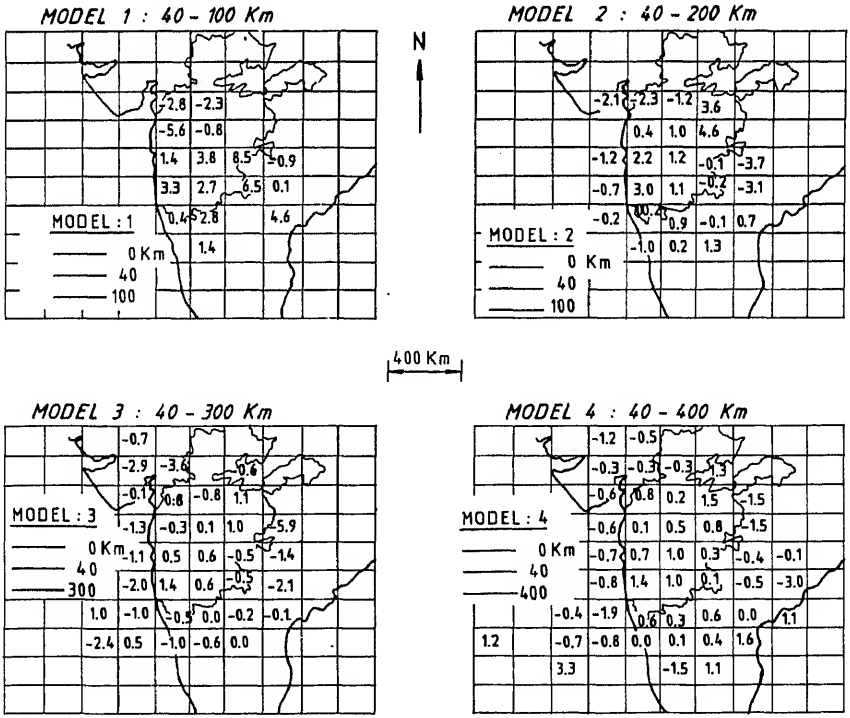

Figure 9. Second layer of 2-layer tomographic models derived using data at all available distances. Numbers indicate percentage velocity perturbations.

indicating lower-than-normal velocities. Note that all these models invariably show the presence of a high velocity region within the DVP surrounded by a relatively low velocity region. The magnitude and lateral extent of the velocity perturbations vary with the model. Although the anomalies are reflected in all the models presented below, the first one with a layer thickness of 40–100 km shows only a small variance improvement (16%) compared with others whose variance improvement ranges from 26–32%, suggesting that the high velocity anomaly (upto 4%) is confined to a depth range of 100–400 km (table 3). To further constrain the anomalous domain we then analysed a large set of three-layer models. Two of these (with variance improvements 53% and 63% respectively) are shown in figure 10, which show that the high velocity anomaly decreases both in magnitude and areal extent for the layer 0–100 km compared with that for the layer 0–150 km. Significantly, the anomaly remains unaltered for depths of 400 km. In order to further test that the anomalies exposed by the above models are not an artefact of the choice of the number of layers, we also tested a suite of 4 layered models for inverting the travel time residuals. Figure 11 and table 4 show the model with various layers lying between 0 and 40 km, 40 and 200 km, 200 and 400 km and 400 and 600 km (variance improvement 46%). These models show that the high velocity anomaly is confined to layers 2 and 3 in the depth range of 40–400 km. As the depth to the top of the anomaly is reasonably well-constrained by the models (figure 10) described earlier we conclude that the high velocity anomaly coinciding with the southern two-thirds of the DVP exists in the depth range of 100–400 km. The 400–600 km layer is characterized by the presence of a very diffused low velocity and is distinct from the overlying layers. Table 4 shows

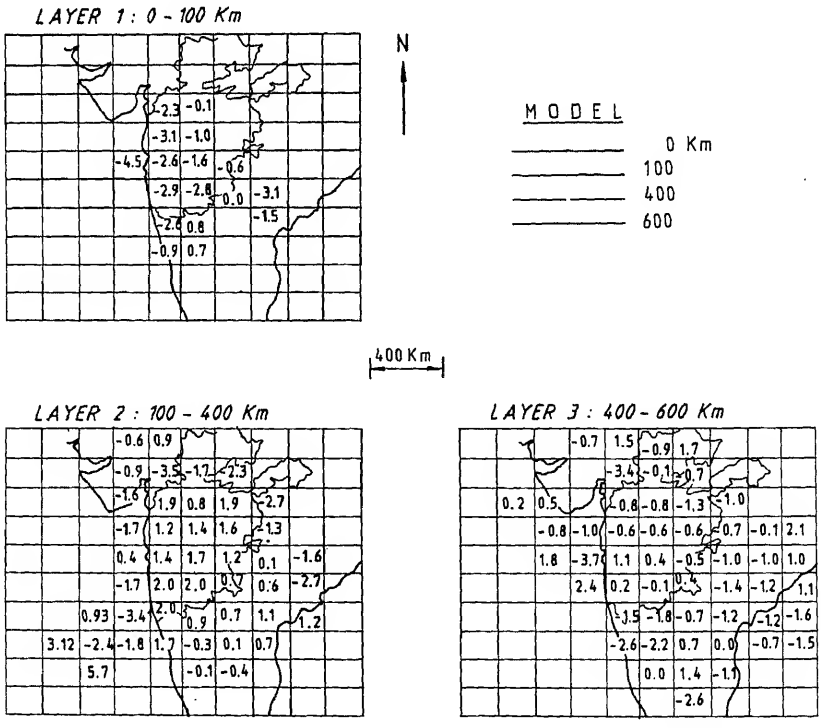

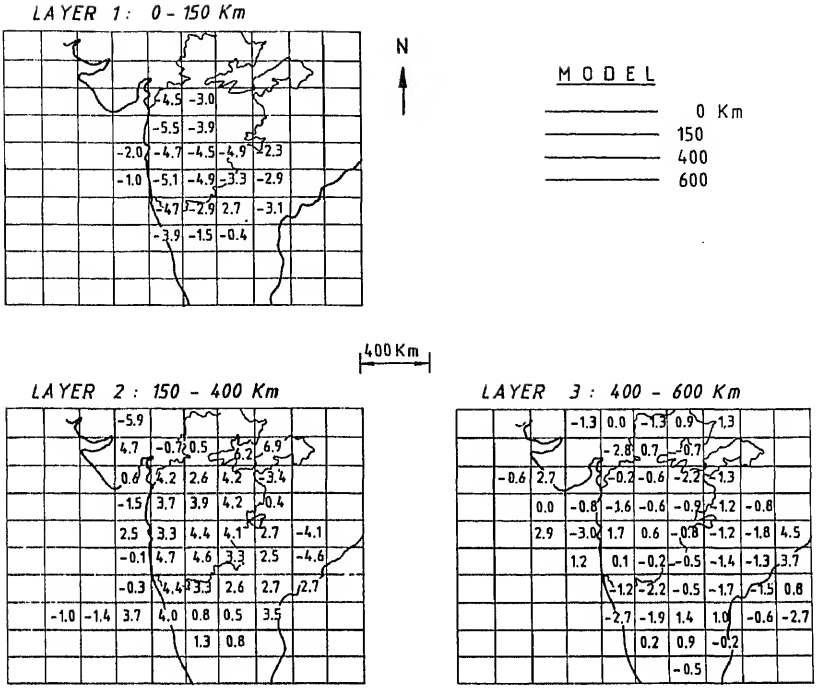

Figure 10b. Velocity perturbations in the three layers (0–150, 150–400, 400–600 km).

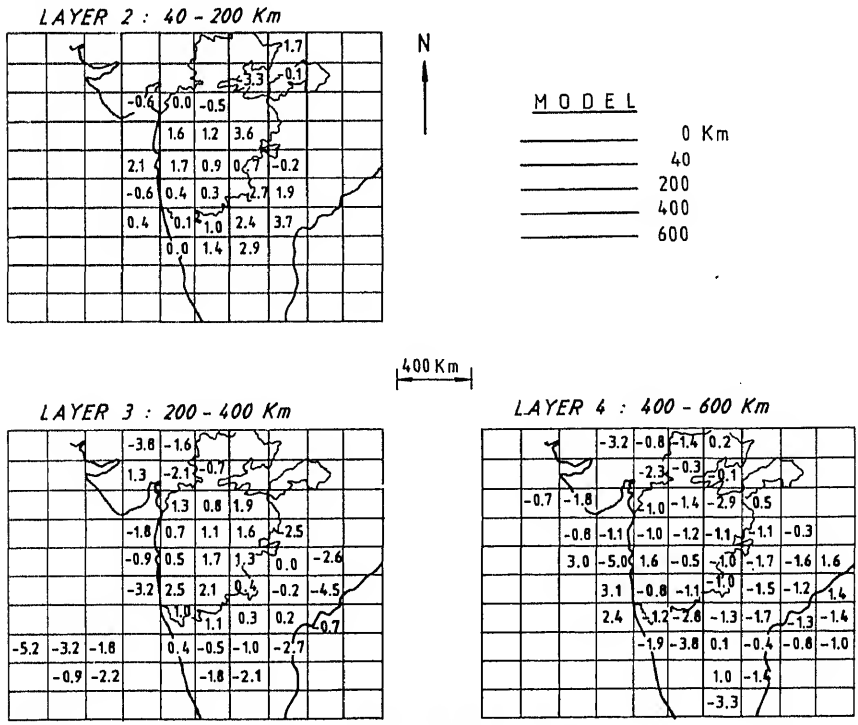

Figure 11. Velocity perturbations in the three sub-crustal layers of four-layer models.

Table 4. Full three-dimensional inversion for the four-layer model.

—up=N OW—

Layer 1

HYB 1	DHL 2	AUB 3	BIR 4	LTR 5	POO 6	GUL 7	SOP 8		
−3·16	−2·08	−1·81	−0·66	−2·37	−5·10	−7·14	−0·12		
182	17	39	41	46	112	29	36		
0·9114	0·9188	0·9421	0·9539	0·9543	0·9464	0·9194	0·9421		
2·55	2·76	2·16	1·81	1·78	1·90	2·51	2·08		
UJN 9	BHA 10	SAT 11	KOP 12	DWR 13	HPT 14	SLM 15	MPU 16		
−2·68	−5·57	−2·63	−1·10	−2·20	1·56	−8·67	−7·25		
30	27	75	73	59	73	12	21		
0·9522	0·9159	0·9369	0·9331	0·9143	0·8996	0·7747	0·9450		
1·80	2·56	2·04	2·05	2·43	2·71	4·15	2·02		

Layer 2

17	18	19	20	21	22	23	24	25	26
0	0	1	1	0	0	2	1·66 5 0·9804 1·50	3	0
27	28	29	30	31	32	33	34	35	36
0	0	0	3	2	1	−3·30 5 0·9557 2·19	−0·12 5 0·9657 1·94	2	0
37	38	39	40	41	42	43	44	45	46
0	0	1	−0·61 6 0·9765 1·53	0·00 22 0·9859 1·20	−0·54 13 0·9772 1·52	3	3	0	0
47	48	49	50	51	52	53	54	55	56
0	0	0	3	1·58 58 0·9804	1·22 78 0·9822	3·55 6 0·9691	3	0	1

57	58	59	60	61	62	63	64	65	66
			2·08	1·72	0·88	0·65	−0·28		
0	0	0	11	166	118	49	21	2	0
			0·9652	0·9916	0·9942	0·9913	0·9831		
			1·95	0·86	0·70	0·91	1·27		
67	68	69	70	71	72	73	74	75	76
			−0·55	0·44	0·32	2·69	1·91		
0	0	1	9	117	80	204	136	0	0
			0·9678	0·9908	0·9927	0·9891	0·9835		
			1·80	0·87	0·80	0·99	1·23		
77	78	79	80	81	82	83	84	85	86
			0·38	0·13	1·01	2·40	3·71		
0	0	4	6	66	93	22	15	0	0
			0·9718	0·9893	0·9879	0·9838	0·9689		
			1·73	0·94	1·01	1·28	1·60		
87	88	89	90	91	92	93	94	95	96
				−0·04	1·43	2·91			
0	0	0	2	7	66	28	0	0	0
				0·9759	0·9815	0·9752			
				1·53	1·29	1·54			
97	98	99	100	101	102	103	104	105	106
0	0	0	0	0	2	2	0	0	0
107	108	109	110	111	112	113	114	115	116
0	0	0	0	0	0	0	0	0	0

Layer 3

117	118	119	120	121	122	123	124	125	126
			−3·78	−1·64					
0	1	4	16	6	2	0	1	0	0
			0·9828	0·9726					
			1·40	1·77					

(continued)

Table 4. (*continued*)

127	128	129	130	131	132	133	134	135
			1·28	−2·14	−0·71			
0	0	1	15	29	16	3	0	0
			0·9755	0·9844	0·9903			
			1·67	1·33	1·05			
137	138	139	140	141	142	143	144	145
				1·32	0·75	1·92		
0	0	2	0	39	40	17	4	0
				0·9926	0·9916	0·9894		
				0·91	0·98	1·10		
147	148	149	150	151	152	153	154	155
			−1·82	0·67	1·13	1·60	−2·49	
0	0	4	7	62	102	51	7	2
			0·8625	0·9940	0·9956	0·9944	0·9920	
			2·76	0·82	0·69	0·79	0·96	
157	158	159	160	161	162	163	164	165
			−0·90	0·52	1·72	1·29	−0·04	−2·64
0	0	2	8	115	135	86	59	9
			0·9405	0·9940	0·9953	0·9955	0·9949	0·9796
			2·11	0·81	0·70	0·70	0·75	1·50
167	168	169	170	171	172	173	174	175
			−3·19	2·50	2·12	0·35	−0·17	−4·51
0	0	1	7	45	103	75	132	41
			0·9784	0·9933	0·9952	0·9947	0·9943	0·9657
			1·55	0·86	0·71	0·76	0·80	1·89
177	178	179	180	181	182	183	184	185

−0·52	−0·32	−1·78		0·37	−0·46	−1·02	−2·72		
5	5	8	4	8	31	41	12	3	2
0·9712	0·9271	0·9619		0·9824	0·9868	0·9879	0·9556		
1·73	2·68	2·07		1·39	1·21	1·15	2·11		
197	198	199	200	201	202	203	204	205	206
	−0·90	2·15			−1·75	−2·08			
2	6	5	1	2	5	7	4	1	0
					0·9842	0·9466			
					1·33	2·41			
207	208	209	210	211	212	213	214	215	216
0	3	1	0	0	0	4	0	0	0

Layer 4

217	218	219	220	221	222	223	224	225	226
			−3·22	−0·80	−1·37	0·17			
0	0	1	6	28	22	6	3	1	1
			0·9694	0·9887	0·9927	0·9665			
			1·86	1·13	0·92	−0·25			
227	228	229	230	231	232	233	234	235	236
				−2·33	−0·32	−0·14			
4	2	0	1	24	25	15	2	3	0
				0·9895	0·9944	0·9864			
				1·10	0·80	1·26			
237	238	239	240	241	242	243	244	245	246
	−0·69	−1·77		−0·97	−1·36	−2·85	0·47		
2	6	5	1	19	42	30	8	3	4
	0·9773	0·6567		0·9914	0·9954	0·9953	0·9775		
	1·58	4·30		0·99	0·71	0·73	1·62		
247	248	249	250	251	252	253	254	255	256
		−0·78	−1·10	−0·99	−1·24	−1·12	−1·17	−0·32	

(*continued*)

Table 4. (*continued*)

0	2	9	6	19	74	66	32	26	4
		0·8991	0·9581	0·9943	0·9966	0·9967	0·9944	0·9885	
		2·56	2·15	0·80	0·60	0·60	0·80	1·15	
257	258	259	260	261	262	263	264	265	266
		3·03	−5·01	1·62	−0·50	−1·05	−1·72	−1·61	1·62
0	0	8	12	20	87	80	73	42	7
		0·9716	0·9770	0·9906	0·9958	0·9966	0·9970	0·9956	0·9733
		1·78	1·61	1·03	0·67	0·61	0·58	0·70	1·71
267	268	269	270	271	272	273	274	275	276
			3·12	−0·83	−1·09	−1·04	−1·53	−1·16	1·37
0	0	0	5	9	75	117	73	73	11
			0·9434	0·9898	0·9953	0·9968	0·9966	0·9935	0·9635
			2·51	1·08	0·72	0·58	0·62	0·86	1·97
277	278	279	280	281	282	283	284	285	286
			2·39	−1·17	−2·86	−1·32	−1·71	−1·26	−1·41
0	0	4	5	7	37	64	36	50	25
			0·9797	0·9791	0·9912	0·9956	0·9955	0·9950	0·9404
			1·53	1·55	0·99	0·70	0·71	0·76	2·52
287	288	289	290	291	292	293	294	295	296
				−1·91	−3·84	0·08	−0·45	−0·79	−1·01
0	2	3	3	6	12	32	34	12	8
				0·9713	0·9764	0·9931	0·9929	0·9564	0·9159
				1·80	1·64	0·88	0·90	1·76	2·96
297	298	299	300	301	302	303	304	305	306
						0·99	−1·36		
2	2	0	3	3	4	9	6	3	4
						0·9832	0·9837		
						1·39	1·36		
307	308	309	310	311	312	313	314	315	316
						−3·34			
0	0	1	1	3	3	5	2	4	2
						0·9724			

e diagonal elements of the resolution matrix along with the standard errors for this layer model.

). Interpretation

xistence of large-scale velocity anomalies in the upper mantle no longer evokes any rprise. Regional studies of one-dimensional velocity structure using travel-times, nthetic seismograms, and surface-wave dispersion, show that heterogeneous ructure of the upper mantle is a rule rather than an exception in almost any region here observations are available. Teleseismic-residual studies show that velocity nomalies with dimensions of a few tens to a few hundreds of kilometers exist in the ust and upper mantle in North America and also in many other regions of the orld (Aki 1982; Iyer 1984, 1988a, b; Thurber and Aki 1987; Iyer and Hitchcock 988). In general, low-velocity anomalies are easier to interpret than high-velocity nomalies as the former seem to be generally associated with regions of young olcanism or recent orogeny. Some typical examples are: the Yellowstone hot spot yer *et al* 1981); Rio Grande Rift (Parker *et al* 1984); Imperial Valley Spreading Centre Humphreys *et al* 1984); Eastern U.S. (Taylor and Toksoz 1979); the Rhinegraben Raikes and Bonjer 1983); and the Tarbela Area of Lesser Himalaya (Menke 1977). Higher-than-normal velocities, invariably found in active subduction zones and aleo-subduction zones are also reasonably well understood as they delineate ubducting plates (for e.g., Japan: Hirahara 1981; Carapathian Arc: Romania: Oncescu *al* 1984). Other high-velocity anomalies, not so well understood, are found in the pper mantle beneath the Baltic Shield (Husebye and Hovland 1982); Eastern Senegal, Vest Africa (Dorbath *et al* 1983); the Alps (Baer 1980); the North China Basin hedlock and Roecker 1987); the Timber Mountain Caldera Complex, Nevada (Evans nd Oliver 1987); and the Southern Sierra Nevada, California (Humphreys *et al* 1984; Humphreys 1987), to name a few. Humphreys (1987) interprets the vertical, tongue-haped, high-velocity anomaly extending to depths of 300–400 km in Sierra Nevada, s representing a descending sub-crustal lithosphere caused by small-scale convection. vailable case histories on large-scale high-velocity anomalies, though similar in size nd velocity contrast, are simply too few to allow any detailed comparisons with the nomaly which we have delineated beneath the DVP.

A fundamental question to be addressed regarding the DVP anomaly is the llowing. Is the anomaly at all related to the Deccan volcanism or is it simply an ntegral part of the architecture of the upper mantle of the Indian shield? There is nough evidence from global and continental scale geophysical data to show that old ontinents are indeed far from being homogeneous in their deep crust and upper antle structure. Our modelling results lead to startling revelations indicating the resence of an anomalously thick high-velocity region beneath the DVP. The presence f such an anomaly at depths much greater than the conventionally accepted plate hickness (of about 100–200 km) could be best explained in the light of the concept f continental tectosphere (Jordan 1975, 1979a, b) and stabilization of cratons (Pollack 986). The existence of lithospheric roots to depths as great as 400 km has been nferred earlier in Western North America, Superior Province of Canada and South frica based on petrological, geothermal and seismological investigations (Grand and Helmberger 1984; Pollack 1986; Lam and Jordan 1987; Silver and Chan 1988). The

(west to east and north to south) taken from the 5 mgal contour Bouguer gravity anomaly map of India. These indicate the presence of a long wavelength, 35 mgal gravity low present over the region of high-velocity anomaly. A preliminary inversion of the data delineates the lower density region roughly lying within the high velocity anomalous region in the depth range of 100–300 km, with a density contrast of about −0·006 to −0·013 grams per cc (D Srinagesh, personal communication).

The other line of evidence is from *S*-wave residuals at POO relative to HYB taken from ISC catalogues (figure 12). In spite of the poor quality of data and consequent high scatter, it is quite obvious that we see an azimuthal pattern broadly similar to that shown by *P*-wave residuals at POO. The *S*-residuals are about three times as large as the corresponding *P*-wave residuals shown alongside for comparison. Shear wave structure beneath the DVP delineated by Montagner (1986) using surface wave data also reveals the existence of a high-velocity anomalous zone in the depth range of 85–250 km. However, the continuation of this anomaly beyond 250 km depth is not observed due to data constraints in the surface wave study.

11. Source of Deccan basalts

Let us now consider the question of the source of Deccan basalts in the light of the existence of a deep continental root under this region, which must have acquired a coherent stable structure long before the Gondwanaland break-up considering that the craton came into existence earlier than at least 2·5 billion years. The formation of tectosphere due to the depletion of volatiles which elevates the solidus, renders the upper mantle region more resistant to subsequent melting. Such stable regions are observed to have normal shield heat flow values (Pollack 1986). This is in conformity with the observed normal heat flow over DVP (Gupta and Gaur 1984). The very presence of the tectosphere beneath the DVP would therefore inhibit the development of large scale perforations which are believed to have been responsible for the extrusion of such extensive flood basalts, implying the absence of their source region directly beneath the DVP. On the other hand, it is significant to note that in all the models, the per cent velocity anomaly beneath the westernmost part of the DVP in the depth range of 40–200 km is relatively less than that observed in other parts. This is also reflected in the results of surface wave study (Nataf *et al* 1984) showing a regional low shear wave velocity enveloping the entire Arabian Sea extending from the east coast of Africa to the west coat of India. However, it is significant to observe that the above low velocity zone is confined to the west of our westernmost profile 2.

Also, recent studies of major and trace element abundances and inter-element ratios as well as Sr isotopic ratios in selected samples combined with extensive field checks in the western parts of the DVP show that the flow sections do not correspond to a classical layer cake-sequence. Instead, they appear to be comprised of a sequence of thicker and older formations in the north which become thinner in the south and are superceded by southward thickening of younger ones that taper out further southwards. This interlocking sequence strongly suggests that the flows are derived

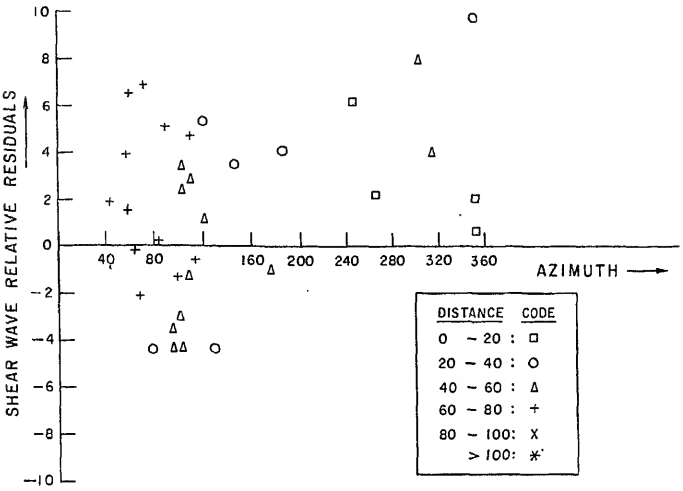

RELATIVE SHEAR WAVE TRAVEL TIME RESIDUALS
AT POONA WITH RESPECT TO HYDERABAD

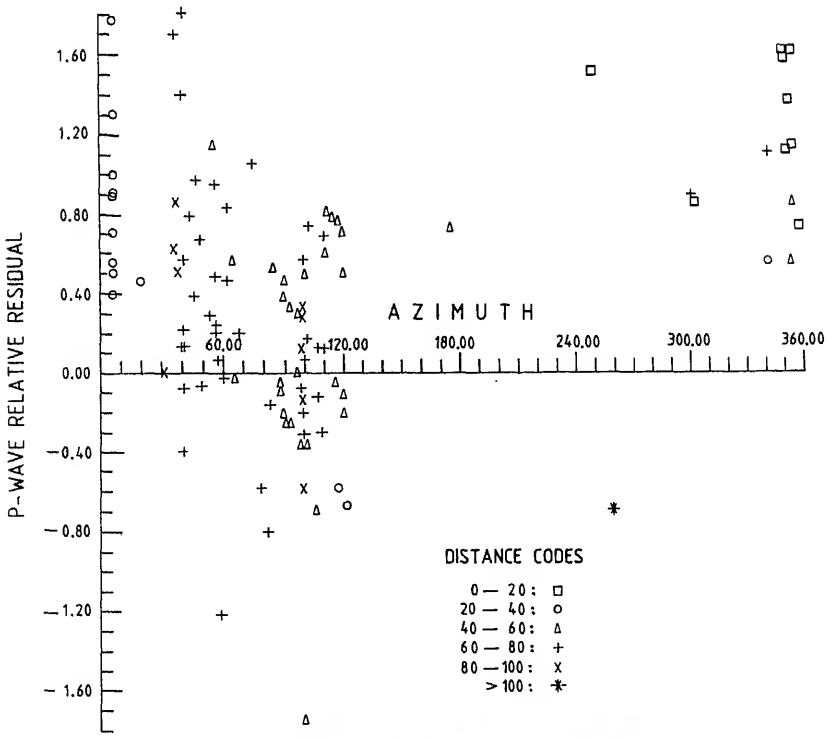

PLOT FOR POONA 75-81

of fissures tapping the lower crust or upper mantle directly beneath the DVP. Further, Nd and Sr isotopic values of least contaminated Deccan Tholeiites from different areas of the DVP fall in a restricted field of high ε_{Nd} which closely approach those of old and present-day Central Indian ridge basalts. This strongly suggests that the Deccan basalts were derived from the same large region of isotopically homogeneous oceanic mantle (Mahoney 1988) which feeds the Central Indian ridge. Considering further that the bulk of Deccan basalts were formed about 65 Ma ago shortly after the rifting between India and Madagascar (80 Ma) when the ridge axis jumped towards India (Norton and Sclater 1979; Schlich 1982), a more natural channel for their outpouring would appear to be associated with the rift systems that eventually fashioned the Indian west coast passive continental margin. If the above visualization of the formation of Deccan basalts is correct, we should expect to see a low velocity zone (LVZ) on the western periphery of the DVP representing the source of the Deccan basalts perhaps characterized by high heat flow values but no thermal anomaly over the DVP. While the heat flow over the LVZ still remains to be measured, the other two predictions from the model are indeed confirmed by observational evidence.

12. Conclusions

Using teleseismic *P*-wave residual tomography, we have identified a large region in the upper mantle beneath the Deccan volcanic province in which the *P*-wave velocity is higher than that in the surrounding region by 1 to 4%. This high velocity anomaly exists coherently in the depth range of 100–400 km. This implies that a coherent, colder and comparatively rigid lithospheric root extends to a depth of about 400 km beneath the DVP. The anomaly in the depth range of 400–600 km is distinctly weaker and appears to be decoupled from the overlying layers. This is as we expect owing to diminished ability of the asthenosphere to retain heterogeneities over extended periods of geologic times. Persistence of the anomaly in the upper mantle is however maintained through a stable geochemical reordering and formation of a tectosphere beneath the craton which together translate coherently over the underlying weaker mantle.

Acknowledgements

Support for this work came from three organizations: the Indo-US Subcommission on Education and Culture which awarded a fellowship to Iyer to spend 13 months in India; the National Geophysical Research Institute which provided full research support; and the U.S. Geological Survey which permitted Iyer's visit to India and completion of the research on his return to USA. Special thanks are due to the Director and staff of the Indian Institute of American Studies, New Delhi for efficiently managing Iyer's fellowship and assisting him in innumerable ways. We are greatly indebted to the various universities, colleges and many individuals for the warm cooperation extended to us in running our field stations during this work. We are very grateful to these organisations and also to many field assistants from NGRI, who participated in the experiment, to Phil Dawson for extensive support in data

analysis and to Tim Hitchcock and M Jayarama Rao for help throughout the project including preparation of figures for this manuscript. Grateful thanks are also due to M/s. N K Venkatesh and G Ramakrishna Rao for the excellent typing of the manuscript.

References

Achauer U, Greene L, Evans J R and Iyer H M 1986 Nature of magma chamber underlying the Mono craters area, eastern California, as determined from teleseismic travel time residuals; *J. Geophys. Res.* **91** 13872–13891

Aki K 1982 Three-dimensional seismic inhomogeneities in the lithosphere and asthenospehre: evidence for decoupling in the lithosphere and flow in the asthenosphere; *Rev. Geophys. Space Phys.* **20** 161–170

Aki K, Christoffersson A and Husebeye E S 1927 Determination of the three-dimensional seismic structure of the lithosphere; *J. Geophys. Res.* **82** 277–296

Baer M 1980 Relative travel time residuals for teleseismic events at the new Swiss seismic station network; *Ann. Geophys.* **36** 119–126

Dorbath C, Dorbath L, Le page A and Gaulon R 1983 The West-African craton margin in eastern Senegal; a seismological study; *Ann. Geophys.* **1** 25–36

Ellsworth W L and Koyanagi R Y 1977 Three-dimensional crust and mantle structure of Kilanea Volcano, Hawaii; *J. Geophys. Res.* **82** 5379–5394

Evans J R 1982 Compressional wave velocity structure of the upper 350 km under the eastern Snake River Plain near Rexburg, Idaho; *J. Geophys. Res.* **87** 2654–2670

Evans J R and Oliver H W 1987 Comparison of Timber Mountain caldera complex, Nevada, with Yellowstone; speculations on mechanisms (Abs), Abstract Volume; *Hawaii Symposium on How Volcanoes Work* (Hilo, Hawaii: Hawaiian Volcano Observatory) p. 67

Grand S P and Helmberger D 1984 Upper mantle shear structure of North America; *Geophys. J. R. Astron. Soc.* **76** 399–438

Gupta M L and Gaur V K 1984 Surface heat flow and probable evolution of Deccan volcanism; *Tectonophysics* **105** 309–318

Hirahara K 1981 Three-dimensional seismic structure beneath southwest Japan: the subducting-phillippine sea plate; *Tectonophysics* **79** 1–44

Herrin E 1968a Seismological tables for *P*; *Seismol. Soc. Am. Bull.* **58** 1193–1241

Herrin E 1968b *P*-wave velocity distribution in the mantle; *Seismol. Soc. Am. Bull.* **58** 1223–1225

Humphreys E 1987 Mantle dynamics of the southern Great Basin-Sierra Nevada region (Abs); *EOS Trans. Am. Geophys Union* **68** 1450

Humphreys E and Clayton R W 1988 Adaptation of back-projection tomography to seismic travel time problems; *J. Geophys. Res.* **93** 1073–1085

Humphreys E, Clayton R W and Hager B H 1984 A tomographic image of mantle structure beneath southern California; *Geophys. Res. Lett.* **11** 625–627

Husebye E S and Hovland J 1982 On upper mantle seismic heterogeneities beneath Fennoscandia; *Tectonophysics* **90** 1–17

Iyer H M 1984 Geophysical evidence for the locations, shapes and sizes, and internal structures of magma chambers beneath regions of Quaternary volcanism. In *Relative contributions of mantle, oceanic crust, and continental crust to magma genesis*, (eds) S Moorbath, R N Thompson and E R Oxburg (Philos Trans. R. Soc. London) **A310** 473–510

Iyer H M 1988a *Seismic tomographys. Encyclopedia of geophysics* (ed.) D James, (Van Nostrand Reinhold and Co.) (in press)

Iyer H M 1988b Seismological detection and delineation of magma chambers beneath intraplate volcanic centres in western USA. In *Modelling volcanic processes* (eds) C King and R Scaroa (Braunschweig/ Wiesbaden: Friedr. Vieweg and Sohn) pp. 1–56

Iyer H M, Evans J R, Zandt G, Stewart R M, Coakley J M and Roloff J N 1981 A deep low-velocity body under the Yellowstone caldera, Wyoming: delineation using teleseismic *P*-wave residuals and tectonic interpretation; *Geol. Soc. Am. Bull.* **92** Part I (Summary), 792–798; part II (full text in microfische edition) 1471–1646

Iyer H M and Hitchcock T 1988 Upper mantle velocity structure in continental US and Canada. Geophysical framework of the Continental United States; *Geol.* Soc. *Am. Mem.* (in Press)

Jordan T H 1975 The continental tectosphere; *Rev. Geophys. Space Phys.* **13** 1–12
Jordan T H 1979a Lateral heterogeneity and mantle dynamics; *Nature (London)* **257** 745–750
Jordan T H 1979b The deep structure of continents; *Sci. Am.* **240** 92–107
Kaila K L 1982 Deep seismic sounding studies in India; *Geophys. Res. Bull. NGRI, India* (Special Issue) **20** 309–328
Kaila K L, Tewari H C and Sarma, P L N 1981 Crustal structure from deep seismic sounding studies along Navibandar-Amreli profile in Saurashtra, India. In *Deccan volcanism and related basalt provinces in other parts of the world* (eds) K V Subba Rao and R N Sukheswala, Geol. Soc. India Memoir No. 3 pp. 218–232
Kaila K L, Reddy P R, Dixit M M and Koteswara Rao P 1985 Crustal structure across the Narmada-Son lineament, Central India from deep seismic soundings; *J. Geol. Soc. India* **26** 465–480
Kailasam L N 1975 Epirogenic studies in India with reference to recent vertical movements; *Tectonophysics* **29** 505–521
Lam A L L and Jordan T H 1987 How thick are the continents; *J. Geophys. Res.* **92** 14007–14026
Mahoney J J 1988 Deccan basalts. In *continental flood basalts* (ed.) J D Macdougall (Kluiser, Norwell, MA)
Menke W H 1977 Lateral inhomogeneities in *P* velocity under the Tarbela array of the lesser Himalayas of Pakistan; *Bull. Seismol. Soc. Am.* **67** 725–734
Montagner J P 1986 Regional three-dimensional structures using long period surface waves; *Ann. Geophys.* **4** 283–294
Morgan W J 1972 Deep mantle convection plumes and plate motions; *Bull. Am. Assoc. Petrol Geol.* **56** 203–213
Nataf H C, Nakanishi I and Anderson D L 1984 Anisotrophy and shear-velocity heterogeneities in the upper mantle; *Geophys. Res. Lett.* **11** 109–112
Norton I O and Sclater J G 1979 A model for evolution of the Indian Ocean and break-up of Gondwanaland; *J. Geophys. Res.* **84** 6803–6830
Oncescu M C, Burlacu V, Anghel M and Smalbergher V 1984 Three-dimensional *p*-wave velocity image under the Carpathinan Arc; *Tectonophysics* **106** 305–319
Parker E C, Davis P M, Evans J R, Iyer H M and Olsen K H 1984 Upwarp of anomalous asthenosphere beneath the Rio qrande rift; *Nature (London)* **312** 354–356
Pollack H N 1986 Cratonization and thermal evolution of the mantle; *Earth. Planet. Sci. Lett.*, **80** 175–182
Qureshy M N 1981 Gravity anomalies, isostasy and crust mantle relations in the Deccan Trap and contiguous regions, India. In *Deccan volcanism and related baslt provinces in other parts of the world* (eds) K V Subba Rao and R N Sukheswala, Geol. Soc. India Memoir No. 3 185–197
Raikes S and Bonjer K P 1983 Large-scale mantle heterogeneity beneath the Rheinish Massif and its vicinity from teleseismic *p*-residuals measurements. In *Plateau uplift* (eds) K Fuchs *et al* (Berlin Heidelberg: Springer-Verlag) 315–331
Shedlock K M and Roecker S W 1987 Elastic wave velocity structure of the crust and upper mantle beneath the North China Basin; *J. Geophys. Res.* **92** 9327–9350
Schlich R 1982 The Indian Ocean: Aseismic ridges, spreading centres, and oceanic basins. In *The oceans basins and margins, Vol. 6 The Indian Ocean* (eds) A E M Nairn and F G Stelhi (New York: Plenum Press) 51–147
Silver P G and Chan W W 1988 Implications for continental structure and evolution from seismic anisotropy; *Nature (London)* **335** 34–39
Takin M 1966 An interpretation of the positive gravity anomaly over Bombay on the west coast of India; *Geophys. J. R. Astron. Soc.* **11** 527–537
Taylor S R and Toksoz M N 1979 Three-dimensional crust and upper mantle structure of the northern United States; *J. Geophys. Res.* **84** 7627–7644
Thurber C H and Aki K 1987 Three-dimensional seismic imaging; *Ann. Rev. Earth Planet. Sci.* **15** 115–139

Proc. Indian Acad. Sci. (Earth Planet. Sci.), Vol. 98, No. 1, April 1989, pp. 61–70.

Rupture zones of great earthquakes in the Himalayan region

PETER MOLNAR and M R PANDEY*

Department of Earth, Atmospheric and Planetary Sciences, Massachusetts Institute of Technology, Cambridge, MA 02139, USA

*Department of Mines and Geology, Ministry of Industry, His Majesty's Government of Nepal, Kathmandu, Nepal

Abstract. The four major earthquakes that have occurred in the Himalayan region since 1897 seem to have ruptured as little as about 15% or 20% to perhaps as much as 45% of the thrust zone separating the underthrusting Indian Shield and the overthrusting Himalayan crystalline nappes. Because of various difficulties in estimating the rupture zones for each of these earthquakes, we cannot place a tight constraint on the fraction of the Himalayan belt for which the risk of an imminent great earthquake is high. If a slip between the Indian Shield and the Himalayan crystalline nappes occurs largely by slip associated with major earthquakes, then recurrence intervals of such earthquakes are likely to be between 200 and 500 years, with a likely value of 300 years.

Keywords. Rupture zone; earthquakes; Himalaya.

1. Introduction

Four great earthquakes have occurred in the Himalayan region in the last 100 years. The 1897 Assam earthquake seems to have ruptured a gently dipping plane beneath the Shillong Plateau (Oldham 1899; Seeber and Armbruster 1981; Molnar 1987b), and the rupture may have extended north beneath the Himalaya. The earthquakes of 1905, 1934 and 1950 occurred within the Himalaya, and were responsible for extensive damage along the Himalaya in zones up to 300 km in length. Earthquakes of this type almost surely constitute the most serious seismic hazard to the residents of the Himalaya and the neighbourhood.

Several aspects of the structure and tectonics suggest that major earthquakes in the Himalaya occur as the Indian shield is thrust beneath the Himalaya (Seeber and Armbruster 1981). Fault plane solutions of nearly all moderate earthquakes ($5{\cdot}5 \leqslant M \leqslant 7$) in the Himalaya indicate thrust faulting with one nodal plane dipping gently north or northeast and with the other nodal plane striking parallel to the range and dipping steeply south or southwest (figure 1) (e.g. Fitch 1970; Rastogi 1974; Molnar *et al* 1973, 1977; Chandra 1978; Baranowski *et al* 1984; Ni and Barazangi 1984). The gently northward or northeastward dipping planes almost surely are the fault planes. Focal depths of about 15 km for these earthquakes are consistent with their occurring on the top surface of the Indian shield as it underthrusts the Himalaya (e.g. Molnar and Chen 1982; Baranowski *et al* 1984; Ni and Barazangi 1984). Gravity anomalies over the Indo-Gangetic Plains and the Himalaya are consistent with the Indian plate extending intact northward from the Indo-Gangetic Plains

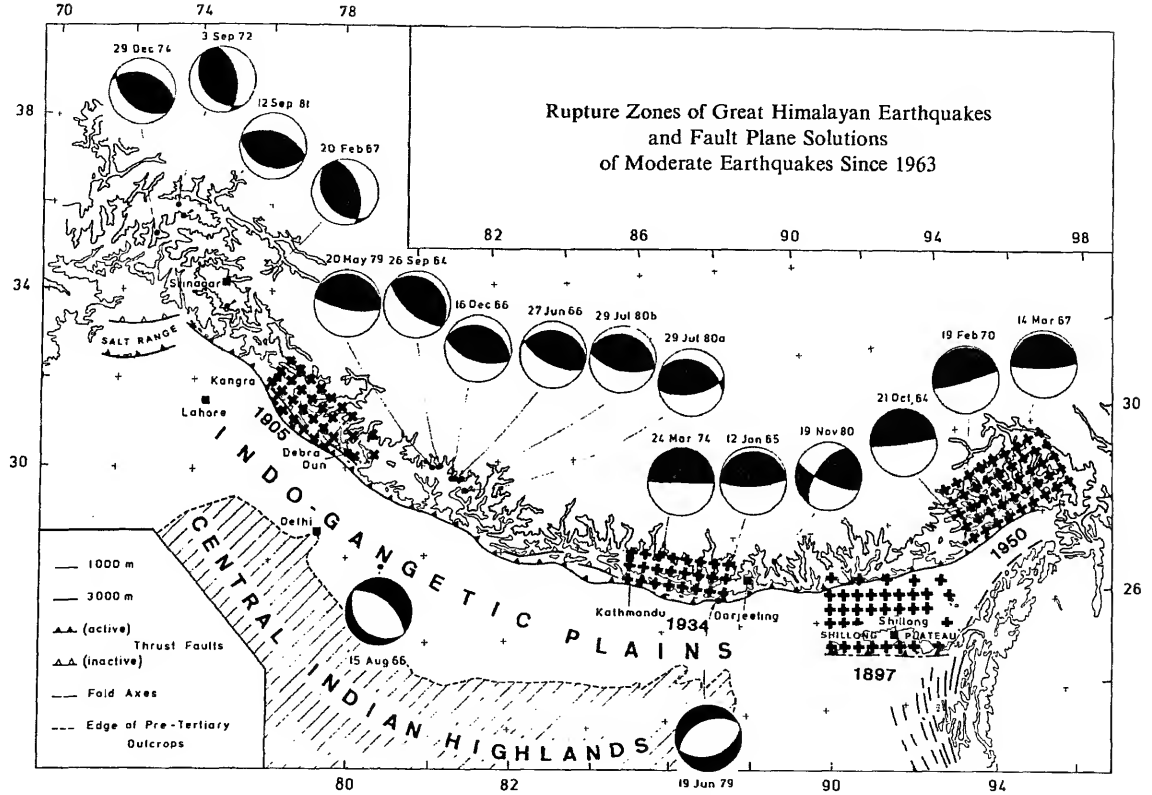

Figure 1. Rupture zone of great Himalayan earthquakes and fault plane solution of moderate earthquakes. Shaded areas show the approximate areas underlain by the rupture zones of the four major earthquakes in the Himalaya since 1897. Lower hemisphere projections of the focal spheres, with blackened quadrants showing those with compressional first motions, were taken from Molnar *et al* (1977), Baranowski *et al* (1984), and Ni and Barazangi (1984).

Himalaya, with an abrupt increase in elevation along the southern margin of the range, the mature landscape of the Lesser Himalaya, and the sharp incision of the Greater Himalaya, is consistent with the Indian plate underthrusting the Lesser Himalaya along a gentle plane that becomes steeper beneath the Greater Himalaya (Molnar 1987c). Thus, several observations suggest that the Indian shield is being underthrust coherently beneath the Lesser Himalaya along a gently dipping fault that steepens northward.

None of the four great earthquakes seems to be associated with primary surface faulting, and therefore the types of faults that ruptured cannot be proven definitively. Seeber and Armbruster (1981) suggested that the great Himalayan earthquakes occurred on a gently dipping thrust fault that underlies the entire Himalaya and part of the Indo-Gangetic Plains. We proceed with the assumption that this contention is basically correct, but we disagree with their estimates of the dimensions of the rupture zones, and in particular, with their inference that the ruptures extend beneath the Indo-Gangetic Plains.

We review briefly the constraints on the rupture zones of the four great Himalayan earthquakes of 1897, 1905, 1934 and 1950, and we also report some tentative implications for recurrence intervals of great earthquakes in the Himalayan region.

2. Rupture zones of great Himalayan earthquakes

2.1 *The 1897 Assam earthquake*

Virtually everything that is known about the effects of this earthquake is given in Oldham's (1899) report. Later, others have extracted factual material to draw conclusions about the style and extent of faulting associated with that earthquake (e.g. Richter 1958; Seeber and Armbruster 1981; Molnar 1987b).

Very high accelerations and particularly great destruction were noted at numerous localities on the Shillong Plateau, and there seems little doubt that the plateau is close to the rupture zone. Indisputable evidence of surface faulting was found only on the Shillong Plateau, but the short segments and varying orientations of such faults suggest that this faulting was secondary, not primary. Warping and tilting of the earth's surface, as reflected by changes in drainage indicated important strains associated with the earthquake. Finally, a nearly continuous belt of landslides along the southern edge of the plateau suggested high accelerations there. Oldham (1899) inferred that a slip occurred on a thrust fault that dips gently northward from the southern edge of the Shillong Plateau, an inference that he later abandoned, but that seems reasonable (e.g. Seeber and Armbruster 1981; Molnar 1987b).

The likelihood of such a thrust fault cannot be denied, but its proof is lacking. The east-west striking Dauki fault, which bounds the southern edge of the Shillong Plateau, marks a vertical separation of the Pre-Tertiary basement of more than 10 km (e.g. Evans 1964; Sengupta 1966). Although Evans (1964) inferred a large component of strike-slip faulting, thrust faulting can account for most of the observations that he presented. The very large isostatic gravity anomalies of the Shillong Plateau (e.g. Verma *et al* 1976; Verma 1985) imply that the strength of the Indian lithosphere must support the plateau, and therefore underthrusting of the strong Indian plate beneath the Shillong Plateau seems likely. Neither the locations of microearthquakes (Khattri *et al* 1983; Kayal 1987) nor fault plane solutions and locations of moderate

earthquakes (Chen and Molnar 1989) give a hint of such a fault. The five moderate earthquakes studied by Chen and Molnar (1989) occurred at depths between 25 and 50 km, too deep to have occurred on a gently dipping plane that crops out as the Dauki fault, and four of the fault plane solutions show faulting on relatively steep places (30°–60°). Thus, although Oldham's (1899) inference of a gently dipping plane seems reasonable, it is not proven.

The extent of the rupture remains in dispute. Damage associated with the 1897 earthquake was not confined to the Shillong Plateau. Oldham (1899) noted that much of the damage, particularly west and south of the plateau, could be associated with fissuring, and he specially noted that the soil conditions associated with and without fissures were different. Thus, he considered this damage to be due to superficial deformation and not to faulting of the underlying basement. One of us, Molnar (1987b), found his arguments convincing, but Seeber and Armbruster (1981) inferred that the rupture extended 100 km south and 200 km west of the plateau. The numerous reports of aftershocks felt on the plateau and just north of it and their paucity from areas to the south or west (Oldham 1899) also support the contention that the fault that ruptured underlies the plateau but not the idea that this rupture zone extends south and west of the plateau.

The eastern limit of the rupture is poorly defined, largely because Oldham and his deputies were unable to gather much data from that area. From the few observations Oldham (1899) reported, Molnar (1987b) inferred an east-west extent of the rupture of 200 ± 40 km, from the western margin of the Shillong Plateau, considerably less than the 550 km suggested by Seeber and Armbruster (1981).

The northern limit of the rupture is also uncertain. Reports of landslides and damage in Bhutan (Oldham 1899) allow the possibility that the rupture reached as far north as the Himalaya, as Seeber and Armbruster (1981) suggested. In any case, for evaluating earthquake hazards in the Himalaya, knowing the northward extent of the rupture is probably less important than determining the degree to which the 1897 earthquake relieved strain caused by the convergence of the Indian plate with the Himalaya. If the 1897 earthquake did relieve such strain, then obviously its occurrence must be considered in evaluating the earthquake hazard of the Himalaya. If, instead, the 1897 earthquake did not relieve such strain, and if the convergence of the Shillong Plateau with the Himalaya occurs essentially as rapidly as that between the rest of the Indian subcontinent and the Himalaya, then clearly the 1897 earthquake could be ignored in evaluating the earthquake hazard in the Himalaya. The available evidence seems to allow either possibility.

2.2 *The 1905 Kangra earthquake*

Middlemiss's (1910) report contained virtually all the published factual material concerning the macroseismic effects of this earthquake. The highest intensity, X on the Rossi-Forel scale, was felt near the towns of Kangra and Dharamsala. The intensity decreased sharply to the west, with the intensity VIII and X isoseismals separated by only 15 km. To the east, the decrease in intensity was more gradual. The intensity VIII, IX and X isoseismals are all aligned northwest-southwest, parallel to the trend of the range and surrounding the Main Boundary Fault, the thrust fault separating Tertiary from pre-Tertiary rock at the foot of the Himalaya. The limited number of observations northeast and immediately southeast of the $I =$ VIII isoseismal make

occurred by slip on a gently northeastward dipping plane, but there is no proof of this and little evidence to constrain the northeast limit of the rupture.

Damage associated with the 1905 earthquake was greater in Dehra Dun and Mussoori, about 250 km southeast of Kangra, than in most of the area southwest and northeast of these two towns. Accordingly, Middlemiss (1910) drew an isolated contour of intensity VIII surrounding Dehra Dun and Mussoori. This contour must close southeast of Dehra Dun, because very little damage was reported at Rishikesh, Hardwar, and neighbouring towns. Very few observations, however, define the closure to the northwest and probably are insufficient to rule out the possibility that the two separate $I = \text{VIII}$ isoseismals ought to be connected.

Relevelling in 1906 along a line across the Siwalik Hills to Dehra Dun, which had been surveyed in 1862, and its continuation to Mussoori, which had been surveyed in 1904, revealed 4 cm of uplift. Middlemiss (1910) and Seeber and Armbruster (1981) associated this uplift with the 1905 earthquake, but we remain unconvinced of this association. The amount of only 4 cm seems small to be associated with the rupture of a major earthquake. Moreover, the uplifted part lies in a topographic basin flanked by ranges that clearly have risen in late Cenozoic time. Thus ascribing the 4 cm of uplift to the 1905 earthquake seems to us to be risky.

The extent of the rupture is poorly defined, and several different possible rupture zones seem to be allowed (Molnar 1987a). One is that rupture occurred only beneath the area delimited by the $I = \text{VIII}$ isoseismal surrounding Kangra, Dharamsala, a zone about 100 km in length. A second possibility is that the two separate areas encompassed by the time $I = \text{VIII}$ isoseismals ruptured, for a total of about 200 km of the Himalayan front. Third, perhaps the entire zone from northwest of Kangra to southeast of Dehra Dun, 280 km in length, ruptured, as Seeber and Armbruster (1981) inferred. Included within the latter, two plausible rupture zones is the possibility that the slip on the southeastern part of the zone was less than that in the northwest, where the maximum intensity was greater. In evaluating the earthquake hazard, it seems reasonable to assume that only the segment approximately 100 km in length surrounding Kangra ruptured in 1905, but also to consider the possibility that the entire zone 280 km in length ruptured.

2.3 *The 1935 Bihar-Nepal earthquake*

Although the 1934 earthquake was recorded by more than 100 seismograph stations, to the best of our knowledge, there are not enough consistent P wave first motions to determine a fault plane solution. Singh and Gupta (1980) inferred from surface waves that strike-slip faulting had occurred, but they did not show their data to be inconsistent with thrust faulting. Chen and Molnar (1977) assumed thrust faulting and used the amplitude spectra of surface waves to infer a seismic moment. Because the inferred value of the moment is inversely proportional to the assumed dip for slip on gently dipping planes, however, their value is very uncertain. Most of what we know of this event derives from macroseismic observations.

Two important sources of macroseismic data were published independently and separately from one another: Dunn *et al* (1939) gave extensive information on the effects of the earthquake in India and along three traverses into Nepal, and Rana

(1936) presented extensive data from the interior of Nepal. Neither Rana nor Dunn and his co-workers seem to have been aware of the others' work. Thus the agreement of the two reports concerning areas discussed by both gives credibility to the areas discussed by only one of them (Pandey and Molnar 1988).

Dunn *et al* (1939) reported three areas of very extensive damage to which they assigned an intensity of $I = \text{IX}$ and X on the Mercalli scale: a belt along the India-Nepal border, a narrow zone along the Ganga river through Monghyr, and the Kathmandu valley in Nepal. The damage in all three areas seems to be due, at least in large part, to local site conditions. The extensive damage along the India-Nepal border is primarily due to slumping (the "slump belt"). Evidence for faulting in the basement is absent, and several observations imply that the slumping was superficial (Dunn *et al* 1939; Pandey and Molnar 1988). Localized high intensities had been noted at Monghyr in association with other important Himalayan earthquakes (Baird Smith 1843; Dunn *et al* 1939). Similarly, the contrast in damage within and surrounding the Kathmandu valley, both in 1934 and in 1833, when a smaller earthquake caused extensive damage, implies that local conditions are largely responsible for this localized damage. Moreover, a recent study of variations in earth noise in the Kathmandu valley shows marked variations that correlate with variations in damage in 1934 (Pandey, unpublished data, 1986). Thus, the areas assigned the highest intensity by Dunn *et al* (1939) do not seem to place useful constraints on the extent of the rupture.

Following the 1934 earthquake, JB Auden made three excursions into Nepal to evaluate the damage: one to Kathmandu, a second into the frontal range of the Himalaya in eastern Nepal, and a third, a traverse across the Lesser Himalaya of easternmost Nepal and the frontier with India to Darjeeling. Except for the Kathmandu valley, Auden saw little evidence for destruction as severe as that in the slump belt. These observations, together with an apparent mislocation of the epicenter of mainshock, led to the inference that the rupture zone underlies the slump belt in the Indo-Gangetic Plains and not the Himalaya (Dunn *et al* 1939; Richter 1958; Singh and Gupta 1980; Seeber and Armbruster 1981).

Ironically, Auden did not visit most of the areas of Nepal where destruction appears to have been most severe, and where it cannot be easily ascribed to local conditions. Rana (1936) reported almost complete destruction of the area north of Auden's central route and west of his eastern route, an area that includes Chen and Molnar's (1977) relocated epicenter of the 1934 earthquake. The severity of the destruction decreased eastward; Darjeeling was not affected much. To the west the level of destruction diminished more gradually to the area just south of Kathmandu, but west of Kathmandu, there was almost no destruction. Thus, the rupture zone probably underlies the Lesser Himalaya of eastern Nepal. The region of most severe destruction spans a segment parallel to the Himalaya approximately 100 km in length, but destruction was not negligible in the area from the eastern frontier of Nepal to just west of Kathmandu, about 300 km in length. Thus the length of the rupture zone is best described as 200 ± 100 km.

2.4 *The 1950 Assam (or Chayu) earthquake*

This earthquake occurred at the northeast end of the Himalaya; although the

epicenter lies in China, numerous aftershocks beneath the Himalaya in eastern Assam (e.g. Chen and Molnar 1977) imply that at least part of the rupture zone underlies the Himalaya.

Tandon (1955) reported a fault plane solution with numerous compressional first motions at stations north, northwest, and northeast of the earthquake. He inferred normal faulting, either on a steeply northward or on a gently southward dipping plane. Ben-Menahem *et al* (1974) revised and added data and inferred a large component of right-lateral strike-slip faulting on a north-northwest trending steeply east-dipping plane. They used surface waves and the existence of scattered aftershocks south-southeast of the epicenter of the mainshock to corroborate this solution. Chen and Molnar (1977) found the *P*-wave first motions used by Ben-Menahem *et al* (1974) to be consistent with thrust faulting on either a gently north-northwest or a steeply south-southeast dipping plane, similar to those of moderate earthquakes (figure 1). Because of the extensive aftershock activity beneath the Himalaya and the similar solutions for nearby moderate earthquakes (figure 1), they inferred thrust faulting on the gently dipping planes. This solution, however, does not agree with Ben-Menahem *et al*'s (1974) measured ratios of Love to Rayleigh wave amplitudes, and the possibility that two separate planes ruptured should not be overlooked (Molnar *et al* 1977; Molnar and Deng 1984). Finally, a re-examination of the aftershocks of the 1950 earthquake shows that if only those earthquakes recorded by more than 50 stations are considered, nearly all of the relocated aftershocks lie beneath the Himalaya in a zone extending roughly 250 ± 50 km west of the epicenter of the mainshock and about 100 km wide (Molnar, unpublished data, 1985). Thus, we presume that rupture occurred primarily on a gently north-northeast dipping thrust fault.

The remoteness of the region affected by the 1950 earthquake prohibited a comprehensive investigation of the damage associated with it. Apparently no special investigation of the damage in the epicentral region was made. Ramachandra Rao (1953) showed several maps of intensity distributions for India, and all indicate a maximum intensity, $I = \text{XI}$ (or XII) on the Modified Mercalli scale, along the Himalaya to about 250 km west of the epicenter. The absence of data within the Himalaya limits the northward extent of this isoseismal. A Chinese map shows these isoseismals closing just east of the epicenter (Anonymous 1979), consistent with the rupture underlying the Himalaya. Thus, given both the aftershock distribution and the isoseismals, we infer that dimensions of the rupture zone are about 250 km in its east-west dimension of about 100 km north-south.

3. Summary and implications

The lengths of the rupture zones parallel to the Himalaya for all four earthquakes exceed 100 km; those for the events of 1897, 1934 and 1950 probably are at least 200 km; and all may reach 300 km, but probably not more than that. Thus, if the slip during the 1897 Assam earthquake relieved the strain in the Himalaya and accommodated some of the convergence between India and the Himalaya, the strain along nearly half of the 2500 km of the Himalaya might have been relieved in the last 100 years. Alternatively, if the 1897 Assam earthquake did not relieve such strain, perhaps strain along as little as only 15–20% of the Himalaya chain was relieved. If we

choose conservative, but probable, lengths for the ruptures of 200 km (1897), 100 km (1905), 200 km (1934), and 250 km (1950), then 30–35% of the Himalayan chain ruptured in the last 100 years. This large range of uncertainty ($30\% \pm 15\%$) for the fraction of the chain along which strain seems to have been relieved since 1897 underscores our ignorance of the seismic hazard in the Himalaya.

If (1) the convergence of the Indian plate with respect to the Himalaya occurs largely by slip associated with great earthquakes, if (2) these four earthquakes relieved all of the strain that had accumulated since the last such earthquakes in the same areas, and if (3) the rate of 4 great earthquakes per century were representative of earthquake recurrence in the Himalayan region, then recurrence intervals should be between about 200 and 500 years, with a most probable value of 300 years. The areas most likely to rupture next are those that did not rupture in 1897, 1905, 1934, or 1950 (e.g. Khattri and Tyagi 1983).

Clearly none of the three assumptions listed above are proven, and there is reason to doubt each of them. Several earthquakes with $M = 7{\cdot}5$ have occurred this century. They, as well as fault creep, may contribute a non-negligible fraction of the convergence. The possibility that different amounts of slip occurred on different parts of the 1905 rupture zone, and the differences in the measured seismic moments, if both very uncertain, for the 1934 and 1950 earthquakes imply that the amounts of slip associated with ruptures in different parts of the Himalaya have been different. Consequently, recurrence intervals for different segments also should be very different from one another. Finally, although major earthquakes did occur during the last century before 1897, reports of them (e.g. Baird Smith 1843; Oldham 1883; Dunn *et al* 1939; Seeber and Armbruster 1981) do not suggest that any was as large as those in 1897, 1905, 1934, or 1950. Thus, the last 100 years may not be representative of the seismic history of the Himalaya for the last few thousand years.

Studies of the great Himalayan earthquakes clearly are vital for evaluating the earthquake hazard, but enough remains unknown about each event that alone they do not place a tight constraint on the earthquake hazard. The value of these studies could be enhanced by a thorough study of archived historic documents that give information about earthquakes prior to 1897.

Because the geologic record is not likely to contain a complete record of earthquakes that did not cause surface faulting, techniques of Quaternary geology may not provide tight constraints on the average recurrence intervals of earthquakes along the Himalaya. Obtaining such constraints probably will require a synthesis of geologic, geophysical, and historical data of various kinds. Among such data are those that constrain average Quaternary, Holocene, or more recent (geodetically measured) slip rates on the main active thrust fault in the Himalaya would be very important in future estimates of recurrence intervals.

Acknowledgements

This work has been supported in part by the National Aeronautical and Space Administration under Grant NAG5-795 and by the National Science Foundation under Grant 8500810-EAR. We thank L Jenatton for drafting figure 1 and D Frank

eferences

onymous 1979 *Maps of isoseismals of Chinese earthquakes* (Beijing: Seismology Publishing House)

ird Smith R 1843 Memoir on Indian earthquakes. Part II. Historical summary of Indian earthquakes with some remarks on the general distribution of subterranean disturbing forces throughout India and its frontier countries; *J. Asiatic Soc. Bengal* **12** 1029–1056

ranowski J, Armbruster J, Seeber L and Molnar P 1984 Focal depths and fault plane solutions of earthquakes and active tectonics of the Himalaya; *J. Geophys. Res.* **89** 6918–6928

n-Menahem A, Aboudi E and Schild R 1974 The source of the great Assam earthquake – an intraplate wedge motion; *Phys. Earth Planet. Int.* **9** 265–269

ıandra U 1978 Seismicity, earthquake mechanisms and tectonics along the Himalayan mountain range and vicinity; *Phys. Earth Planet. Int.* **16** 109–131

ıen W-P and Molnar P 1977 Seismic moments of major earthquakes and the average rate of slip in Central Asia; *J. Geophys. Res.* **82** 2945–2969

ıen W-P and Molnar P 1989 Source parameters of earthquakes beneath the Shillong Plateau and the northern Indoburman ranges; *J. Geophys. Res.* (submitted)

ınn J A, Auden J B, Ghosh A M N and Wadia D N 1939 The Bihar-Nepal earthquake of 1934; *Geol. Surv. India Mem.* 73

ans P 1964 The tectonic framework of Assam; *J. Geol. Soc. India* **5** 80–96

tch T J 1970 Earthquake mechanisms in the Himalayan, Burmese and Andaman regions and continental tectonics in Central Asia; *J. Geophys. Res.* **75** 2699–2709

ayal J R 1987 Microseismicity and source mechanism study: Shillong Plateau, northeast India; *Bull. Seismol. Soc. Am.* **77** 184–194

hattri K and Tyagi A K 1983 Seismicity patterns in the Himalayan plate boundary and identification of the areas of high seismic potential; *Tectonophysics* **96** 281–297

nattri K, Wyss M, Gaur V K, Saha S N and Bansal V K 1983 Local seismic activity in the region of the Assam gap, northeast India; *Bull. Seismol. Soc. Am.* **73** 459–469

von-Caen H and Molnar P 1983 Constraints on the structure of the Himalaya from an analysis of gravity anomalies and a flextural model of the lithosphere; *J. Geophys. Res.* **88** 8171–8191

von-Caen H and Molnar P 1985 Gravity anomalies, flexture of the Indian plate, and the structure, support and evolution of the Himalaya and Ganga basin; *Tectonics* **4** 513–538

iddlemiss C S 1910 The Kangra earthquake of 4th April 1905; *Mem. Geol. Surv. India* Vol. 37, Geol. Surv. India, Calcutta (reprinted 1981)

olnar P 1987a The distribution of intensity associated with the 1905 Kangra earthquake and bounds on the extent of the rupture zone; *J. Geol. Soc. India* **29** 221–229

olnar P 1987b The distribution of intensity associated with the great 1897 Assam earthquake and bounds on the extent of the rupture zone; *J. Geol. Soc. India* **30** 13–27

olnar P 1987c Inversion of profiles of uplift rates for the geometry of dip-slip faults at depth, with examples from the Alps and the Himalaya; *Ann. Geophiscae* **5** 663–670

olnar P and Chen W-P 1982 Seismicity and mountain building. In *Mountain building processes* (ed.) K Hsu (London: Academic Press)

olnar P and Deng Qidong 1984 Faulting associated with large earthquakes and the average rate of deformation in central and eastern Asia; *J. Geophys. Res.* **89** 6203–6227

olnar P, Fitch T J and Wu F T 1973 Fault plane solutions of shallow earthquakes and contemporary tectonics of Asia; *Earth Planet. Sci. Lett.* **16** 101–112

olnar P, Chen W-P, Fitch T J, Tapponnier P, Warsi W E K and Wu F T 1977 Structure and tectonics of the Himalaya: A brief summary of relevant geophysical observations. In *Himalaya: Sciences de la Terre* (Paris: Centre National de la Recheche Scientifique) pp. 269–294

i J and Barazangi M 1984 Seismotectonics of the Himalayan collision zone; geometry of the underthrusting Indian plate beneath the Himalaya; *J. Geophys. Res.* **89** 1147–1163

ldham T 1883 A catalogue of Indian earthquakes from the earliest time to the end of 1869 AD; *Mem. Geol. Surv. India* 163–215

ldham R D 1899 Report on the great earthquake of 12th June 1897; *Mem. Geol. Surv. India* Vol. 29, Geol. Surv. India, Calcutta (reprinted 1981)

andey M R and Molnar P 1988 The distribution of intensity of the Bihar-Nepal earthquake of 15 January 1934 and bounds on the extent of the rupture zone; *J. Geol. Soc. Nepal* **5** 22–44

Ramachandra Rao M B 1953 A compilation of papers on the Assam earthquake of August 15, 195 No. 1, The Central Board of Geophysics, Govt. of India p. 112

Rana J B (Maj. Gen. Brahma Sumsher) 1935 *Nepalko maha Bhukampa* (*The great earthquake of* (published in Nepali by the author in Kathmandu)

Rastogi B K 1974 Earthquake mechanisms and plate tectonics in the Himalayan region; *Tectonoph* 47–56

Richter C F 1958 *Elementary seismology* (San Francisco: W H Freeman) p. 768

Seeber L and Armbruster J 1981 Great detachment earthquakes along the Himalayan arc and lo forecasts. In *Earthquake prediction: An international review* (eds) D W Simpson and P G R (Washington DC: Am. Geophys. Union) Maurice Ewing Series 4, pp. 259–277

Sengupta S 1966 Geological and geophysical studies in the western part of Bengal basin, India; *Am Petrol. Geol.* **50** 1001–1017

Singh D D and Gupta H K 1980 Source dynamics of two great earthquakes of the Indian subconti Bihar-Nepal earthquake of January 15, 1934 and the Quetta earthquake of May 30, 1935; *Bull.* Soc. Am. **70** 757–773

Tandon A N 1955 Direction of faulting in the great Assam earthquake of August 15, 1950; *I Meteorol. Geophys.* **6** 61–64

Verma R K 1985 *Gravity, seismicity and tectonics of the Indian Peninsula and the Himalayas* (Hi Massachusetts: D. Reidel) p. 213

Verma R K, Mukhopadhyay M and Ahluwalia M S 1976 Seismicity, gravity and tectonics of n India and northern Burma; *Bull. Seismol. Soc. Am.* **66** 1683–1694

Proc. Indian Acad. Sci. (Earth Planet. Sci.), Vol. 98, No. 1, April 1989, pp. 71–89.
© Printed in India.

Active tectonics of the Himalaya

JAMES F NI
Department of Physics, New Mexico State University, Las Cruces, NM 88003, USA

Abstract. The Himalayan mountains are a product of the collision between India and Eurasia which began in the Eocene. In the early stage of continental collision the development of a suture zone between two colliding plates took place. The continued convergence is accommodated along the suture zone and in the back-arc region. Further convergence results in intracrustal megathrust within the leading edge of the advancing Indian plate. In the Himalaya this stage is characterized by the intense uplift of the High Himalaya, the development of the Tibetan Plateau and the breaking-up of the central and eastern Asian continent. Although numerous models for the evolution of the Himalaya have been proposed, the available geological and geophysical data are consistent with an underthrusting model in which the Indian continental lithosphere underthrusts beneath the Himalaya and southern Tibet. Reflection profiles across the entire Himalaya and Tibet are needed to prove the existence of such underthrusting. Geodetic surveys across the High Himalaya are needed to determine the present state of the MCT as well as the rate of uplift and shortening within the Himalaya. Paleoseismicity studies are necessary to resolve the temporal and spatial patterns of major earthquake faulting along the segmented Himalayan mountains.

Keywords. Himalayan mountains; continental collision; earthquakes; active tectonics; tectonic setting; Main boundary thrust; Tethyan slab.

1. Introduction

The Himalaya is the largest mountain chain in the world. Accordingly, understanding the mechanics responsible for its formation and for its support must be two of the most important geological problems. Moreover, study of the active tectonics of the Himalayan mountain belt is important because such a region contains information that is unavailable in other, older mountain belts, but necessary in order to understand how mountain building takes place.

Early episodes in orogenic research (last quarter of the 18th and first half of the 19th centuries) were characterized by the interpretation that mountain belts are a result of vertical uplift. It was not until the late 19th century that the role of horizontal movements became more widely appreciated. The development of geosynclinal theory in the early 20th century to explain the prehistory of mountain belts and the subsequent horizontal shortening in orogeny as expressed by fold and nappe structures delayed a more accurate understanding of mountain building. As the concept of plate tectonics was developed during the 1960s, numerous models for the evolution of the Himalaya were proposed. The past decade has included a transition from a focus on testing of the Himalayan collision models to research based more on

This review focuses on the deep crustal and uppermost mantle structures of the Himalaya, because these features reflect the mechanical processes that result in mountain building. The review also will discuss recent work on the Pakistan Himalaya.

2. Collision models

Early ideas about the architecture of the Himalaya assumed that the Himalayan Mountains rest on a rigid substratum that is similar to the rocks beneath the Indian Shield. However, geodetic measurements (plumb line) of Pratt (1855) showed that the observed deflection was much smaller than expected for a rigid model. Shortly following this experiment the concept of isostasy was born and a floating Himalayan range with a "crustal root" became the dominant geological thinking for the early twentieth century. With the improvement of gravity meters, numerous studies have shown that gravity measurements deviate from local isostatic equilibrium. This discovery suggested that the Himalaya is not completely supported by the buoyancy force; rather it is held up, at least in part, by an upward force. Searching for the origin of this force is essential to understanding the dynamics of mountain building.

The concept of underthrusting of one continental lithosphere beneath another as the cause of mountain building and plateau uplift was first proposed by Argand (1924). With the advent of the new global tectonics (e.g. Isacks *et al* 1968) a number of different mechanisms for the uplift of the Himalaya and Tibet have been developed. Dewey and Bird (1970) suggested that the Himalaya was formed solely by the collision of an Atlantic-type continental margin with the Asian continent bordered by a marginal trench. In their model they assumed that the buoyancy of the continental lithosphere prevents further subduction and they overlooked the possible significance of intracontinental thrusts. Powell and Conaghan (1973) pointed out that the geological history of the Himalaya does not agree with the simple continent–continent collision model of Dewey and Bird (1970), because the collision itself did not directly produce the present-day Himalaya. Alternatively, Powell and Conaghan (1973, 1975) and Powell (1979) proposed an "evolutionary" model (figure 1) invoking two phases of orogeny. In their model, the first phase is related to active Mesozoic-early Tertiary subduction zones along the present-day Indus-Tsangpo suture, analogous to the North American Cordilleras. This phase ended in the Eocene (e.g. Molnar and Tapponnier 1975; Tapponnier and Molnar 1977) when India collided with Asia. The Indus-Tsangpo suture is a direct result of this collision. The second phase involves formation of intracontinental fractures within the northern Indian margin during the Middle Tertiary and underthrusting of the Indian continent along this fracture from Miocene time to the present.

Since 1973, increasing amounts of data on the Himalaya and Tibet have become available and, consequently, many plate tectonic models have been proposed for the evolution of the Himalaya (e.g. LeFort 1975; Molnar *et al* 1977; Bird 1978; Seeber *et al* 1981; Chen and Molnar 1981; Barazangi and Ni 1982; Molnar and Chen 1982; Ni and Barazangi 1984; Molnar 1984). Among these models, much of the debate about the tectonics of the Himalaya is concerned with the nature of the Main Boundary Thrust (MBT) and Main Central Thrust (MCT). According to LeFort (1975), the Himalaya was formed by the imbrication of slices of India's northern margin. In his evolutionary model (figure 1), the MBT and MCT are assumed to be similar, but successive,

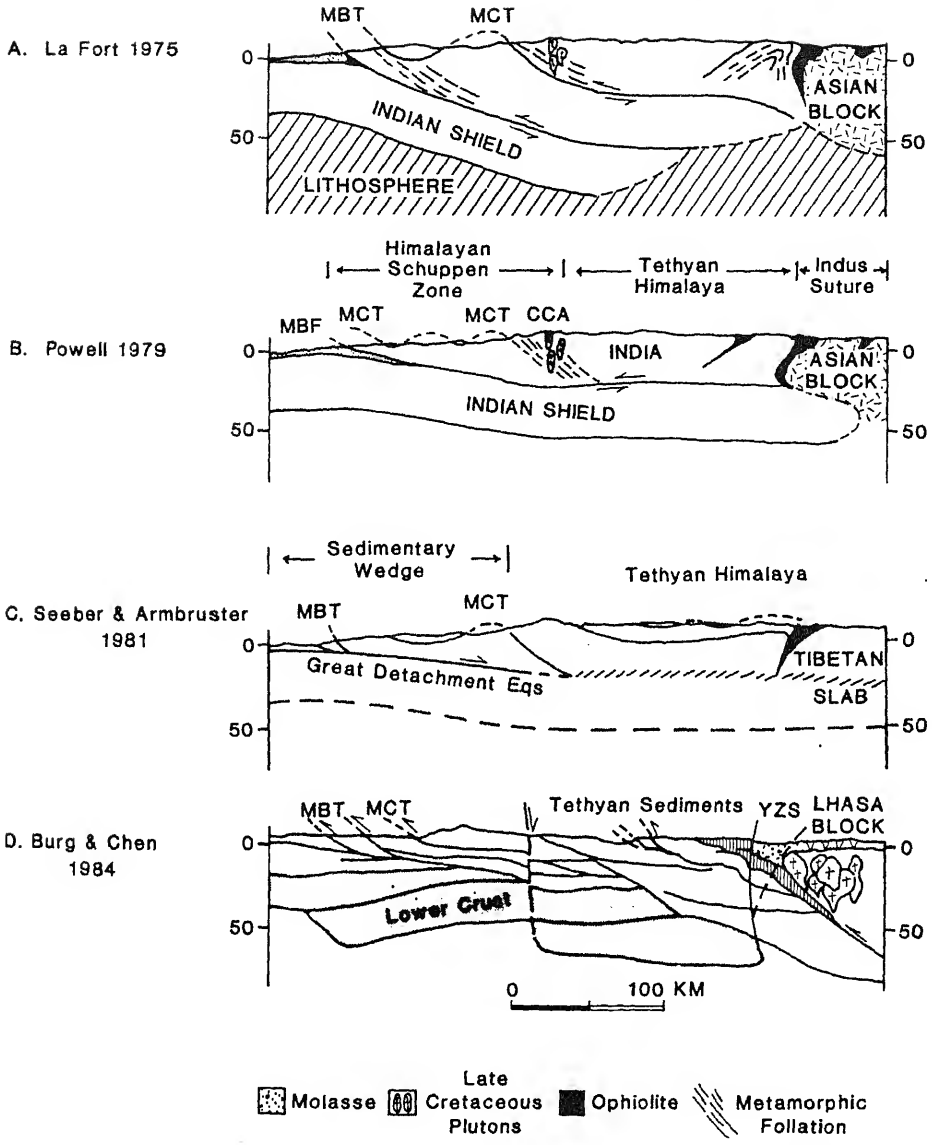

Figure 1. Comparison of tectonic models of the Himalaya. A. After La Fort (1975). The Himalaya was formed by imbrication of slices of India's northern margin. B. After Powell (1979). The MCT and MBT are fundamentally different structures in this model. C. After Seeber and Armbruster (1981). All the elements in this model are active simultaneously and subduction proceeds without fundamental changes in the structure. This model was named the "steady-state" model. D. After Burg and Chen (1984). In their model, decoupling and thrusting, which separate lower and upper crustal layers, occur contemporaneously with each other.

tectonic thrusts. The southern thrust zone (i.e. the MBT) becomes the new boundary of the continental convergent zone, while the older thrust zone (i.e. the MCT) becomes a less active or a dormant feature.

In contrast, Seeber and Armbruster (1981) proposed a "steady-state" model

(figure 1) for the evolution of the Himalaya. This model requires that the MBT and MCT are contemporaneous features. Central to this model is a detachment (decollement) surface underlying the entire Himalaya. The detachment represents the upper surface of the underthrusting Indian plate. Seeber *et al* (1981) also postulated the presence of a Basement Thrust (BT) where the northerly and relatively steeply dipping MCT merges with the shallow dipping detachment surface at depth (see figure 11 of Seeber *et al* 1981). The BT zone represents the front of the overriding crystalline basement (analogous to a bulldozer blade), and it is along this front where the sedimentary rocks above the Indian Shield are scraped off.

A more complex model for the Himalaya has been proposed by Hirn *et al* (1984a) and Burg and Chen (1984) (figure 1). Their model is mostly based on the interpretation of recent reflection data in which a variation in the level of the Moho has been suggested. In their model, decoupling and thrusting, which separate lower and upper crustal layers, occur contemporaneously with each other. However, polarities of thrusting are opposite to each other (figure 1).

3. Tectonic setting

The hypotheses of the evolution of the Himalaya discussed above depend largely on understanding the evolution and structure of major tectonic features and their behaviour at depth. The following is a brief summary of the main structural characteristics of these features (figure 2).

3.1 *Indus-Tsangpo suture*

The Indus-Tsangpo suture (e.g. Gansser 1964, 1980; LeFort 1975) marks the northern limit of the Indian subcontinent following the late Cretaceous-early Tertiary closure of the Neo-Tethys. The suture is made up of imbricated melanges of flysch sediments, radiolarite, pillow lavas, volcanics, and basic and ultrabasic rocks that are cut by steep thrust faults (e.g. Stocklin 1980; Allegre *et al* 1984).

3.2 *Main central thrust (MCT)*

The MCT, at the base of the crystalline zone, (e.g. Gansser 1964) dips 30° to 45° northward, separating the Higher Himalaya from the Lesser Himalaya. The thrust is characterized by a zone of intense shearing; no master thrust surface is apparent (e.g. Valdiya 1980; Sinha-Roy 1982). An abrupt change in the style of structures, especially folding, and in the grade of metamorphism is the main manifestation of the presence of the MCT. The MCT appears to have developed since mid-Tertiary time, and there are some geological indications of minor recent movements along the MCT (e.g. Valdiya 1980; Stocklin 1980; Gansser 1982).

3.3 *Main boundary thrust (MCT)*

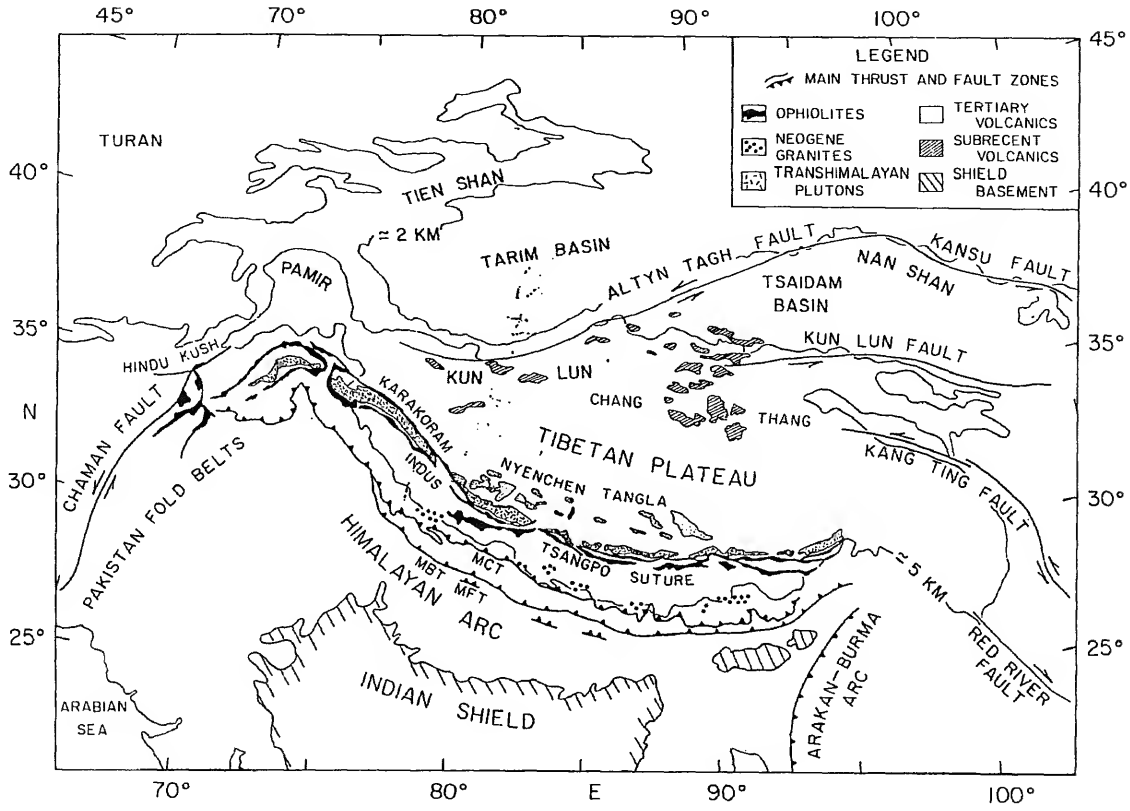

Figure 2. Map of Himalayan arc, Tibetan plateau, and surrounding regions showing major structural features (after Gansser 1964; Molnar and T 1975). MCT, main central thrust; MBT, main boundary thrust; MFT, main frontal thrust. Neogene granites appear to be related to MCT and to the Central Himalaya.

planes of the MBT at the surface gradually flatten out at depth (Valdiya 1980). The MBT has developed since Pliocene time, and abundant geological evidence shows that the thrust zone was active through the Pleistocene (e.g. Mathur and Evans 1964; LeFort 1975; Valdiya 1981).

3.4 *Tethyan slab*

The region between the MCT and the Indus-Tsangpo suture is composed of the Tethyan sedimentary zone in the north and the central crystalline zone in the south, and is often referred to as the Tethyan slab. The richly fossiliferous, platform-type sediments of this region (Paleozoic-Mesozoic age) are clearly of Gondwana affinities and represent the former Indian margin. Burg and Chen (1984) showed that the Tethyan slab consists of several thrust sheets with distinct stratigraphies, states of deformation and metamorphic grades. Crustal shortening of the northern Tethyan slab is produced by decoupling and thrusting of both upper and lower crustal layers (Burg and Chen 1984). As the result of continental collision the Tethyan sediments are also intruded by Tertiary leucogranite. The leucogranite, dated between 10–20 Ma, (LeFort 1975, 1981; Vidal 1978; Wang *et al* 1981) appears to have a certain stratigraphic and structural relationship when compared with the position of the MCT. First, the metamorphic isograde run roughly parallel to the MCT for great distances (e.g. LeFort 1975). Second, the metamorphic isograde are inverted in the upper level of the Lesser Himalaya. A high $^{87}Sr/^{86}Sr$ ratio (e.g. LeFort 1981; Wang *et al* 1981) of the leucogranite clearly indicates that it was derived from a crustal source, however, the source of heat remains an enigma.

3.5 *Normal faulting in the High Himalaya*

Burg *et al* (1984) indicate the existence of an east-west striking, gently north-dipping normal fault of regional extent in the High Himalaya. This normal fault zone separates the highly metamorphosed crystalline rock and a transitional zone from the overlying late Precambrian to Cambrian sedimentary sequence. A similar type of normal faulting has been observed in the Zanskar region of the western Himalaya (Herren 1987). Movement along the shallow-dipping normal fault is believed to be about 20 km and limited to the deformation of upper crust. Analysis of two-mica granite shows that normal faulting is coeval with the south-directed overthrusting along the MCT (Copeland *et al* 1987). Burchfiel and Royden (1985) suggest that the tensional stress induced by the difference in topography between the Indian foreland and the southern edge of the Tibetan Plateau is a possible cause for the extensional faulting parallel to the Himalayan ranges. At present there are little data on these normal faults. It appears that the normal faulting can be considered as an important effect superimposed on the north-south regional compression.

3.6 *Strike-slip faulting*

A secondary effect of the north-south shortening of the Himalaya is the pervasive strike-slip faulting throughout most of the Lesser Himalaya. Valdiya (1976, 1981) indicated that the strike-slip faults have right-laterally displaced the MBT by as much as 12 km. Other examples of strike-slip faulting in the Nepal Himalaya have been

The Himalaya is seismically active. During the last decade not only have four great earthquakes ($M > 8$) occurred along the Himalaya, but also a large number of moderate-sized earthquakes. Local seismic networks are restricted to the western Himalaya and the Assam region. Therefore, earthquake hypocenters for the Himalayan events are based on teleseismic locations. Routine location procedures usually yield reasonably good locations with uncertainties not exceeding 20 km. However, the focal depths of these events can have errors of as much as 50 km. Recently developed techniques of synthetic body wave modelling of P and SH waves not only provide a better constraint on the orientation of nodal planes but also provide good depth control for shallow events to ± 3 km. Using this technique Baranowski *et al* (1984) and Ni and Barazangi (1984) showed that the moderate sized thrust-type events in the central and eastern Himalaya lie between 10 and 15 km depth. Based on a qualitative selection criteria, Ni and Barazangi (1984) showed that the better located epicenters are concentrated in a narrow zone, about 50 km wide, lying just south of the MCT (figure 3). Focal mechanisms obtained from forward waveform modelling indicate thrust faulting with one nodal plane dipping gently ($< 30°$) north or northeast beneath the Himalaya and the other nodal plane dipping steeply southward (figure 3). It is generally accepted that the shallow north-dipping nodal planes are the fault planes (figures 3, 4).

Projection of all reliable thrust-type events along the Himalayan arc into a single cross-section reveals that these events define a simple planar zone, having an apparent northward dip of about 15° (figure 4). This shallow northward dipping zone has been interpreted as a part of the master detachment of the Himalaya (Ni and Barazangi 1984).

Baranowski *et al* (1984) suggested that the orientation of slip vectors is approximately perpendicular to the Himalayan range. Their method of constraining the direction of slips was primarily based on forward modelling of *P* waves (SH waves were used for only a few earthquakes). The orientation of slip vectors is approximately perpendicular to the Himalayan range. Thus, the gravitational spreading of the overriding Himalaya and Tibet contributes greatly to the deformation of the Himalaya. Teleseismic earthquake data indicate that the MBT, rather than the MCT, is currently the active feature of the Himalayan arc. It is most probable that the great Himalayan events occur along the same detachment surface as defined by the moderate-sized thrust-type events (figure 5).

4.2 *P_n and S_n wave propagation beneath the Himalaya*

Variations in P_n and S_n velocities can be used to indicate regional differences in the physical properties of the uppermost mantle. Examples of high P_n velocities (8·2–8·4 km/s) and S_n velocities (4·7 km/s) have been reported for a variety of continental shield regions (Brune and Dorman 1963; Bath 1966; Huestis *et al* 1973), whereas low P_n velocities (7·7–7·8 km/s) and S_n velocities (4·4–4·5 km/s) characterize, for example, most of the Basin and Range province in which the lithosphere is thin and heat flow values are high (Eaton 1980).

P_n and S_n travel times from earthquakes in the Himalaya to the World Wide

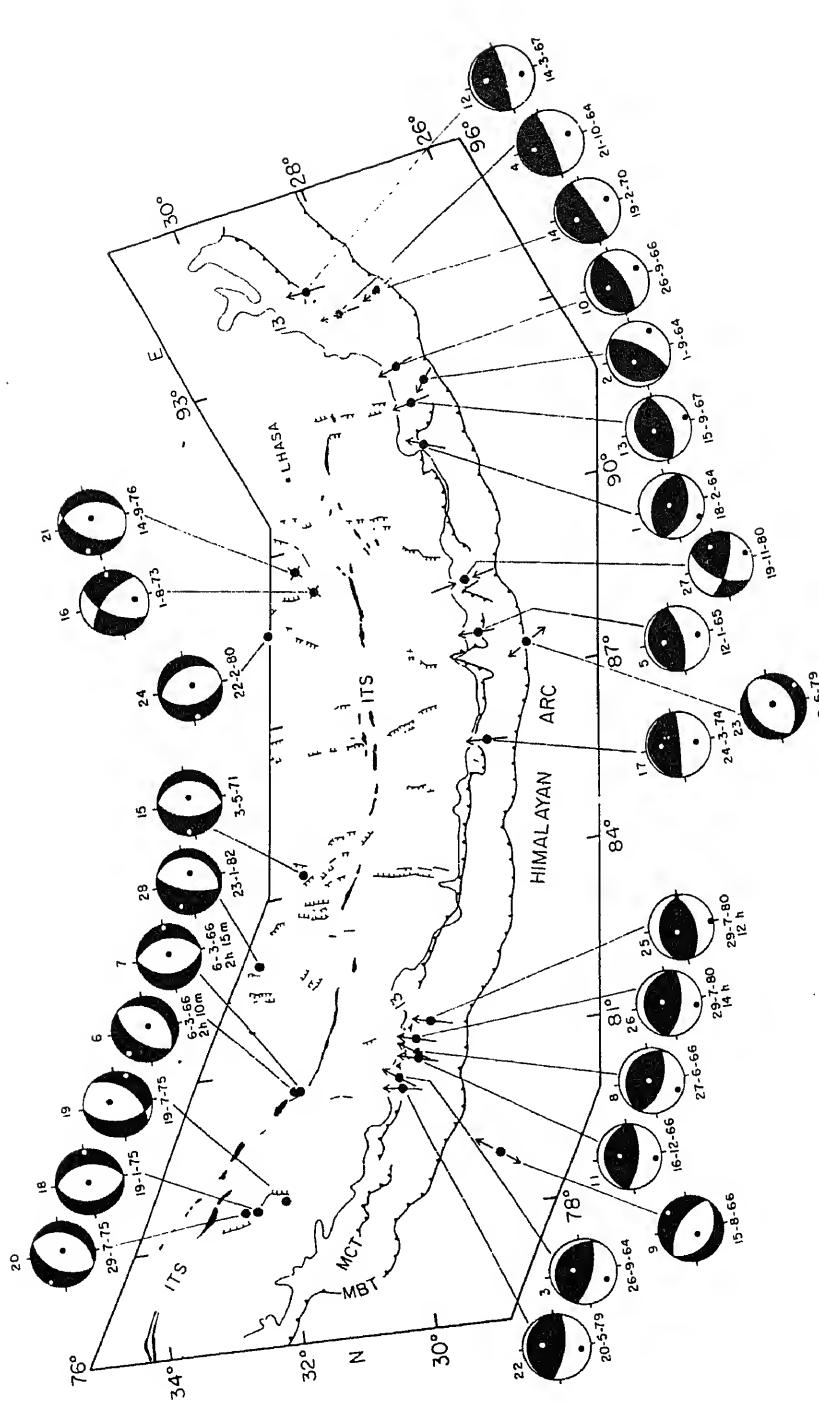

Figure 3. Seismotectonic map of the Himalayan region. Lower hemisphere projections of fault-plane solutions (from Baranowski *et al* 1984; Ni and Barazangi 1984). Positions of ITS (Indus Tsangpo Suture), MCT, MBT and spatially averaged 13,000-foot contour are also shown.

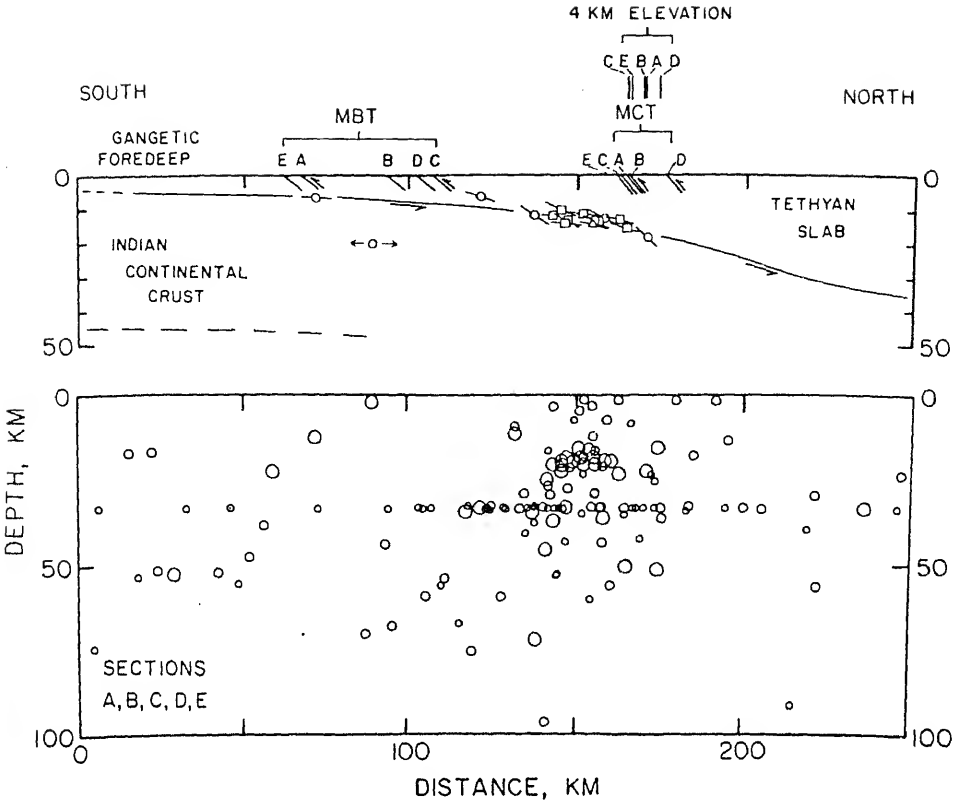

Figure 4. A composite cross-section using the MCT and the 4-km elevation contour as a reference for projection. Bottom section shows ISC hypocenters. The larger the open circle the better the epicenter location. Notice that the majority of earthquakes are located south of the MCT In the top section the projected low-angle nodal planes for thrust-type focal mechanisms are shown as line segments drawn across the accurately located depths of hypocenters. From Ni and Barazangi (1984).

Standard Seismograph Network (WWSSN) stations at northern Afghanistan, India, and to the local network at northern Pakistan, have been used to resolve the uppermost mantle P and S wave velocities. For paths along the Himalaya to the Tarbela Dam network in northern Pakistan, Menke and Jacob (1976) obtained P_n and S_n velocities of $8{\cdot}5 \pm 3{\cdot}5$ km/s and $5{\cdot}00 \pm 2{\cdot}0$ km/s respectively. With WWSSN data, Ni and Barazangi (1983) obtained $8{\cdot}45 \pm 0{\cdot}08$ km/s and $4{\cdot}74 \pm 0{\cdot}5$ km/s (figure 6), which are similar to the corresponding P_n and S_n velocities for the uppermost mantle beneath the Indian Shield and Southern Tibet. The crustal and uppermost mantle velocity structure of the Himalaya derived from body waves (Ni and Barazangi 1983) is consistent with that obtained from surface wave dispersion (Gupta and Narain 1967). The high P_n and S_n velocities indicate that the uppermost mantle structure beneath the Himalaya is not significantly different from that of India and southern Tibet and is consistent with a model in which the Indian continental lithosphere is being underthrust beneath the Himalaya and southern Tibet.

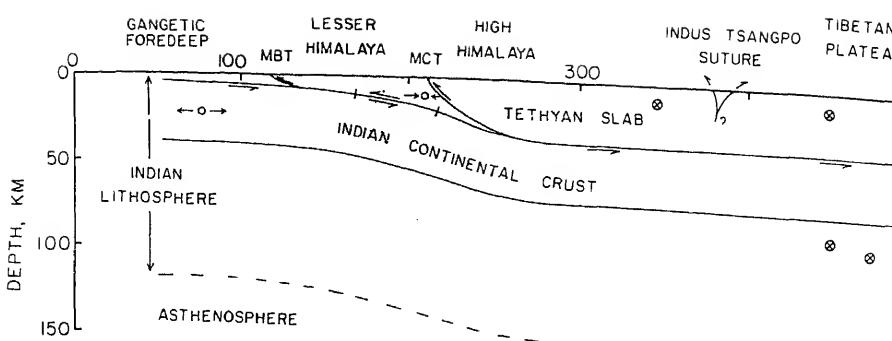

Figure 5. A schematic cross-section of the present geometries of converging plates i Himalaya-Tibetan region. Events with normal-type focal mechanisms located in the sh crust and uppermost mantle of Tibet are shown as open circles with crosses. All Hima thrust-type events can be interpreted most simply to define a part of the detachment be the underthrusting Indian plate and the upper Himalayan crustal blocks.

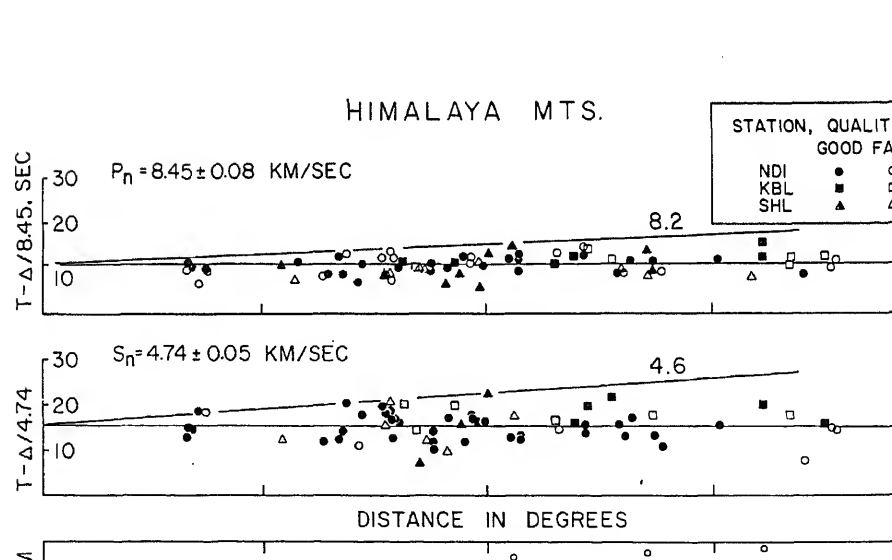

Figure 6. Reduced travel-time plots of P_n and S_n data recorded at station NDI, KB SHL. At least 50% of the propagation paths are within the Tibetan Plateau. The botto shows ISC hypocentral depth vs epicentral distance for events used in the above trave plots.

4.3 *Refraction profiles and wide-angle reflections beneath the Himalaya*

Significant information on the velocity structure of the Himalaya comes from: (i) an unreversed profile that crosses the western Himalaya (Kaila *et al* 1978; Beloussov *et al* 1980); and (ii) wide-angle reflection profiles recorded in Nepal (Hirn and Sapin 1984; Hirn *et al* 1984a, b).

Two spreads, one 6 km long and the other 11 km long, located near the Srinagar region of the Kashmir Himalaya recorded shots fired in Pakistan and USSR. These data recorded clear reflection from the Moho. Kaila *et al* (1978) showed that the Moho is at a depth of about 45 km near Sopur, dips to 54 km in the region of Wular Lake and continues to deepen further toward the north. Such geometry indicates a moderate, 15° to 20° northwesterly dip of the Moho. The dip of the Moho could be an overestimate because the profile is not reversed.

Wide-angle reflection data in the Tethyan and High Himalaya were collected by Hirn and his colleagues. Seismograms recorded at Arun valley and Kathmandu valley from shots in southern Tibet showed two clear phases separated by about 2 s. The later phases were interpreted as a P_mP (Moho) reflection from 75 km depth (Lepine *et al* 1984). The earlier phase was attributed to reflection from the top surface of the underthrusting Indian Plate (Hirn and Sapin 1984). Although Lepine *et al* 1984) suggested that a step in the Moho existed somewhere just north of the High Himalaya, Molnar (1988) indicated that six seismograms are insufficient to constrain the geometry of the Moho.

Most of the evidence supporting a southward dipping Moho beneath the Himalaya is from a fan profile constructed with seismograms at distances of 170 to 300 km recorded in Nepal and southern Tibet (figure 7). The arrival times from the first strong signals recorded by seven stations located north of the High Himalaya (figure 3 of Hirn *et al* 1984a) show a southward dipping reflector from 45 to 50 km depth. Hirn *et al* (1984a) interpreted this reflector as representing a southward dipping Moho. Molnar (1988) argued that this reflector can be associated with reflection from an interface within the crust. Moreover, he pointed out that reflections in the fan profile are consistent with a Moho increasing smoothly from 50 to 55 km beneath the Great Himalaya to about 70 km in the southern Tethyan Himalaya.

4.4 *Gravity anomalies across the Himalaya*

Gravity anomalies in the Himalaya place constraints on the deep structures and the dynamics of mountain building. In the Himalaya large Bouguer anomalies become increasingly negative as the elevation increases, their values reach about −400 mGals over the Great Himalaya (Marussi 1964; Quershy 1969; Quershy and Warsi 1980; Verma and Prasad 1987). This northward decrease in Bouguer anomalies is interpreted to indicate some sort of isostatic compensation in the Himalaya. However, large negative isostatic anomalies (−100 mGals) over the Ganga Basin and (+80 mGals) in the High Himalaya indicate deviation from local isostatic compensation (e.g. Warsi and Molnar 1977; Lyon-Caen and Molnar 1983). The apparent causes of this deviation from isostatic equilibrium are the focus of recent studies (Lyon-Caen and Molnar 1983, 1985). Negative isostatic anomaly over the Ganga Basin can be explained, at least in part, by the several kilometers of low density upper Cenozoic sediments. Positive isostatic anomaly over large parts of the High Himalaya could be a result of thickening of a basaltic layer in the lower crust (Quershy and Warsi 1980).

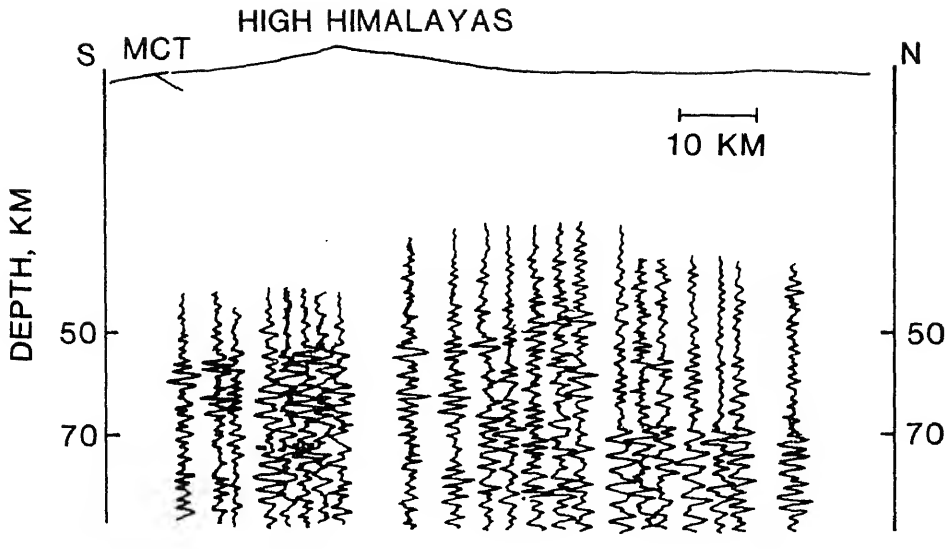

Figure 7. A north-south fan-profile across the Greater Himalaya, from Hirn *et al* (1984a). Reflection times are corrected to a constant offset of 200 km. Reflections from about 70 km on the north and from about 55 km on the south are quite clear. Northward shallowing reflectors to depths of 50 to 45 km are seen on the middle traces. Note strong signals that follow these mid-crust reflectors from 65 km (9th and 10th traces) to about 75 km on the 14th and 15th traces. Thus, the wide angle reflection data are consistent with a northward dipping Moho from 55 km on the southern to 75 km on the northern Greater Himalaya.

Deficiency and excessive distribution of mass in the Himalaya must be supported by stress differences within the lithosphere and mantle. Thus, gravity anomalies in the Himalaya can be used to examine how the mountains are supported. In a simple elastic flexure model where the Indian lithosphere extends to the Indus-Tsangpo suture zone, the overburden is too great to depress the Ganga Basin deeper than observed, and the calculated gravity anomalies are much too negative (Lyon-Caen and Molnar 1983). Therefore, a simple flexure model cannot account for the gravity anomalies across the Himalaya.

The Indian lithosphere underthrusts beneath the Ganga Basin and Lesser Himalaya at a shallower angle than beneath the High Himalaya implying the Moho also has different dips. Recognizing this, Lyon-Caen and Molnar (1985) computed Bouguer gravity anomalies across the Himalaya using an elastic plate model with different flexure rigidity. Their calculations indicate that the load of the mountain is still too great to yield gravity anomalies over the Lesser Himalaya and Ganga Basin that are comparable with the observed values. A moment must be applied to the end of the elastic plate to properly support the Himalayan mountains. This moment can be related to either a horizontal force or a vertical force. Lyon-Caen and Molnar (1985) ruled out the horizontal force because it must have an excess horizontal compressive stress of at least 330 MPa. On the other hand, the vertical force can be related to phase change of the lower crustal material in the underthrusted Indian lithosphere and is more plausible.

In our opinion, analysis of gravity data explains the broad features of the Moho configuration that are consistent with a smoothly increasing Moho from 38 km

eneath the Ganga Basin to about 55 km beneath the High Himalaya. Mountain uilding involves processes not only confined in the lithosphere but also in the upper ıantle. The nature of the forces that support the excess weight of the mountain emain to be discovered.

. Pakistan Himalaya

ıformation about the geometry of the underthrusting Indian plate within the akistan Himalayan foreland and fold-and-thrust belt has been reported by Lillie *t al* (1987). Based on the interpretation of oil company reflection data they showed ıat beneath a salt detachment, the Indian crystalline basement dips gently northward om about 1° beneath the Salt range to about 4° beneath the northern Potwar lateau (figure 8). Their results confirm earlier interpretations that detachment lies ithin an Eocambrian evaporite sequence. The extent of this detachment and the eometry of the Indian plate farther north beneath the Peshawar basin are not clear.

Based on an analysis of local seismicity data Seeber and Armbruster (1979) showed wo northwesterly trending basement features, the Hazara Lower Seismic Zone HLSZ) and the Indus-Kohistan Seismic Zone (IKSZ) (figure 9). They interpreted ıese features as buried extensions of the northwesterly trending Himalayan thrust ıults beyond their surface termination at the western Himalayan Syntaxis. The IKSZ, ıe more active of the two seismic zones, is associated with underthrusting toward the ortheast (Seeber and Armbruster 1979). The HLSZ defines a steeply dipping asement fault which may merge southward with a shallow dipping surface of etachment between the basement and the sedimentary rocks of the Salt Range. roving such a relation, however, requires that one knows the deep structures beneath ıis region.

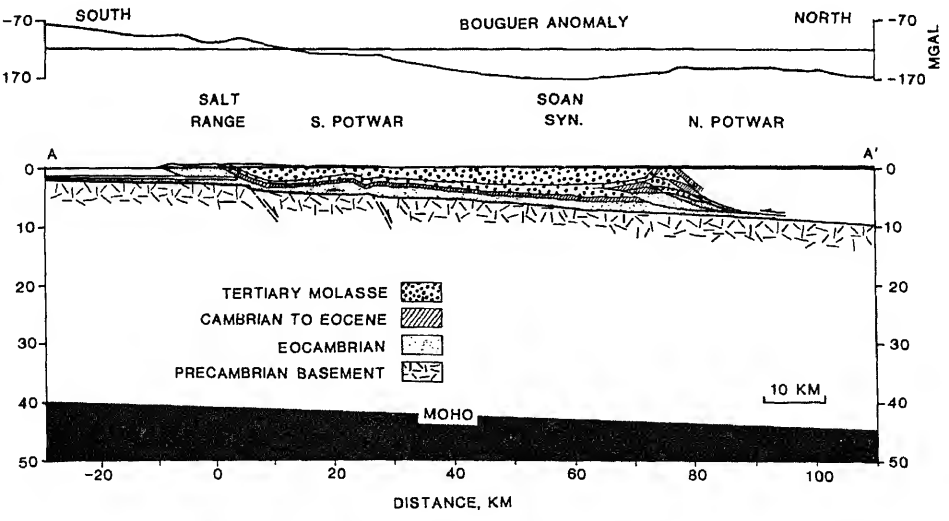

Figure 8. Structural cross-section and Bouguer gravity profile of northern Jhelum Plain, Salt Range and central Potwar Plateau, from Lillie *et al* (1987). The gradient in the Bouguer gravity in this region is about 1 mgal/km and is similar to that of the Indo-Gangetic Plain.

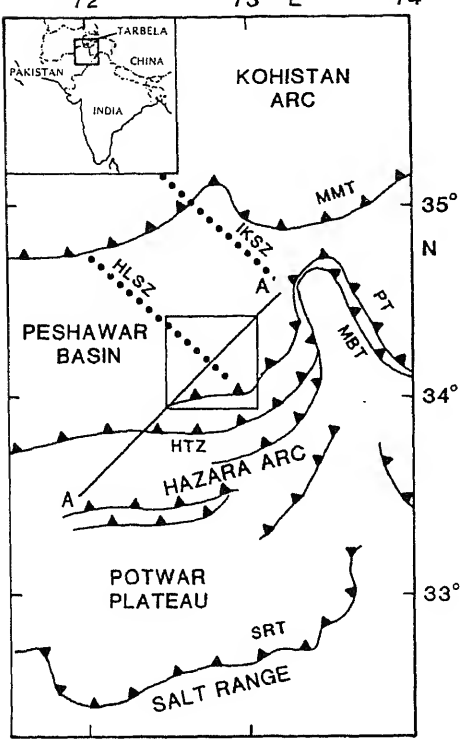

Figure 9. Simplified tectonic map of the western Himalayan syntaxis region. MBT, main boundary thrust; MMT, main mantle thrust; HTZ, Hazara thrust zone; PT, Panyal thrust; SRT, salt range thrust; HLSZ, Hazara lower seismic zone; IKSZ, Indus-Kohistan seismic zone.

A recent study (Ibenbrahim *et al* 1987) of the three-dimensional *P* wave velocity structure beneath the northern Hazara thrust zone and the eastern Peshawar basin from inversion of *P* wave travel time data produced by the Tarbela Dam array indicates that the 6·2 km/s velocity surface dips northerly from about 13 km beneath the Hazara thrust zone (equivalent of MBT of the central Himalaya) to 17 km beneath the northern Peshawar basin. This surface has an apparent dip of about 8° and is interpreted as the top surface of the underthrusting Indian Plate. This result incorporated with observations from the foreland (e.g. Farah *et al* 1977; Yeats and Hussain 1987; Lille *et al* 1987) is used to illustrate the geometry of the underthrusting Indian lithosphere in the Pakistan Himalaya. Beneath the Salt Range and Potwar Plateau the crystalline basement of the Indian Shield dips smoothly northward from about 1° to about 4°. The detachment extends farther north beneath the Peshawar basin with an increased slope of 5°–10° (figure 10). The relocated hypocenters of shallow crustal events cluster at 11–14 km depth and are associated with the activity in the interplate seismic zone beneath the Peshawar basin. A steeper dip of the detachment is consistent with the mechanical thrusting model in which shale or other incompetent materials rather than evaporite form the zone of decollement (Davis *et al* 1983). Thus, an important implication of the steeper underthrusting of the Indian plate beneath the Peshawar basin is that this portion of the detachment appears to involve no salt and is capable of producing great earthquakes.

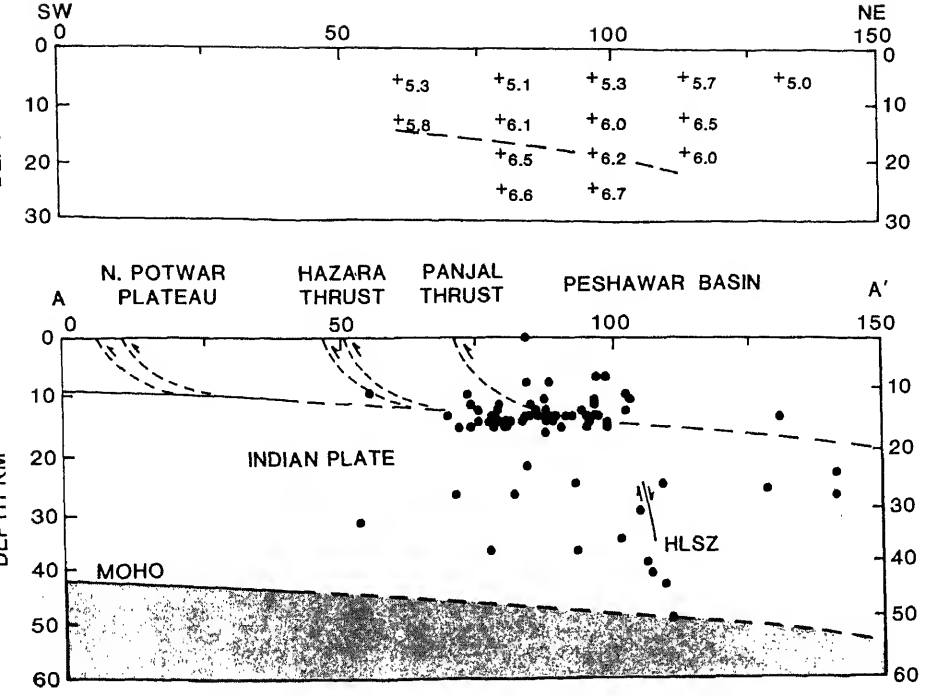

Figure 10. Structure cross-section (AA' in figure 9) shows that the gently dipping Indian plate beneath the Peshawar Basin correlates with the 6·2 km/s *P*-wave velocity contour. From Ibenbrahim *et al* (1987).

6. Rates of uplift of the Himalaya

It has been suggested by many authors that the uplift of the Himalaya occurred during recent geological time, especially during Quaternary and Holocene time (Wadia 1979; Zeitler *et al* 1982; Zeitler 1985; Coward *et al* 1987). A repeated levelling profile across the Himalayan frontal zone indicates as much as 6 mm/yr of uplift in a 12-year period of the front with respect to the Ganga Basin (Chugh 1974; Molnar *et al* 1977). Although the levelling data suggest very rapid uplift, lower rates have been given when longer durations are considered.

Uplift rates using fission track methods imply movements of about 1 mm/yr or less in the western Himalaya. However, higher rates of 7 mm/yr have been reported for the Nanga Parbat-Haramosh region (Zeitler 1985). The increased uplift around the Nanga Parbat-Haramosh massif represents the culmination of Nanga Parbat Gneiss. Several millimeters per year uplift rates in the Higher Himalaya have been inferred from pollen and spores imbedded in the Quaternary sediments (e.g. Xu 1981). Table 1 gives estimates of uplift rates for the Himalaya. These uplift data indicate that rapid and recent uplift applies only to the region in which it is observed and does not suggest that recent uplift is at an accelerating rate.

Table 1. Uplift rates of the Himalayan mountains.

Uplift rates (mm)	Method of determination	Source
0·1 to 4·5	Fission-track dating	Zeitler (1985)
0·6 to 0·8	Fission-track dating	Mehta (1980)
1·0 to 1·4	River profiles	Seeber and Gornitz (1983)
2	Bengal fan deposition	Curray and Moore (1971)
0·1 to 1	River terraces	Iwata *et al* (1984)
1·2 to 1·5	Levelling of river terraces	Iwata (1987)
6	Second order levelling	Chugh (1974)
5 to 12	Flexural modelling	Lyon-Caen and Molnar (1983)

7. Summary

The Himalaya is a product of the collision between India and Eurasia which began in the Eocene. In the earlier stage of continental collision the development of a suture zone between two colliding plates took place. A modern analogue of this stage may be the collision between the northern Australian continental margin and the Banda arc in the Timor island region. The continued convergence is accommodated along the suture zone and in the back-arc region. The Zagros represents an example of this stage. Further convergence results in intracrustal megathrust within the leading edge of the advancing Indian plate. In the Himalaya this stage is characterized by intense uplift of the High Himalaya and the development of the Tibetan Plateau in the back-arc region. The tectonics of the modern Himalaya can be best explained by the model of Ni and Barazangi (1984). In this model (figure 5), the southern edge of the High Himalaya is likened to a curved bulldozer blade that scrapes most sediments from the Indian crust, and underthrusting proceeds without fundamental changes in the major structure.

Geological and geophysical constraints presented in this review are still insufficient to tightly constrain models outlined in the earlier section. Reflection profiles across the entire Himalaya and Tibet are needed to better resolve the deep crustal structures. Dense seismic and geodetic networks in the High Himalaya are needed to resolve the seismogenic nature of the MCT and the detailed structures. Initiation of paleoseimicity studies is necessary to resolve the temporal and spatial patterns of major earthquake faulting along the Himalaya.

References

Allegre C J *et al* 1984 Structure and evolution of the Himalaya-Tibet orogenic belt; *Nature (London)* **307** 17–22

Argand E 1924 La Tectonique de l'Asie; *Int. Geol. Congr. Rep. Sess. 13* **1** 170–732

Baranowski J, Armbruster J, Seeber L and Molnar P 1984 Focal depths and fault plane solutions of earthquakes and active tectonics of the Himalaya; *J. Geophys. Res.* **89** 6918–6928

Barazangi M and Ni J 1982 Velocities and propagation characteristics of P and S beneath the Himalayan arc and Tibetan Plateau: possible evidence for underthrusting of Indian continental lithosphere beneath Tibet; *Geology* **10** 179–185

Kharmabeav I Kh, Kaila K L, Narain H, Marussi A and Finetti J 1980 Structure of the lithosphere along deep seismic sounding profile: Tien Shan-Pamirs-Karakorum-Himalayas; *Tectonophysics* **70** 193–221

Bird P 1978 Initiation of intra-continental subduction in the Himalaya; *J. Geophys. Res* **83** 4975–4987

Brune J and Dorman J 1963 Seismic waves and earth's structure in the Canadian Shield; *Bull. Seismol. Soc. Am.* **43** 167–210

Burchfiel B C and Royden L H 1985 North-south extension within the convergent Himalayan region; *Geology* **13** 679–682

Burg J P and Chen G M 1984 Tectonics and structural zonation of sourthern Tibet, China; *Nature (London)* **331** 219–223

Burg J P, Brunel M, Gapais D, Chen G M and Liu G H 1984 Deformation of leucogranites of the crystalline main central sheet in southern Tibet (China); *J. Struct. Geol.* **6** 535–542

Chen W-P and Molnar P 1981 Constraints on the seismic wave velocity structure beneath the Tibetan Plateau and their tectonic implications; *J. Geophys. Res.* **86** 5937–5962

Chugh R S 1974 Study of recent crustal movements in India and future programs; paper presented at the *International Symposium on Recent Crustal Movements, Zurich*

Copeland P, Harrison T M, Parrish R, Burchfiel B C, Hodges K and Kidd W S F 1987 Constraints on the age of normal faulting, north face of Mt. Everest: Implication for Oligo-Miocene uplift; *EOS Trans. Am. Geophys. Union* **68** 1444

Coward M P, Butler W H, Khan M A and Knipe R J 1987 The tectonic history of Kohistan arc and its implications for Himalayan structure; *J. Geol. Soc. London* **144** 377–391

Curray J R and Moore D G 1971 Growth of the Bengal deep-sea fan and denudation in the Himalayas; *Bull. Geol. Soc. Am.* **82** 563–572

Davis D M, Suppe J and Dahlen F A 1983 Mechanics of fold-and-thrust belts and accretionary wedges; *J. Geophys. Res.* **88** 1153–1172

Dewey J F and Bird J M 1970 Mountain belts and the new global tectonics; *J. Geophys. Res.* **75** 2625–2647

Eaton G P 1980 Geophysical and geological characteristics of the crust of the Basin and Range province, in *Continental tectonics* (ed.) Geophysics Study Committee (Washington DC: National Acad. Sci.) pp. 96–113

Farah A, Mirza M A, Ahman M A and Butt M H 1977 Gravity field of the buried shield in the Punjab plain, Pakistan; *Geol. Soc. Am. Bull.* **88** 1147–1155

Fuchs G R 1975 Contribution to the geology of the northwestern Himalaya; *Abh. Geol. B A* **32** 1–59

Gansser A 1964 *The Geology of the Himalaya* (London, New York, Sydney: Interscience Publishers) p. 289

Gansser A 1977 The great suture zone between Himalaya and Tibet: a preliminary account. In *Colloq. Int. 268, Ecologie et géologiè de l'Himalaya*, Paris 1976, ed. Cent. Natl. Rech. Sci. Vol. Sci. de la Ture, 181–191

Gansser A 1980 The significance of the Himalayan suture zone; *Tectonophysics* **62** 181–191

Gansser A 1982 The morphogenic phase of mountain building. In *Mountain building processes* (ed.) K J Hsu (London: Academic Press) pp. 221–228

Gupta H K and Narain H 1967 Crustal structure of the Himalayan and Tibet Plateau region from surface wave dispersion; *Bull. Seismol. Soc. Am.* **57** 235–248

Herren E 1987 Zanskar shear zone: Northeast-southwest extenstion within the Higher Himalayas (Ladakh, India); *Geology* **15** 409–413

Hirn A and Sapin M 1984 The Himalayan zone of crustal interaction: Suggestions from explosion seismology; *Ann. Geophysicae* **2** 123–130

Hirn A *et al* 1984a Crustal structure and variability of the Himalayan border with Tibet; *Nature (London)* **307** 23–25

Hirn A, Jobert G, Wittlinger G, Xu Zhongxin and Gao Enyuan 1984b Main features of the upper lithosphere in the unit between the high Himalayas and the Yarlung Zhangbo Jiang suture; *Ann. Geophysicae* **2** 113–117

Huestis S, Molnar P and Oliver J 1973 Regional S_n velocities and shear velocity in the upper mantle; *Bull. Seismol. Soc. Am.* **63** 469–475

Ibenbrahim A, Ni J and Gross R 1987 Three-dimensional crustal velocity structure beneath the Tarbela array, Pakistan; *EOS Trans. Am. Geophys. Union* **68** 1373

Isacks B, Oliver J and Sykes L R 1968 Seismology and the new global tectonics; *J. Geophys. Res.* **73** 5855–5900

Iwata S, Sharma T and Yamanaka H 1984 A preliminary report on geomorphology of Central Nepal and Himalayan uplift; *J. Nepal Geol. Soc.* **4** 141–149 (special issue)

Kaila K L, Kirshna V G, Choudhury K and Narain H 1978 Structure of the Kashmir Himalaya from deep seismic soundings; *J. Geol. Soc. India* **19** 1–20

LeFort P 1975 Himalayas: the collided range. Present knowledge of the continental arc; *Am. J. Sci.* **A275** 1–44

LeFort P 1981 Manaslu leucogranite: A collision signature of the Himalaya, a model for its genesis and emplacement; *J. Geophys. Res.* **86** 10545–10568

Lepine J-C, Hirn A, Pandey M R and Tater J M 1984 Features of the *P* waves propagated in the crust of the Himalayas; *Ann. Geophysicae* **2** 119–121

Lillie R J, Johnson G D, Mohammed Y, Zamin A S H and Yeats R S 1987 Structural development within the Himalayan foreland fold-and-thrust belt of Pakistan. In *Sedimentary basins and basin-forming mechanisms* (eds) C Beaumont and A J Tankard; *Canadian Society of Petroleum Geologists, Memoir* **12** 379–392

Lyon-Caen H and Molnar P 1983 Constraints on the structure of the Himalaya from an analysis of gravity anomalies and a flexural model of the lithosphere; *J. Geophys. Res.* **88** 8171–8191

Lyon-Caen H and Molnar P 1985 Gravity anomalies, flexure of the Indian plate, and the structure, support and evolution of the Himalaya and Ganga Basin; *Tectonics* **4** 513–538

Marussi A 1964 Geophysics of the Karakorum Italian expeditions to the Karakorum (L2 and Hindu Kush) Sci. Rept. 2, 1, p. 242

Mathur L P and Evans P 1964 *Oil in India. Sp. Brochure. Int. Geol. Congr. 22nd Session New Delhi* 64–79

Mehta P I C 1980 Tectonic significance of the young mineral dates and rates of cooling and uplift in the Himalayas; *Tectonophysics* **62** 205–212

Menke W H and Jacob K H 1976 Seismicity patterns in Pakistan and northwestern India associated with continental collision; *Bull. Seismol. Soc. Am.* **66** 1695–1711

Molnar P 1984 Structure and tectonics of the Himalaya: Constraints and implications of geophysical data; *Annu. Rev. Earth Planet. Sci.* **12** 489–518

Molnar P 1988 A review of geophysical constraints on the deep structure of the Tibetan Plateau, the Himalaya, and the Karakorum; *Philos. Trans. R. Soc. London* (in Press)

Molnar P and Chen W-P 1982 Seismicity and mountain building. In *Mountain building processes* (ed.) K Hsu (London: Academic Press)

Molnar P and Tapponnier P 1975 Cenozoic tectonics of Asia: Effects of a continental collision; *Science* **189** 419–426

Molnar P, Chen W-P, Fitch T J, Tapponnier P, Warsi W E K and Wu R T 1977 Structure and tectonics of the Himalaya: A brief summary of geophysical observations. In *Colloq. Int. C.N.R.S. Ecologie et Geologie de L'Himalaya vol. 2* 269–294

Nakata T 1988 Active faults of the Himalaya of India and Nepal; *Bull. Geol. Soc. Am.* (in review)

Ni J and Barazangi M 1983 High-frequency seismic wave propagation beneath the Indian Shield, Himalayan arc, Tibetan Plateau, and surrounding regions: high uppermost mantle velocities and efficient S_n propagation beneath Tibet; *Geophys. J. R. Astron. Soc.* **72** 665–689

Ni J and Barazangi M 1984 Seismotectonics of the Himalayan collision zone: Geometry of the underthrusting Indian plate beneath the Himalaya; *J. Geophys. Res.* **89** 1147–1163

Powell C M 1979 A speculative tectonic history of Pakistan and surroundings: some constraints from the Indian Ocean. In *Geodynamics of Pakistan* (eds) A Farah and K DeJong, (Quetta: Geol. Surv. of Pakistan) p. 5–24

Powell C M and Conaghan P J 1973 Plate tectonics and the Himalayas; *Earth Planet. Sci. Lett.* **20** 1–12

Powell C M and Conaghan P J 1975 Tectonic models of the Tibetan Plateau; *Geology* **3** 727–731

Pratt J H 1985 On the attraction of the Himalayan mountains, and of elevated regions beyond them, upon the plumb line in India; *Philos. Trans. R. Soc. London* **145** 53–100

Qureshy M N 1969 Thickening of the basalt layer as a possible cause for the uplift of the Himalayas—a suggestion based on gravity data; *Tectonophysics* **7** 137–157

Qureshy M N and Warsi W E K 1980 A Bouguer anomaly map of India and its relation to broad tectonic elements of the sub-continent; *Geophys. J. R. Astron. Soc.* **61** 235–242

Seeber L and Armbruster J 1979 Seismicity of the Hazara Arc in northern Pakistan: Decollement versus basement folding. In *Geodynamics of Pakistan* (eds) A Farah and K A DeJong (Quetta: Geol. Surv. Pakistan) p. 131–142

Seeber L and Armbruster J 1981 Great detachment earthquakes along the Himalayan arc and long-term

forecasts; *Earthquake prediction: An international review, Maurice Ewing Series 4*, (eds) D W Simpson and P G Richards (Washington DC: Am. Geophys. Union) pp. 259–277

Seeber L, Armbruster J and Quittmeyer R 1981 Seismicity and continental collision in the Himalayan arc. In *Zagros. Hindu Kush, Himalaya, Geodynamic evolution;* Geodynamics Series vol. 3 (Washington DC: Am. Geophys. Union) pp. 215–242

Seeber L and Gornitz V 1983 River profiles along the Himalayan arc as indicators of active tectonics; *Tectonophysics* **92** 335–367

Sinha-Roy S 1982 Himalaya main central thrust and its implications for Himalayan inverted metamorphism; *Tectonophysics* **84** 197–224

Stocklin J 1980 Geology of Nepal and its regional frame; *J. Geol. Soc. London* **137** 1–34

Tapponnier P and Molnar P 1977 Active faulting and tectonics in China; *J. Geophys. Res.* **82** 2905–2930

Verma R K and Prasad K A V L 1987 Analysis of gravity fields in the northwestern Himalayas and Kohistan region using deep seismic sounding data; *Geophys. J. R. Astron. Soc.* **91** 869–889

Valdiya K S 1976 Himalayan transverse faults and folds and their parallelism with subsurface structures of north Indian plains; *Tectonophysics* **23** 353–386

Valdiya K S 1980 The two intracrustal boundary thrusts of the Himalaya; *Tectonophysics* **66** 323–348

Valdiya K S 1981 Tectonics of the central sector of the Himalaya. In *Zagros, Hindu Kush, Himalaya, Geodynamic evolution* Geodynamics Series, (eds) H Gupta and F Delany, vol. 3 (Washington DC: Am. Geophys. Union) and (Boulder: GSA) pp. 87–110

Vidal Ph 1978 Rb-Sr systematics in granite from central Nepal (Manaslu): Significance of the Oligocene age and high 87Sr/86Sr ratio in Himalayan orogeny. Comment; *Geology* **6** 196

Wadia D N 1961 *The Geology of India* Third edn. (London: Macmillan)

Wadia Institute of Himalayan Geology, 1979 Annual Report 1978–79, Dehra Dun, India, 2–45

Wang J, Chen Z, Gui X, Xu R and Zhang Y 1981 Rb-Sr isotopic studies on some intermediate-acid plutons in southern Xizang. In *Geological and ecological studies of Qinghai-Xizang Plateau* (Beijing: Science Press) vol. 1, p. 515–520

Warsi W E K and Molnar P 1977 Gravity anomalies and plate tectonics in the Himalaya, Colloques Internationaux de CNRS, No. 268, *Himalaya: Sciences de la Terre*, Editions du Centre National de la Recherche Scientifique, Paris, 463–478

Xu R 1981 Vegetational changes in the past and the uplift of Qinghai-Xizang plateau. In *Geological and ecological studies of Qinghai-Xizang Plateau* (Beijing: Science Press) vol. 1, 139–144

Yeats R S and Hussain A 1987 Timing of structural events in the Himalayan foothills of northwestern Pakistan; *Geol. Soc. Am. Bull.* **99** 161–176

Zeitler P K 1985 Cooling history of the N W Himalaya, Pakistan; *Tectonics* **4** 127–151

Zeitler P K, Johnson N M, Naeser C W and Tahirkheli A K 1982 Fission-track evidence for Quaternary uplift of the Nanga Parbat region, Pakistan; *Nature (London)* **298** 255–257

New seismological results on the tectonics of the Garhwal Himalaya

K N KHATTRI, RAMESH CHANDER, V K GAUR*, I SARKAR and SUSHILKUMAR

Department of Earth Sciences, University of Roorkee, Roorkee 247 667, India
*National Geophysical Research Institute, Uppal Road, Hyderabad 500 007, India

Abstract. This paper reports data pertaining to 90 local earthquakes recorded during 1984–86 using seismographs in arrays of 5–7 stations deployed near the Main Central Thrust between Bhagirathi and Alakhananda valleys. The results which are also compared with 162 earthquakes recorded in 1979–80 provide a local view that refines and complements information recorded at distant seismic stations.

Keywords. Garhwal Himalaya; local earthquakes; seismo-tectonic model; focal mechanisms.

1. Introduction

Broadly speaking, the Garhwal Himalaya, drained by the Yamuna, the Bhagirathi and the Alakhnanda rivers constitute the middle part of Burrard's and Gansser's Kumaun Himalaya extending from the Sutlej to the Kali river. The meizoseismal area of the 1905 Kangra earthquake (magnitude 8·6) extended into the western part of the Garhwal Himalaya (Molnar, this volume). The eartern part of the region marks the western end of the 700-km-long seismic gap extending up to the rupture zone of the 1934 Bihar-Nepal earthquake (magnitude 8·4). The region has not experienced a major earthquake (magnitude $> 8{\cdot}0$) in recorded history and unless it happens to be an exceptional segment of the Himalaya collision zone distinguished only by strain releases through small and intermediate magnitude earthquakes, the ambient stresses here must be fairly high.

In this study, data for 90 local earthquakes recorded during 1984–86, using portable seismographs in arrays of 5 to 7 stations deployed in the vicinity of the Main Central Thrust (MCT) between Bhagirathi and Alakhnanda valleys, are reported and considered along with the previously published results for 162 earthquakes recorded in 1979–80 in the vicinity of the MCT between the Yamuna and Bhagirathi valleys. The epicentres of these 252 earthquakes define a 140-km-long seismic belt stretching from northwest of the Yamuna valley southeastward upto the Alakhnanda valley. The width of the belt varies between 30 and 50 km. The estimated focal depths of 225 earthquakes were less than 13 km, while those of the remaining 27 were between 13 and 23 km. The first motion data for 50 earthquakes provided two composite focal mechanism solutions. Data for 29 earthquakes defined a strike-slip solution. Twenty of these earthquakes occurred NW of the Bhagirathi river. Data for the other 21 earthquakes defined a thrust solution. Nineteen of these earthquakes occurred SE of the Bhagirathi river. The maximum compressive stress direction is very nearly identical in both cases, being oriented NE–SW. The thrust solution yields a modest plunge of 15° to the NE for the axes of maximum compressive stress.

plate involved in the Himalayan convergence. A general stress-state conducive to thrust or reverse faulting appears to exist in the overriding plate from the ground surface down to its lower boundary where it is in contact with the under-thrusting Indian plate. The strike-slip earthquakes may be explained by postulating a modification of this stress-state through tensile stresses due to a flexure of the overriding plate over a ridge-like feature on the top surface of the subducting plate. The ridge would be a northeastward salient of the Pre-Cambrian Aravalli ranges of Rajasthan whose outcrops can be seen as far north as New Delhi and which probably continue northeastward under the Sindhu-Ganga alluvium and even the Lesser and High Himalaya. The crest of the ridge may be approximately along 78°E. The tensile stresses generated on this account would attenuate with distance perpendicular to the ridge crest. The ridge which is transverse to the Himalaya perhaps decouples the rupture zone of the 1905 Kangra earthquake from the seismic gap that lies east of it, thereby facilitating the strain release on these segments at their separate rates.

The seismic belt associated with the Himalayan collision boundary has so far been delineated mainly on the basis of teleseismic and regional data. Here we present information about earthquake locations and source mechanisms for a part of the Garhwal Himalaya (figure 1) segment of the seismic belt as gleaned from seismograms recorded locally, using portable seismographs deployed in arrays of small areal extent. Combined with data and results from Gaur *et al* (1985) (hereafter referred to as paper I) this provides a unique local view that refines and complements the information recorded at distant seismic stations.

1.1 *Nomenclature*

The administrative districts of Pauri, Chamoli, Uttarkashi, Tehri and Dehradun constitute the region of the Garhwal Himalaya. This region forms a somewhat bigger middle third of Burrard's (see Wadia 151, p. 9 and Gansser 1964, p. 8) "Kumaon Himalaya" which extended from Sutlej to Kali river. Alternatively, the region forms the western, bigger part of Valdiya's (1980, p. 1) "Kumaun Himalaya" which run from the state boundary between Himachal Pradesh and Uttar Pradesh to the international boundary between India and Nepal along the Kali river. The Yamuna, the Bhagirathi and the Alakhnanda are the main rivers of the Garhwal Himalaya.

We shall have occasion to use the terms Lesser and High Himalaya. Originally (Wadia 1951, p. 10) these terms denoted physiographic provinces running along the entire length of the Himalaya. "The High (or Great) Himalaya constitute the innermost line of high ranges rising above the limit of perpetual snow. Their average height extends to 6–7 km. The Lesser Himalaya are a series of ranges closely related to the former but of lower elevation, seldom rising much above 4 to 5 km" (Wadia 1951). Gansser (1964) used terms Lower and Higher Himalaya with the connotation that the boundary between the Lesser and Higher Himalaya is marked by the Main Central Thrust (MCT), the other boundary of the Lesser Himalaya being the Main Boundary Thrust (MBT). According to Valdiya (1980, p. 10), the highest point in Garhwal Himalaya is Nag Tibba (elev. 3022 m), the general elevations being in the range of 1500 to 2500 m.

We shall call the seismic belt in the Garhwal Himalaya as GLHSB, short for

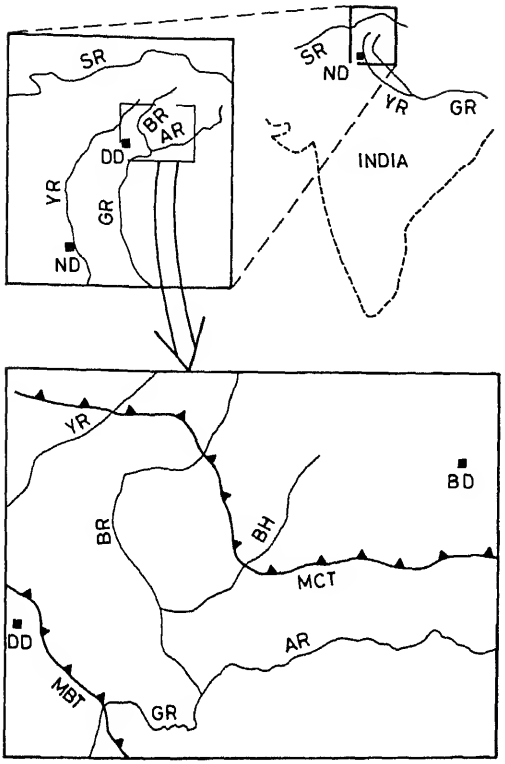

Figure 1. Showing the location of the area of interest in the Himalaya. Abbreviations for river names are: AR, Alakhnanda river; BH, Bhilangana river; BR, Bhagirathi river; GR, Ganga river; SR, Sutlej river and YR, Yamuna river. Abbreviations for place names are: BD, Badrinath; DD, Dehradun and ND, New Delhi. The thrusts shown are the Main Boundary Thrust (MBT) and the Main Central Thrust (MCT).

hwal Lesser Himalaya Seismic Belt. This appellation appears to be strictly true
respect to the earlier definition of the Lesser Himalaya. It takes only minor
rties with Gansser's Lower Himalaya concept because at places in Garhwal the
mic belt appears to lie some distance NE of the MCT.

Relevance of the study

r large earthquakes (magnitudes 8·7, 8·6, 8·4 and 8·7, Richter 1958) have occurred
lifferent parts of the Himalaya in the last nine decades. But the last of them
urred 37 years ago. The meizoseismal area of the 1905 Kangra earthquake
gnitude 8·6) extended well into Garhwal Himalaya from the west. The portion of
hwal Himalaya immediately east of this is a part of the nearly 700-km-long
mic gap recognized by Seeber and Armbruster (1981), Khattri and Tyagi (1983)
Khattri (1987). The region is not known to have experienced a magnitude 8 or
ter earthquake in recorded history and unless it happens to be an exceptional
ment of the Himalaya collision zone in which most of the stress is released through

Further, as noted above, the Garhwal Himalaya are drained by three mighty perennial rivers with numerous tributaries. The region thus possesses a vast potential for irrigation and generation of hydroelectric power. A large number of multipurpose river valley schemes have been conceived for the region and many of them are under execution or in advanced stages of design. The 260 m high earth and rockfill Tehri Dam on the Bhagirathi river is in the early stages of execution. Detailed seismicity information would be vital for planning seismic risk mitigation measures for these projects. Scientifically too, detailed information about earthquake processes in the region would be useful for evolving earthquake prediction and seismotectonic models.

1.3 *Local recording*

Sporadic recording of local earthquakes using one to three seismograph stations has been carried out in the Bhagirathi valley between 1974 and 1977 (Agarwal and Kumar 1982). Four permanent photographically recording seismographs have also been present for some time and are still in operation in the region (Srivastava 1986). But the instruments have low magnification and the array configuration is unsuitable for detecting and locating many local earthquakes. Results of recording local earthquakes with a five-station array (largest dimension 45 km) during 1979–80 were reported in paper I. The array stations were located in the Yamuna and the Bhagirathi valleys in the vicinity of the MCT. We report here analyses of local earthquake data recorded with 5 to 7 element seismograph arrays during 1984–86 in the region immediately SE of that considered in paper I. This region lies between Bhagirathi and Alakhnanda valleys in the vicinity of MCT.

1.4 *Review*

A cardinal fact about the Himalayan seismic belt is that its overall definition so far rests on regional and teleseismic observations of intermediate magnitude earthquakes. The information has been supplemented in recent years by data from a few local networks (Seeber *et al* 1981; Gaur *et al* 1985; Srivastava 1986; Khattri 1987). Hence most of the articles about seismicity of Himalaya refer to the four large and numerous intermediate magnitude earthquakes. We recall here the available models of Himalaya against which we compare our results and conclusions.

The Himalaya is considered to be the result of continent–continent collision of the Indian and Eurasian plates (e.g. LeFort 1975; Valdiya 1980; Seeber *et al* 1981; Khattri 1987). The two continents have sutured along the Indus Suture Thrust. Portions of the northern edge of the Indian plate have been thrusted southwards as a result of continued convergence between India and Eurasia. Two major intraplate thrusts are the MCT and MBT. According to one model, the so-called evolutionary model (e.g. LeFort 1975), the MCT and MBT are similar in nature and along these crustal slices of the Indian plate have been thrusted southwards. In the alternative steady-state model (e.g. Seeber *et al* 1981; Seeber and Armbruster 1981; Ni and Barazangi 1984) the MBT and MCT are different in character. The MCT is a thrust fault that involves the upper crust. The region south of the MCT constitutes a sedimentary wedge consisting of the Ganga foredeep, the other (Siwalik) Himalaya, and the Lesser Himalaya. This

wedge is thought to be underlain by a quasi-horizontal detachment surface coinciding with the upper surface of the subducting Indian lithosphere. Earthquakes of intermediate magnitudes occur near the northern margin of the detachment whereas the great earthquakes further to the south are caused by slip on this detachment.

The faultplane solutions and focal depths determined by Baranowski *et al* (1984) confirm the above model, though they, as well as Lyon–Caen and Molnar (1983), favour a model in which the upper portion of the Indian slab under the Greater Himalaya has been sliced and thrusted southward.

On a more local scale, for the Garhwal Himalaya specially, Agarwal and Kumar (1982) reported their tripartite observations of seismicity in the Bhagirathi valley. They noted sporadic activity along the MCT.

A belt of local earthquake epicentres was defined over a distance of about 70 km from the analyses reported in paper I. The best data pertained to the region between the Yamuna and the Bhagirathi valley which was enclosed within the recording array. In this region the seismic belt was observed to lie distinctly south of the MCT which was thus considered to be seismically inactive in the region. A sinistral offset along on E–W line was observed in the trend of the belt. A composite focal mechanism solution indicated strike-slip faulting. The strikes of the two nodal planes were N–S and E–W. The latter plane was inferred to be the fault plane because the sinistral relative motion observed across it coincided with the sinistral E–W offset in the seismic belt. The focal depth of the majority of the earthquakes was less than 10 km and a case was made that the seismicity may be confined only to the top 20 km of the crust.

The new results presented in this study enable the belt of local earthquakes to be defined over a further distance of 70 km between the Bhagirathi and Alakhnanda valleys. The estimated focal depths of earthquakes are again predominantly shallow. A composite 'thrust' solution has been observed for earthquakes SE of the Bhagirathi valley. The seismicity in the Garhwal Himalaya appears to be confined primarily to the overriding slice of the plate which may be composed of the sedimentary wedge and the Tethyan slab according to Seeber and Armbruster (1981), of the upper portion of the Indian plate itself (Baranowski *et al* 1984).

2. Seismicity

The sites in the Bhagirathi and Alakhnanda valley occupied with portable seismographs during parts of 1984–86 are shown in figure 2. The details of the station networks operated are given in table 1. Earthquakes occurring locally as well as at regional and teleseismic distances were recorded. But we present data for local

Table 1. Details about seismograph arrays operated during 1984–86.

List of stations in the array	Period of operation
AKM, CHA, LMG	November–December 1984
AKM, CHA, GHU, LMG, DHO	January–March 1985
AKM, CHA, GHU, DHO, LAT	April–June 1985
AKM, CHA, GHU, DDA, DAB, TIL, UKH	October 1985–June 1986

Note: The station codes match with those shown in figure 2

Layer 1	17	5·2	2·97
Layer 2	Infinite	6·0	3·43

earthquakes only because by doing so at least the estimates of epicentral locations can be relied upon for earthquakes occurring within or close to a seismograph station array.

2.1 *Data analysed*

The data for only those earthquakes were analysed which provided a minimum of five-wave arrival times in the following combinations.

(i) P readings at 5 stations;
(ii) P readings at 4 stations and S reading at one of the 4 stations;
(iii) P readings at 3 stations and S readings at two of these stations.

A restriction was also imposed that the difference in arrival times of P and S waves should be less than 10 s. The aim was to improve the chances that the first arriving P wave would be a direct wave. A simple application of the head wave theory (Dobrin 1976) shows that in the context of the wave speed model of table 2, this would be the case for earthquakes with focal depths less than 13 km. Still, in every case, an attempt was made to use as much data for an earthquake as possible and available within these restrictions.

2.2 *Hypocentral parameter estimation procedure*

The same computer program was employed for this purpose as discussed and used in paper I.

2.3 *Crustal model*

Estimation of the four hypocentral parameters (viz. epicentral latitude and longitude, hypocentral depth and origin time) from arrival times of P and S waves requires information about the distribution of P and S wave speeds between the earthquake focus and the stations. We are unaware that any study elucidating this information has been carried out in the region of interest, namely the region along the GLHSB between the Bhagirathi and the Alakhnanda rivers. We adopted for the purpose a uniform half-space model with a P wave speed of 5·2 km/s and P to S wave speed ratio of 1·75, close to 1·73 for a Poisson solid. This P wave speed is the same as estimated by Chander *et al* (1986) for the region in the vicinity of the MCT between Yamuna and Bhagirathi valleys immediately to the NW of the region of interest here. We offer the following remarks in defence of this simple wave speed model. Many investigators (e.g. Kaila *et al* 1968; Tandon and Dubey 1973; Verma 1974) have attempted to estimate

ve also been used to estimate seismic wave speeds in the first and second crustal yers. The above mentioned result (5·2 km/s) for the first crustal layer applies to the gion between Yamuna and Bhagirathi valleys near the MCT, while the result 0 km/s) for the second crustal layer (Kumar *et al* 1987) applies strictly to the region mediately NW of that. Both these values have been adopted for the region of the LHSB southeast of the Bhagirathi valley as being the values estimated for the region osest to the region of interest. The depth to the interface between the two layers has ot been estimated in these studies. We assume that the interface in question is the rust surface between the colliding lithospheric plates in the Lesser and High imalaya. The surface may be delineated approximately by the foci of intermediate agnitude thrust earthquakes (Ni and Barazangi 1984) in the Himalaya seismic belt. he depth to the interface beneath the MCT is estimated by us to be 17 km from Ni d Barazangi's figure 11 (middle part). The interface dip of 15° has been estimated by and Barazangi but may be ignored when only the order of magnitude of the travel nes of head waves travelling predominantly parallel to the strike of the interface is ing considered. Since only eight out of 92 earthquakes had estimated focal depths low 13 km in the context of the model of table 2, these were the only earthquakes for ich there was a need to consider at least a two-layered half space model. This tifies the use of the simple half-space model on grounds of convenience and its atively minor influence on the results obtained.

4 *Seismicity results*

e stringent conditions on phase data discussed in the foregoing were met for only 41 rthquakes recorded during the 1984–85 season and 49 events during the 1985–86 ason. The data for these 90 events are considered along with 162 events considered paper I which met the same requirements. However, we recall that the hypocentral rameters of the latter events had been estimated using a P wave speed of 5 km/s. The 252 epicentres are plotted in figure 2. The seismic belt delineated by these local ents is compared with that defined by regionally and teleseismically located events 1684 to 1985 in figure 3. Two depth sections along the perpendicular to the trend the seismic belt (local earthquakes only) are shown in figures 4 and 5. The coda agnitude of these events is in the range of 2 to 4.

5 *Belt of seismicity*

e 252 epicentres of the local earthquakes recorded during 1979–80 and 1984–86 fine a definite seismic belt extending over a distance of about 140 km from NW of muna river to Alakhnanda river. The width of the belt appears to vary between 30 d 50 km. Around 78·5°E longitude the belt appears to have a 50 km long, N–S nding offshoot to the south. The concentration of epicentres between Yamuna and agirathi valleys clearly defines a sinistral E–W oriented offset in the belt (figure 2).

6 *Focal depth*

frequency/km table (table 3) and a histogram (figure 6) were prepared for the

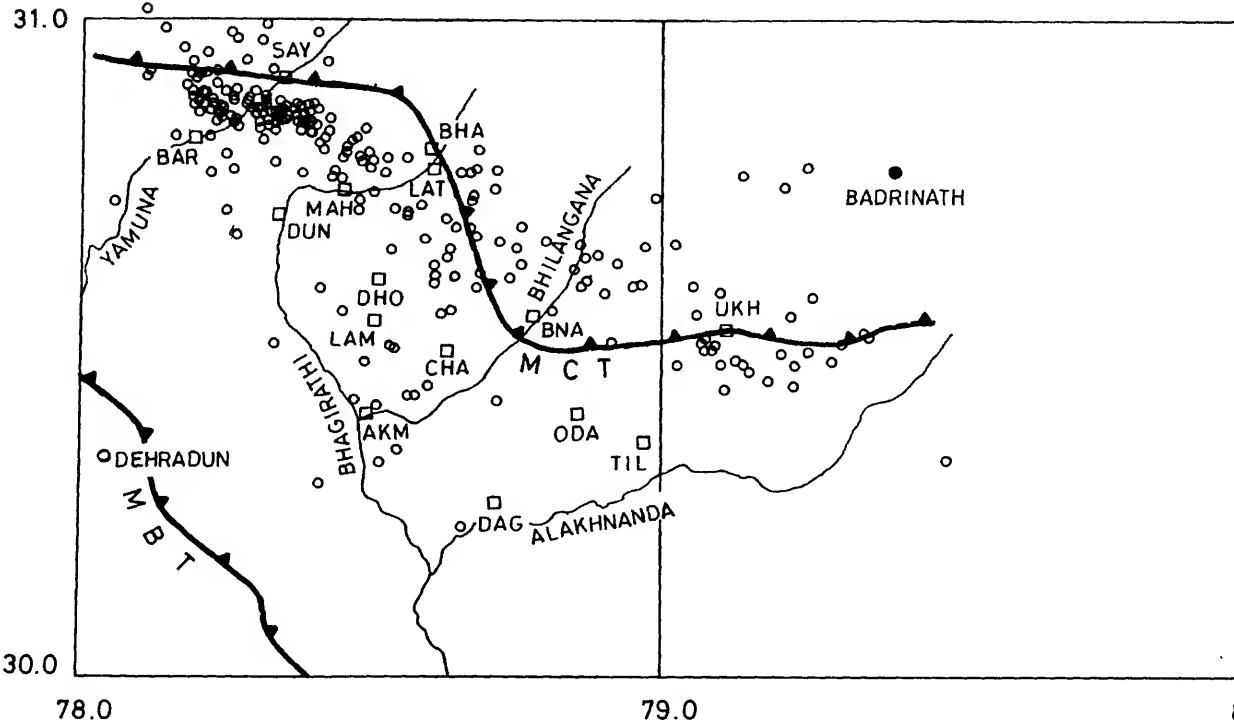

Figure 2. A combined plot epicentres of local earthquakes recorded in the Garhwal Himalaya during 1984–86 (90 events) and 1979–80 (1
represent epicentres and squares stations. The stations operated during 1984–86 and are shown here as AKM, LAM, DHO, LAT, BNA,
UKH, DHO. The schedule indicating the stations operating at a given time during 1984–86 is given in table 1.

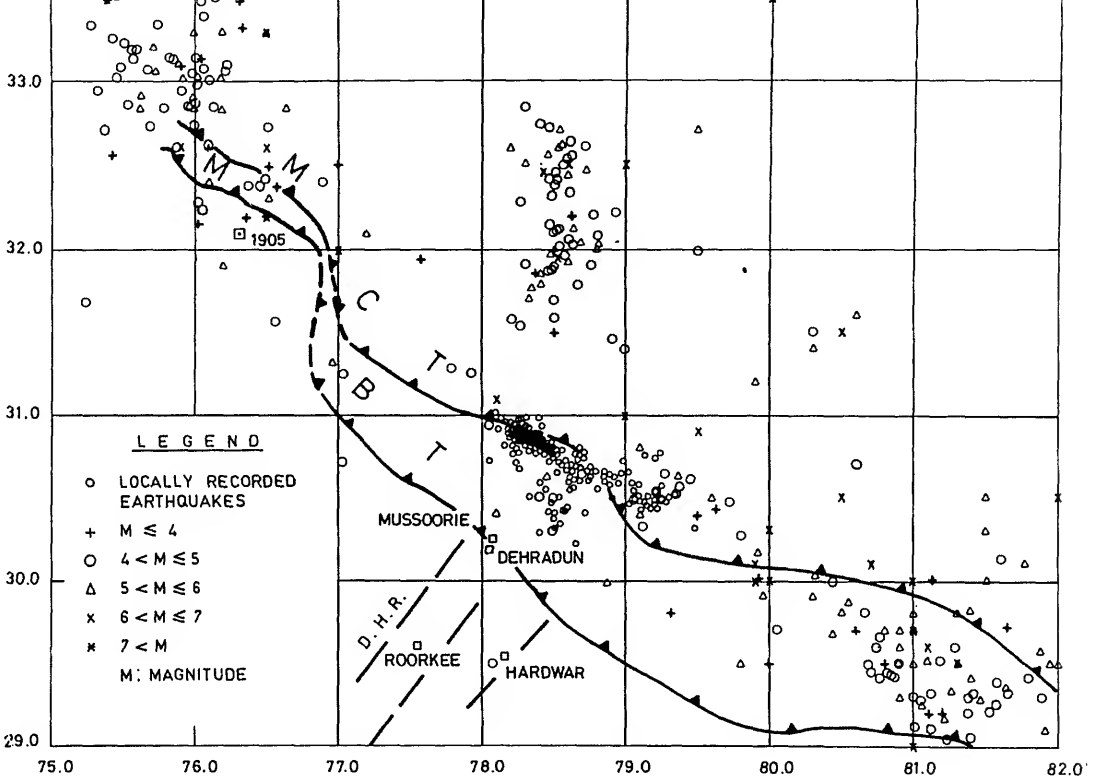

Figure 3. Relation of local earthquakes shown in figure 2 with the seismicity belt delineated from regional and teleseismic data for the perio The epicentre of the 1905 Kangra earthquake (M = 8·6) is also included. The location of this earthquake has been taken from Molnar Delhi–Hardwar Ridge.

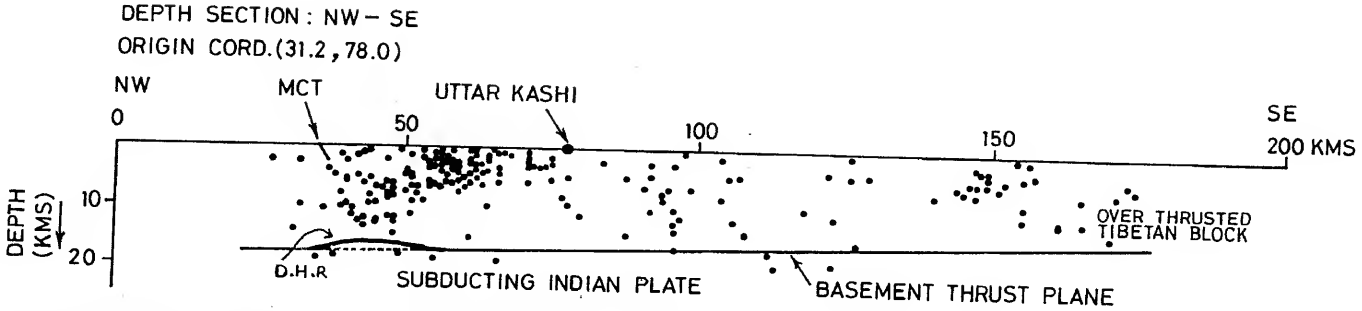

Figure 4. NW-SE oriented depth section for local earthquakes of figure 2. Only the westernmost crossing of the MCT with the section line is shown. DHR, Delhi-Hardwar Ridge.

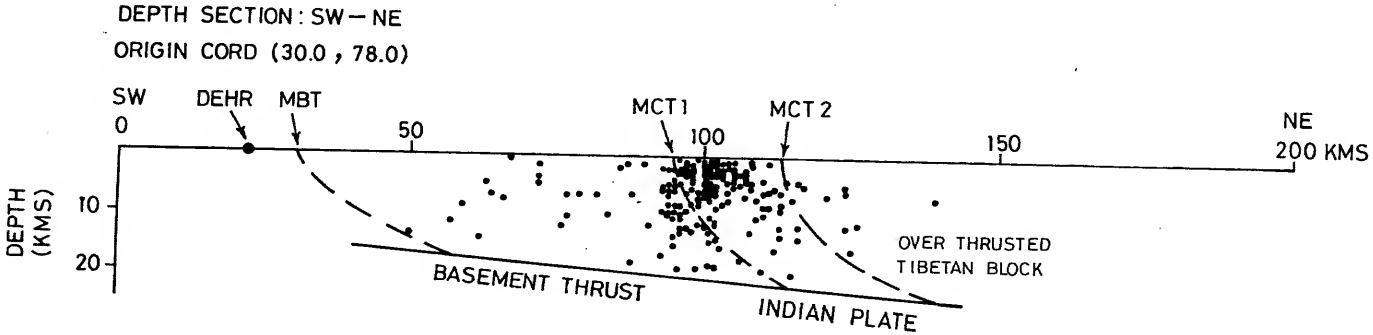

Figure 5. SW-NE oriented depth section for local earthquakes figure 2. MCT1 and MCT2 mark the southwesternmost and northeastern most locations of the meandearing trace of MCT according to Gansser (1964). DEHR, Dehradun.

Table 3. Distribution of estimated focal depths in 1 km intervals.

Depth interval (km)	Number of earthquakes in the interval	Cumulative Number
−1–0	1	1
0–1	20	21
1–2	23	44
2–3	25	69
3–4	19	88
4–5	20	108
5–6	22	130
6–7	25	155
7–8	11	166
8–9	16	182
9–10	11	193
10–11	11	204
11–12	12	216
12–13	9	225
13–14	9	234
14–15	3	237
15–16	4	241
16–17	2	243
17–18	3	246
18–19	2	248
19–20	0	248
20–21	2	250
21–22	1	251
22–23	1	252

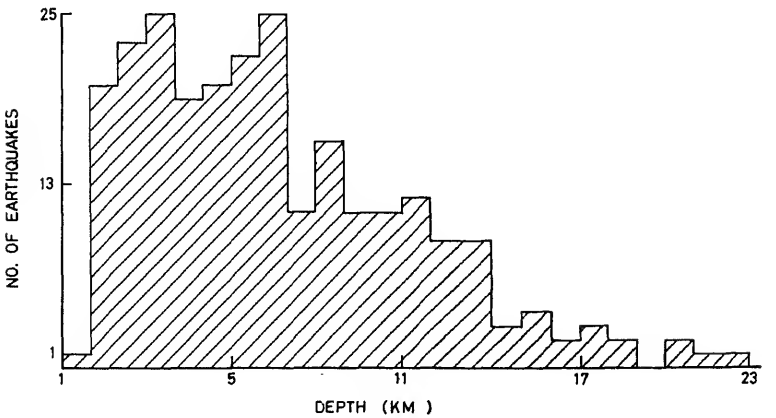

Figure 6. Histogram showing the number of earthquakes versus depth of focus for an estimated 252 earthquakes.

estimated focal depths of the 252 earthquakes. The estimated focal depth did not exceed 23 km in any case. It was less than 10 km for 193 earthquakes and between 10 and 13 km for another 32 earthquakes. In all 27 (or about 10%) earthquakes were assigned estimated focal depths in the range of 13 to 23 km. The preponderance of very shallow earthquakes among the local earthquakes considered is manifest.

2.7 *Activity with time*

The frequency of earthquake occurrence in time is not uniform along the trend of the GLHSB. The region with the highest level of activity in this regard is the part of the belt between the Yamuna and Bhagirathi valleys. The next most active part of this stretch of the belt is considered on available data to be between the Mandakini and Alakhnanda rivers. This stretch of the belt appears to be most active, however, when the number of earthquakes located from regional and teleseismic observation in the period 1684–1985 is considered.

3. Focal mechanisms

Focal machanisms of earthquakes have provided crucial evidence for sea floor spreading and plate tectonic hypotheses. Fitch (1970) presented the first focal mechanism solutions based on teleseismic and regional data for earthquakes in the Himalayan region. The results for the four earthquakes which occurred just east of Garhwal and were considered by Fitch showed support for the view that the Indian lithospheric plate was underthrusting the Himalaya. Subsequently many other investigators have presented such solutions for the Himalaya, but none of them referred párticularly to the Garhwal Himalaya. Among the Himalaya earthquakes with available focal mechanism solutions, six occurring in the India–Nepal Border region immediately east of the Garhwal Himalaya showed thrust-faulting and had reliably determined focal depths in the range of 12 to 18 km (Ni and Barazangi 1984; Baranowski *et al* 1984).

The seismograms recorded during 1984–86 were also examined for the sense of ground motion in the first *P* waves. Reliable readings were obtained at one or more stations for 28 earthquakes. The data were consistent with two distinct composite focal mechanism solutions as follows.

Data from 20 earthquakes were consistent enough to yield the composite solution of figure 7. Five of the earthquakes occurred at focal depths of 15 to 20 km. We take the NE dipping nodal plane with reverse fault motion as the fault plane. This is consistent with the view held by earlier workers (e.g. Fitch 1970; Chandra 1978) for Himalayan earthquake to take the northerly dipping plane as the fault plane. Ni and Barazangi (1984) and Baranowski *et al* (1984) reported thrust faulting in the 12 to 18 km range. The NE dipping plane of figure 6 has a dip of 60° and it should strictly be termed a reverse fault. Since it refers mainly to shallower earthquakes, it is in conformity with the geological observations and opinion (e.g. Valdiya 1986) that the thrust faults in the Himalaya are listric with steeper dips at shallow depths and gentler dips at greater depths. Accordingly, we also call our reverse fault solution as a 'thrust' solution. Numerical data used for this solution is given in table 4.

Data from eight earthquakes were found to be consistent with the same strike-slip

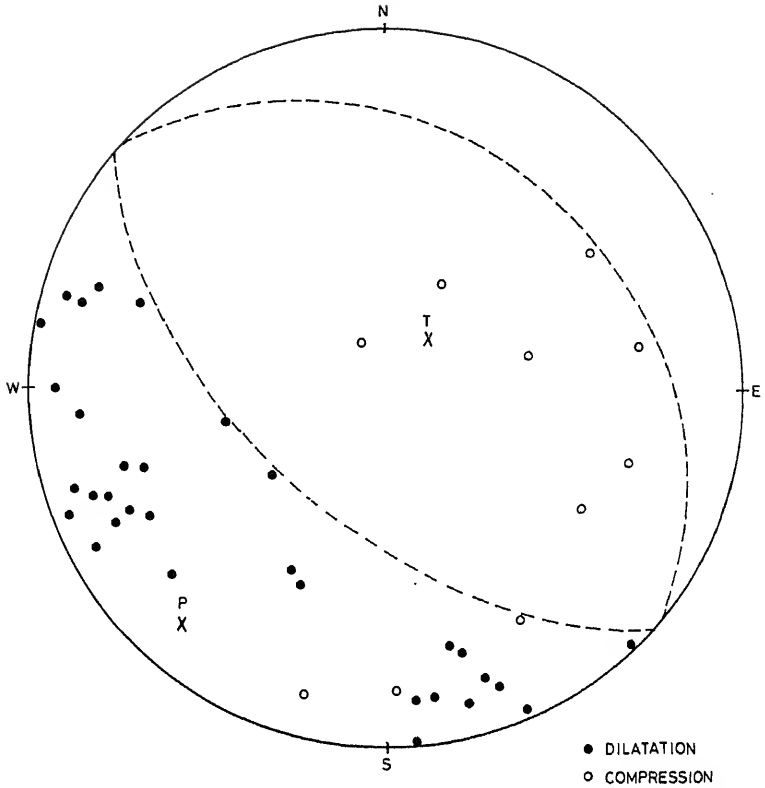

Figure 7. Composite focal mechanism solution in which only data from 1984–86 were involved. Equal area projection of the upper half of the focal sphere is shown. P and T mark the positions of the pressure and tension axes. The north-easterly dipping nodal plane is identified as the fault plane.

Table 4. Numerical data for the thrust solution of figure 6.

	Strike	Dip
Nodal plane 1	N48°W–S48°E	60° along N42°E
Nodal plane 2	N48°W–S48°E	30° along S42°W
	Trend	Plunge
Pressure axis	N42°E–S42°W	15° along N42°E
Tension axis	N42°E–S42°W	75° along S42°W
b axis	N48°W–S48°E	Nil

solution as obtained in paper I from 1979–80 recordings. Seven of the eight earthquakes had their epicentres in the SE part of the region where earthquakes used in solution of paper I had occurred. One of these seven earthquakes had an estimated focal depth of 17·7 km while the rest had focal depths shallover than 15 km. The eight earthquakes occurred well inside the region of earthquakes contributing to the above 'thrust' solution. The data on first motion for these earthquakes are shown in figure 8 plotted on the data and strike-slip solution of paper I. The new data 1984–86 provide

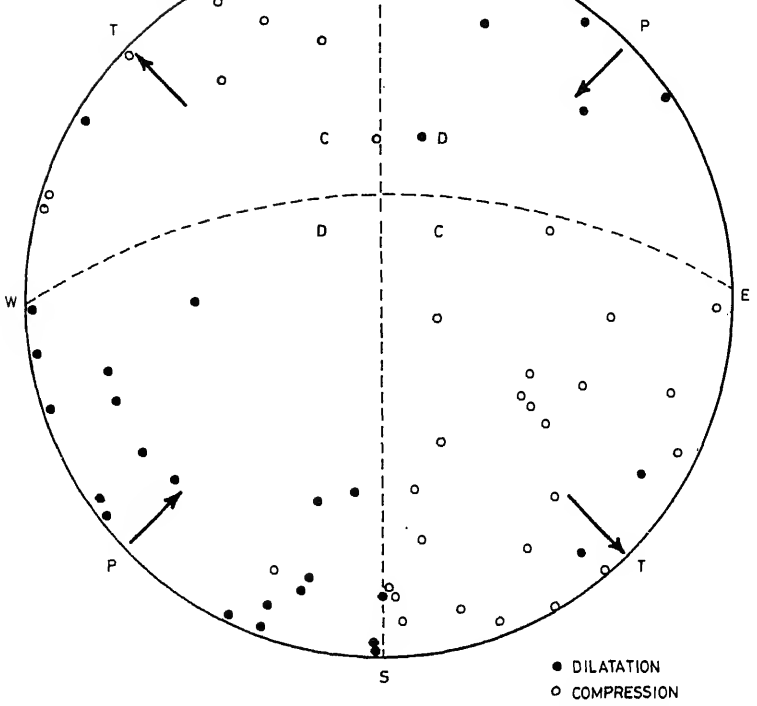

Figure 8. Composite focal mechanism solution in which 1984–86 data are combined with the 1979–80 data. Equal area projection of the upper half of the focal sphere is shown. P and T mark the positions of the pressure and tension axes.

no reason to change the earlier conclusion regarding E–W nodal plane with sinistral relative motion as the fault plane, because it matches with a sinistral E–W offset in the epicentral belt.

The epicentres of all earthquakes whose data were used in obtaining the composite solutions are shown in figure 9 where *T* and *S* mark the epicentral positions according to whether the corresponding first motion data appear in figures 6 or 7 respectively.

A remarkable feature of the composite solutions is that the direction of compressive stress is very nearly the same NE–SW in both cases (figures 6–8).

4. Discussion

It is evident from a review of literature and the foregoing analyses that investigations so far made, of Himalayan earthquakes based on magnitude, may be divided into three categories. Investigations of large (magnitude >8) earthquakes are mainly based on a visual inspection of the effects, in the four known cases of the last nine decades. Only for the 1934 Bihar-Nepal and 1950 Assam earthquakes are some instrumental investigations available (apart from estimation of hypocentral

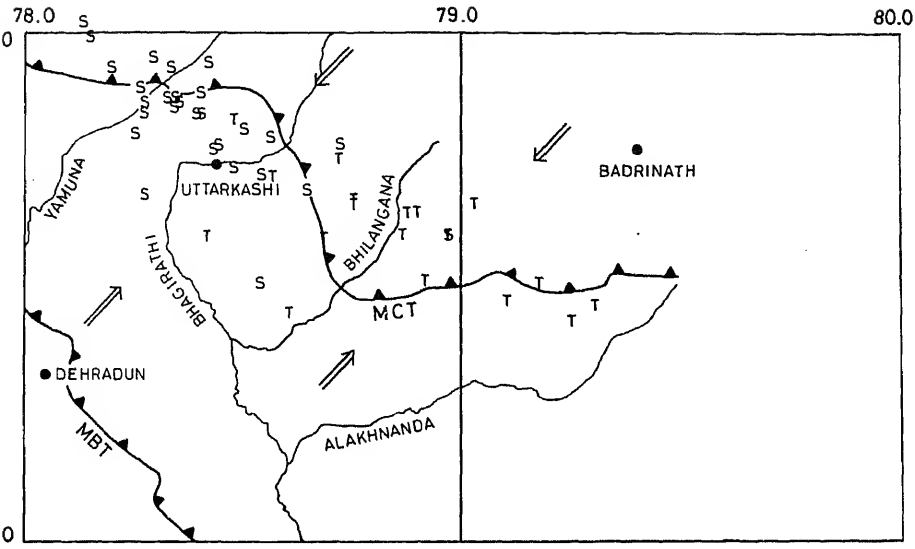

Figure 9. Epicentres of the earthquakes whose first motion data were used in the composite plots. *T* and *S* mark the epicentre positions according as the data for the corresponding earthquake were utilized in the thrust solution of figure 6 or strike-slip of figure 7. The large arrows indicate continuity in the maximum compressive stress direction across the 140 km length of the belt.

rameters and magnitudes). The intermediate magnitude earthquakes have been orded at regional and teleseismic stations and have yielded data on hypocentral rameters, magnitudes, focal mechanisms, space-time seismicity studies, etc. In the t few decades local networks have started to yield information on small magnitude thquakes in the Himalaya. The networks operated by our group in Garhwal malaya during 1979–80 and 1984–86 have yielded data on only one earthquake for ich NOAA also has provided hypocentral data. In the modelling of seismicity of malaya attention has only been paid (e.g. Seeber and Armbruster 1981; Khattri and agi 1983; Baranowski *et al* 1984; Ni and Barazangi 1984, 1987) to large and ermediate magnitude earthquakes.

The belt of local earthquakes epicentres investigated by us in the Garhwal malaya appears to agree with that deduced from regional and teleseismic data ure 3). The epicentre of the earthquake of 28 December 1979 was located using al data and by NOAA using regional and teleseismic data. The estimates of the o epicentres differed by 23 km of map distance. This implies that the epicentral ordinates and focal depths of intermediate magnitude earthquakes are subject to certainties of this order. We thus take the view that the agreement between small d intermediate magnitude earthquake epicentre belts may be regarded as tentative d subject to further verification.

Depthwise, the small magnitude earthquakes in the Garhwal Himalaya, according our estimates, have shallow foci from ground surface down to a depth of about km in a very large number of cases. On the other hand, the accurate focal depth

depthwise region of low seismicity in the 12 to 15 km range has been speculated upon by Chander *et al* (1985) but bears further investigation. Also, we still hold the view put forward in paper I on the basis of numerical experiments with observed and synthetic data and multilayered wave speed models that the focal depths in the range of 30 to 70 km reported by ISC and NEIS for Himalayan earthquakes are probably unreliable. This is borne out by the data presented in many figures by Ni and Barazangi (1984) and Baranowski *et al* (1984).

The relation of the seismic belt to the MCT is of interest. Seeber and Armbruster (1981) regarded the seismic belt to be down dip of the MCT. Baranowski *et al* (1984) and Ni and Barazangi (1984) argued that the belt lies between MBT and MCT mostly close to the latter. The same inference was also drawn in paper I. However, the surface location of the MCT is a matter of debate among investigators. The trace of the MCT shown in the figures of the present article is taken from the tectonic map of Gansser (1964) because he was one of the propounders of the MCT concept and his map is widely available and frequently referred. The results of seismicity obtained in this article on being combined with those of paper I show that over a distance of about 140 km, the seismic belt follows a straighter course than the surface trace of the MCT. In fact the seismic belt and the MCT criss-cross each other in this part of the Garhwal Himalaya.

The status of the MCT and the MBT in regard to the current seismotectonics of the Himalaya is a matter of debate among the earth scientists. For example, LeFort (1975) considered MCT and MBT as successive tectonic boundary thrusts. MBT is the current boundary of the continental convergence zone while the MCT is a less active or dormant feature. Seeber and Armbruster (1981) argued that MBT and MCT are contemporaneous and that MCT is currently active. Ni and Barazangi (1984) state that it is the MBT and nearby surface and blind thrusts rather than the MCT that are presently the most active structures in the Himalaya. Chander (1987, in press) found that the coseismic ground elevation changes observed during the 1905 Kangra earthquake can be explained only by assuming that slip did not take place on the MBT. Lastly Krishnaswamy *et al* (1970) observed that coseismic slip did not occur on MBT or any other thrust in the Himalaya. We thus take the view that the current seismotectonics of the Himalaya is associated with buried (or blind) thrust(s) corresponding to the upper surface of the subducting Indian plate.

The main cause of the stresses responsible for the small magnitude earthquakes recorded by us is probably the same as that responsible for relative displacements between the overriding and the subducting plates in the Himalaya. They are likely to be conducive to thrust earthquakes. Locally the elastic (plastic) response of the overriding plate to topographic relief in the underthrusting slab may lead to perturbations of this stress regime. Chandra (1978) put forward the agrument that the normal faulting during the 1975 Kinnaur earthquake, approximately 150 km north of MCT near 78°E, was in response to stresses induced by a north-eastward extending salient of the northeast trending Precambrian Aravalli ranges of Rajasthan under the Sindhu-Ganga (Indo-Gangetic) alluvium and the Lesser and High Himalaya. We recapitulate in figure 10 how the principal stresses for a thrust fault or earthquake can be modified with a superimposed tensile stress to produce principal stresses suitable for strike slip faulting and earthquakes. We thus argue (figure 11) that in the region of GLHSB between the Yamuna and Bhagirathi valleys, the flexing of the overriding rock material in response to the presence of the same Aravalli salient on the under-

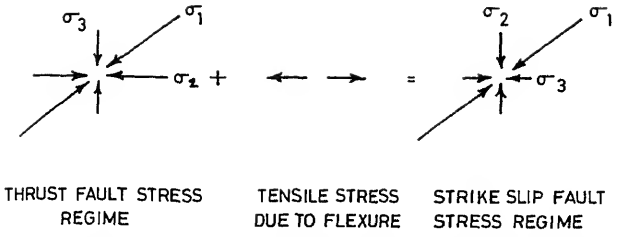

Figure 10. Schematic drawing to show the alteration of a thrust-fault stress regime to a strike-slip fault stress regime due to action of stresses arising from flexure in the lithospheric plate.

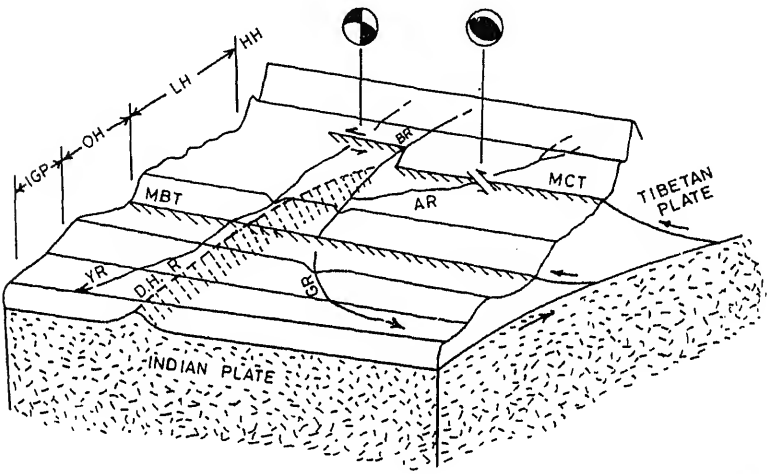

Figure 11. A cartoon to show the origin of flexure in the overriding plate due to topographic relief in the subducting plate. DHR is the Delhi–Hardwar Ridge, a postulated buried northeastward salient of the Pre-Cambrian Aravalli ranges of Rajasthan under the Sindhu Ganga (Indo-Gangetic) Plains (SGP) and Outer (OH), Lesser (LH), Bhagirathi (BR), Ganga (GR) and Yamuna (YR).

thrusting Indian slab gives rise to tensile stresses that modify the configuration of stresses that would have been conducive to thrust earthquakes in the absence of the salient into a stress configuration conducive to strike-slip earthquakes. South east of the Bhagirathi valley, the influence of this superimposed tensile stress regime wanes sufficiently with the result 'thrust' faulting is observed even at shallow levels under the Lesser Himalaya. We however note that in a setting as complex as the Himalaya other processes can give rise to strike-slip faulting.

5. Conclusions

(i) Our observations with seismograph arrays of small areal extent in the Garhwal Himalaya have so far shed light only on the small magnitude local earthquakes.
(ii) The belt of local earthquakes has been defined over a distance of 140 km parallel to the general strike of the mountains in the Garhwal Himalaya.

(iii) The belt of local earthquakes appears to coincide with the belt of intermediate magnitude earthquakes. However, as uncertainties in the locations of the latter events are greater, this agreement can only be regarded as being tentative.
(iv) The seismic belt follows a straighter course than the outcrop of the MCT in the Garhwal Himalaya and the two criss—cross each other.
(v) The vast majority of earthquakes have focal depths of less than 13 km.
(vi) The first motion data of this paper on being combined with that of paper I indicate strike-slip and thrust mechanisms in operation along the 140 km length of the GLHSB, investigated. Both solutions indicated a NE–SW oriented compressive maximum principal stress.
(vii) The composite solution indicating thrust-faulting establishes that the overall stress regime in the region is conducive to thrust or reverse fault earthquakes.
(viii) The strike slip earthquakes in the region occupied by the valleys of Yamuna to Bhagirathi, may be the result of an aberration of this stress regime due to tensile stresses induced in the overriding slab, in response to topographic relief on the subducting slab surface.
(ix) The seismic risk in eastern Garhwal Himalaya is high because it lies in the area of a seismic gap along the Himalayan collision zone.

Acknowledgements

The authors are grateful to the Department of Science and Technology and the Department of Earth Sciences of the University of Roorkee for support of this investigation in all respects.

References

Agarwal P N and Kumar A 1982 Microearthquake recording for engineering applications. In *Engineering geosciences* (ed.) B B S Singhal (Meerut: Sarita Prakashan) pp. 181–186

Baranowski J, Armbruster J, Seeber L and Molnar P 1984 Focal depths and fault plane solutions of earthquakes and active tectonics of the Himalaya; *J. Geophys. Res.* **89** 6918–6928

Chandra U 1978 Seismicity, earthquakes mechanisms and tectonics along the Himalayan Mountain range and vicinity; *Phys. Earth Planet. Inter.* **16** 109–131

Chander R 1987 On the interpretation of some observations regarding ground level changes during the 1905 Kangra earthquake, NW Himalaya (submitted)

Chander R, Khattri K N, Sangvai P M, Sarkar I and Gaur V K 1985 A strategy for hypocentral parameter estimation for microearthquake surveys at engineering sites; *Bull. Indian Soc. Earthquake Tech.* **22** 1–8

Chander R, Sarkar I, Khattri K N and Gaur V K 1986 Upper crustal compressional wave velocity in the Garhwal Himalaya; *Tectonophysics* **124** 133–140

Dobrin M 1976 *Introduction to geophysical prospecting* (New York: McGraw Hill Book Co.)

Fitch T J 1970 Earthquake mechanisms and Tectonics in the Himalayan, Burmese and Andaman regions and continental tectonics in central Asia; *J. Geophys. Res.* **73** 777–784

Gansser A 1964 *Geology of the Himalayas* (New York: Interscience) p. 289

Gaur A 1964 *Geology of Himalayas* (New York: Interscience) p. 289

Gaur V K, Chander R, Sarkar I, Khattri K N and Sinvhal H 1985 Seismicity and state of stress from investigations of local earthquakes in the Kumaun Himalaya; *Tectonophysics* **118** 243–251

Kaila K L, Reddy R P and Narain H 1968 Crustal structure in the Himalayan foothills area of North India from *P* wave data of shallow earthquakes; *Bull. Seismol. Soc. Am.* **58** 597–612

Khattri K N 1987 Great earthquakes, seismicity gaps and potential for earthquake disaster along the Himalayan plate boundary; *Tectonophysics* **38** 79–92

attri K N and Tyagi A K 1983 Seismicity patterns in the Himalayan plate boundary and identification of areas of high seismic potential; *Tectonophysics* **96** 281–297

shnaswamy V S, Jalote S P and Shome S K 1970 Recent crustal movements in NW Himalaya and gengetic foredeep and related patterns of seismicity; *Proc. IV Symp. on Earthquake Engg. Univ. of Roorkee* (Meerut: Sarita Prakashan) pp. 419–439

nar S, Chandcr R and Khattri K N 1987 Compressional wave speed in the second crustal layer in Garhwal Himalaya; *J. Assoc. Expl. Geophys.* **8** 219–225

on-Caen H and Molnar P 1983 Constraints on structure of the Himalaya from an analysis of gravity anomalies and a flexural model of the lithosphere; *J. Geophys. Res.* **88** 8171–8191

Fort P 1975 Himalayas: The collided range. Present knowledge of the collided arc; *Am. J. Sci.* **A275** 1–44

lnar P 1987 The distribution of intensity associated with the 1905 Kangra earthquake and bound on extent of rupture zone; *J. Geol. Soc. India* **29** 221–229

J and Barazangi M 1984 Seismotectonics of the Himalayan collision zone: Geometry of the under-thrusting Indian plate beneath the Himalaya; *J. Geophys. Res.* **89** 1147–1163

hter C F 1956 *Elementary seismology* (San Francisco: W H Freeman and Co.)

ber L and Armbruster J G 1981 Great detachment earthquakes along the Himalayan arc and long term forecasting. In *Earthquake prediction. An international review* (Washington DC: Am. Geophys. Union)

ber L, Armbruster J G and Quittmeyer R C ,1981 Seismicity. and continental subduction in the Himalayan arc; *Interunion Commission on Geodynamic Working Group* 6 Volumes (Washington D.C.: Am. Geophys. Union) pp. 215–242

vastava H N 1986 Status of seismicity and observational networks. In *Proceedings of the National Meet of Earthquake Mechanism and Mitigation*, Department of Science and Technology, Government of India, New Delhi, pp. 51–58

don A N and Dubey R K 1973 A study of crustal structure beneath the Himalaya from body waves; *Pure Appl. Geophys.* **3** 2207–2216

diya K S 1980 *Geology of the Kumaun Himalaya* (Dehradun: Wadia Institute of Himalayan Geology) p. 289

diya K S 1986 Neotectonics activities in the Himalayan belt; *Proceedings of International Symposium on Neotectonics in South Asia* (Dehradun Survey of India) p. 434

ma G S 1974 Structure of the foothills of the Himalaya; *Pure Appl. Geophys.* **112** 18–76

dia D N 1953 *Geology of India* (London: Macmillan and Co.) p. 531

n intermediate-term prediction of strong earthquakes in the malayan arc region using pattern recognition algorithm M8

S C BHATIA, S V CHALAM, V K GAUR, V I KEILIS-BOROK* and V G KOSOBOKOV*

National Geophysical Research Institute, Hyderabad 500 007, India
* Institute of Physics of the Earth, Moscow, USSR

Abstract. Seismicity of the Himalayan arc lying within the limits shown in figure 1 and covering the period 1964 to 1987 was scanned using M8 algorithm with a view to identifying the times of increased probabilities (TIPs) of the occurrence of earthquakes of magnitude greater than or equal to 7·0, during the period 1970 to 1987. In this period, TIPs occupy 18% of the space time considered. One of these precedes the only earthquake in this magnitude range which occurred during the period. Two numerical parameters used in the algorithm, namely the magnitude thresholds, had to be altered for the present study owing to incomplete data. Further monitoring of TIPs is however warranted, both for testing the predictive capability of this algorithm in the Himalayan region and for creating a base for the search of short-term precursors.

Keywords. Himalaya; intermediate term prediction; M8 algorithm; pattern recognition algorithm; times of increased probabilities; seismicity.

Introduction

any scheme of pattern recognition, distinctive patterns of attributes describing the its of events (objects) of a particular class are first established in the course of a rning process. The ensemble of objects which are thus unequivocally grouped into o or more classes and the attributes describing them, constitute the learning material m which recognition rules are abstracted. These rules are then applied to recognition new objects, that is assigning them to the appropriate class, which is the ultimate ective. For predicting earthquakes, the objective is to recognize instants of times ich presage the approach of a strong earthquake. This can be attempted by ablishing premonitory patterns based on the analysis of past data and designing appropriate pattern recognition algorithm.

Earthquake sequences constitute so far the longest and the least incomplete data relevant to earthquake prediction in many parts of the world. This is also largely e for the Himalayan region. Here we analyse the earthquake sequences in the malayan region using the M8 algorithm designed by Keilis-Borok and Kosobokov 84) to test the possibility of diagnosing the approach of a strong earthquake. The monitory patterns expressed by this algorithm appear to be rather similar in widely erent regions of the world (Gabrielov *et al* 1986).

t is of course recognized, at the very outset, that the symptoms of an approaching thquake can be quite different from one case to another. This may happen because

SEISMICITY OF HIMALAYAN ARC

MAGNITUDE 6 AND ABOVE

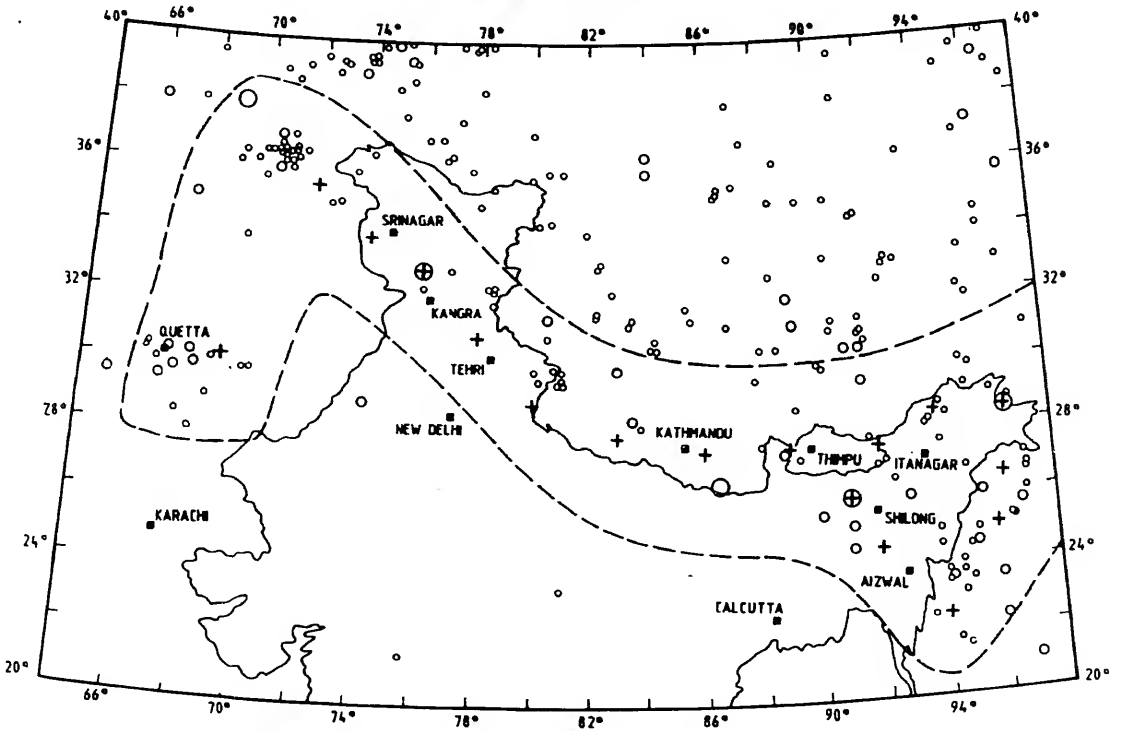

MAGNITUDE

- ○ 6 – 6.9
- ○ 7 – 7.9
- ◯ ≥ 8 –

INDEX

- —— Teritory of present study
- \+ Centres of the indidual squares
- ■ Cities

the distinctive seismotectonic environment of different seismic regions or due to homogeneous distribution of rock materials and stresses within the same region. en earthquakes occurring in the same area may show different premonitory sociations if the stress regime and rock properties preparatory to fracture have been eatly altered by earlier or neighbouring earthquakes. The nature of earthquake quences is therefore so diverse (Gabrielov *et al* 1987), as to defy classification and strate attempts to abstract from them a consistent set of premonitory signals. In der to circumvent this problem, Allen *et al* (1984) and Gabrielov *et al* (1986) devised scheme of integral representation of earthquake sequences which smoothens the ersity of seismicity patterns without, however, losing any premonitory signals that y be contained in the data. This is realized in the following way.

First, the earthquake flow within a certain large territory is carefully scanned. veral integral functions (attributes) describing the nature (traits) of the earthquake quence in the region are then evaluated within a sliding time window, each assigned the instant of time that terminates the window. In all, 14 functions describing the lowing traits can be formed: level of seismicity, seismic quiescence, variation of smicity, spatial concentration, clustering in time and space, contrast of seismicity adjacent areas and long term interaction.

Figure 2 shows a schematic representation of traits and the manner of their aluation along the time axis. Appropriate pattern recognition algorithms can be veloped using some or all of these traits. Diagnosis of the time of increased obability of occurrence of a strong earthquake (TIP) is made by applying the propriate recognition rules. After a TIP has been diagnosed, a strong earthquake magnitude greater than or equal to a threshold magnitude M_0 is expected to occur hin a few hundred kilometers over the next few years. This is called an ermediate-term prediction. A magnitude threshold M_0 is determined for each ion on the basis of its past history of strong earthquakes.

To ensure uniform diagnostics of TIPs for different regions, the functions describing ious traits are normalized, as described below. The sequence of main shocks is t isolated, the number of aftershocks being considered as one of the characteristic ctions of the corresponding main shock. In order to smoothen the earthquake quence, their traits are first defined within a wide time window and epicentral area. xt, groups are formed corresponding to each of the functions, which comprise a of these functions evaluated for different arguments. For example, the group of function describing the intensity of earthquake flow consists of the values of the ction evaluated for different magnitude ranges. Each function is then quantized two or three discrete intervals, and various combinations of these are used to gnose a TIP.

Two related algorithms for such diagnosis of TIPs are available; one called CN, igned by Allen *et al* (1984) and the other, M8 designed by Keilis-Borok and sobokov (1984). Their application to different regions of the world is described by brielov *et al* (1986). Algorithm M8, used in the present study, is described below.

Pattern recognition algorithm M8

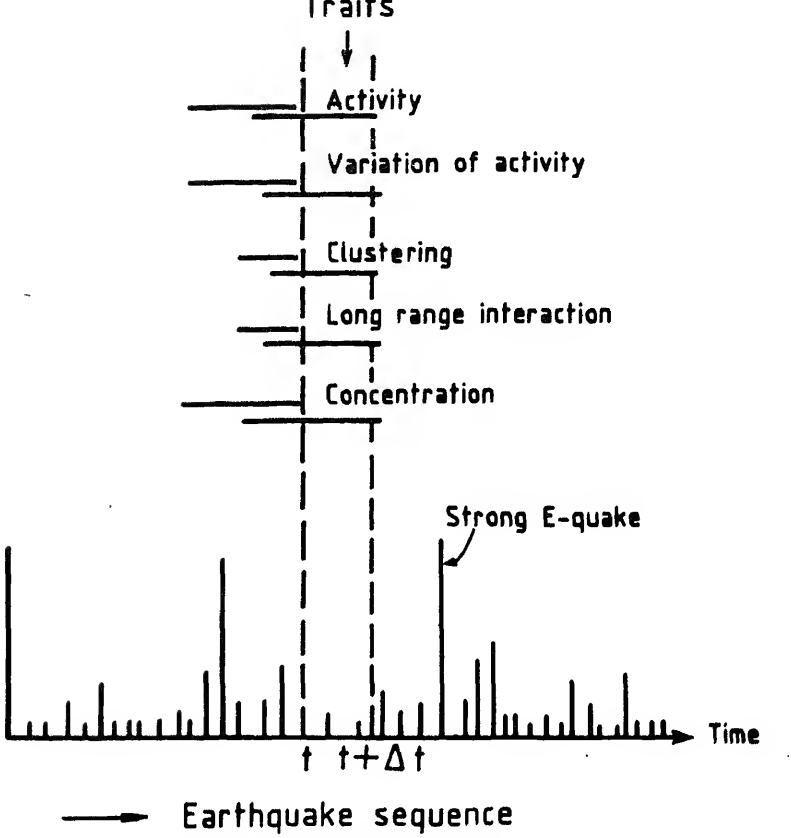

Figure 2. Schematic representation of the sequence of earthquake occurrence and evaluation of intrinsic traits for PR methods. Vertical lines on the time axis show the occurrence of earthquakes (the length being proportional to the magnitude). Various traits are evaluated along sliding time window at Δt steps. Broken vertical lines show this at t and $t + \Delta t$ time instants.

of sources and clustering of sources, measured by the maximal number of aftershocks of the main shocks. The territory under study is scanned by a network of overlapping squares. These squares are centred at appropriate points which show comparatively greater seismic activity with respect to their surroundings. The side length (L) of each square in degrees of the great circle is determined by the relation

$$L(M_0) = \exp(M_0 - 5{\cdot}6) + 1.$$

The above functions are evaluated from the data of earthquake flow in these squares. Each of the first three functions is determined twice, for two different magnitude thresholds M_1 and M_2. The set of values of a function evaluated for different arguments together constitute a 'group'. The values M_1 and M_2 are determined by the criterion that the average annual number of such main shocks is greater than or equal to the predetermined numbers n_1 and n_2 respectively. These values of n_1 and n_2 are consistently adopted for all squares within a region and for all regions, in order to normalize the seismic activity. In defining the spatial concentration, the main shocks

to be considered, lie within the magnitude range M_1 to $(M_0 - 0{\cdot}2)$ while for clustering they lie in the range $(M_0 - 2{\cdot}0)$ to $(M_0 - 0{\cdot}1)$. The flow of main shocks is thus normalized with respect to M_0. The time window for which the functions are evaluated is 6 years for the first three functions and one year for clustering. The sliding step is chosen appropriately, say 6 months.

A function is identified as being abnormally large when its value exceeds the prescribed value, say the 10% percentile of the range of values of the function. Pattern M8, is said to have occurred if at two successive instants of time $K-1$ and K, at least a prescribed number H of individual functions attain abnormally large values, and there are at least a prescribed number G of groups which have at least one member that attains an abnormally large value. A TIP is then declared at the time instant K. The duration of TIP is a suitable multiple (say 10) of the sliding time step. The free parameters of algorithm M8 were determined by Keilis-Borok and Kosobokov (1984) by establishing TIP diagnosis in respect of the strongest earthquakes of magnitude 8 or greater that occurred between 1970 and 1983 in different parts of the earth. The algorithm was later successfully applied to other regions as well, with minimal readaptation of parameters; only the magnitude threshold M_0 had to be adjusted for every region (Gabrielov *et al* 1986). For example, M_0 was 8 for Mexico and 6 for Western Canada. The success-to-failure score was no worse than in the original data-fitting (Keilis-Borok and Kosobokov 1984). Similar results were obtained in tests for algorithm CN (Gabrielov *et al* 1986) with a very low value of M_0 equal to 4·5.

However, as this test is retrospective, it cannot be considered to be conclusive. But it does support the concept of global self-similarity of earthquake flow (Sadovsky *et al* 1982; Gabrielov *et al* 1986) and warrants similar tests to be made for other regions.

3. The region

The region considered for this study is the Himalayan sector (figure 1) of the Alpide-Himalayan fold belt, including the Indus-Ganga-Brahmaputra foredeep to the south of the ranges and part of the Burmese arc. The evolution of the Himalaya is traced to the collision of the Indian plate with the Eurasian plate. Its present-day seismicity is attributed to continued convergence of the Indian plate towards the north by underthrusting beneath the Tibetan plateau. Owing to the gentle dip of this underthrusting plane which leads to a wide zone of frictional contact, the seismic activity along the belt is quite diffuse and mostly confined within a depth of about 20 km. At its eastern extremity however, along the Arakan-Yoma fold belt, hypocentral depths range from shallow to intermediate (about 200 km). Although major earthquakes periodically occur all along the Himalayan collision boundary to relieve the accumulating strains, some parts of the belt show more prolific seismicity, notable among which is the eastern segment.

Four devastating earthquakes of magnitude greater than 8·4 have ruptured the various segments of the 2400 km long Himalayan arc during the past 100 years, leaving seismic gaps of different lengths in between. Unfortunately, our knowledge about the seismicity of the Himalaya in preceding centuries is very sketchy although no earthquakes of comparable magnitude are known to have occurred since the

sixteenth century. It is therefore difficult to estimate the recurrence period of g
earthquakes in the region, although earthquakes of magnitudes less than 5 are q
frequent, interspersed occasionally by earthquakes of magnitude 5 to 6. Since 1
however, the entire region seems to have entered a period of quiescence as fa
earthquakes of magnitude 7 or greater are concerned.

4. The data

The earthquake catalogue selected for the present study was taken from the NC
World Hypocenter Data File issue of 1987. More detailed catalogues based on l
networks are still restricted to small areas and limited time-intervals. A more comp
global catalogue is of course produced by the International Seismological Centr
Newbury, England, but the long delay in dissemination of this catalogue mak
unsuitable for this study.

The main shocks were isolated from the aftershocks by the algorithm describe
Keilis-Borok *et al* (1980) using the space and time windows given in table 1.

Epicentral locations of the main shocks are given in tables 2 and 3. The terri
lying between latitudes 21·0°N and 36·5°N and longitudes 65·6°E–99·0°E was caref
scanned (figure 1). It is framed by the Hindu Kush mountains in the northwest fam
for their strong seismicity at intermediate depths, and by the parameridional Sich
seismic belt lying between 102°E and 105°E.

The temporal chart of the main shocks given in table 4 depicts a magnitude-
distribution of earthquakes in the various rectangular areas bounded by latitu
17°N–45°N and longitudes 60°E–105°E. It may be recalled that algorithm M8
only be applied to diagnose TIPs for the period which starts 7 years after the
availability of a sufficiently complete catalogue, as some of the functions are evalua
from data within a time window of six years prior to the instant of their evaluat
Also, the data pertaining to the first 6 years are necessary to establish as to wh
values of the functions are abnormally large. Table 4 shows that the catalogu
relatively complete only for magnitudes greater than 4·5–5·0, and that too after 1

Table 1. Windows for the identification of aftershocks (reproduced from Keilis-Borok *et al* 1980).

M	R (km)	T (days)
2·5	19·5	6·0
3·0	22·5	11·5
3·5	26·0	22·0
4·0	30·0	42·0
4·5	35·0	83·0
5·0	40·0	155·0
5·5	47·0	290·0
6·0	54·0	510·0
6·5	61·0	790·0
7·0	70·0	915·0
7·5	81·0	960·0
8·0	94·0	985·0

Table 2. Magnitude of the largest earthquake in each of the zones defined by the latitude and longitude.

Latitude (N) \ Longitude (E)	60·0		65·0		70·0		75·0		80·0		85·0		90·0		95·0		100·0		105
45·0	—	—	0·0	—	—	0·0	4·8	8·7	6·5	7·2	8·3	6·6	7·3	7·5	4·6	4·8	6·5	5·6	
	0·0	4·3	6·5	5·5	5·5	7·6	6·8	7·1	7·3	7·2	6·8	5·6	4·7	5·3	4·8	4·7	—	7·0	
41·0	4·9	7·0	4·7	7·1	6·1	7·8	8·6	6·8	5·1	7·3	4·6	4·9	6·5	—	7·6	4·0	—	5·0	
	4·9	5·1	7·2	8·1	7·6	7·0	6·4	6·0	5·0	5·8	6·8	5·5	6·3	4·6	7·2	6·5	7·2	7·0	
37·0	4·5	3·9	5·6	6·6	8·1	6·8	6·8	6·3	6·3	7·2	6·9	6·0	5·0	6·2	5·5	7·6	8·3	6·8	
	5·3	—	5·8	7·6	5·8	6·0	5·6	6·5	6·5	5·2	5·5	6·0	6·5	6·1	6·5	4·9	6·0	5·5	
33·0	6·3	0·0	5·6	5·3	4·9	5·2	8·6	7·1	6·5	6·8	6·3	7·1	8·0	6·0	5·8	7·7	7·4	7·4	
	5·4	4·8	7·5	7·0	6·1	4·6	4·2	5·5	7·7	7·3	5·8	6·2	7·9	5·0	6·0	6·5	7·4	6·0	
29·0	6·7	7·0	5·4	6·8	0·0	7·1	4·7	5·6	4·7	7·0	5·7	6·3	6·8	7·9	8·7	6·3	6·8	7·5	
	6·5	5·2	5·9	5·6	5·0	—	0·0	—	0·0	—	8·4	5·5	7·1	7·2	7·6	6·5	7·3	6·0	
25·0	4·7	8·3	5·6	5·2	5·6	—	—	0·0	6·5	—	4·8	6·3	7·6	7·2	7·8	7·0	7·2	7·5	
	5·5	0·0	0·0	0·0	—	5·4	6·3	4·9	5·5	0·0	0·0	5·5	5·2	6·5	7·0	7·3	7·0	6·6	
21·0	4·8	0·0	—	5·2	—	4·5	—	—	—	—	4·4	—	5·2	5·5	7·9	5·5	6·8	6·8	
	5·6	—	—	—	0·0	6·0	—	0·0	5·7	—	5·0	—	—	5·6	5·6	5·9	—	4·7	
17·0	—	—	—	—	—	—	—	—	—	—	—	—	—	—	7·3	—	—	—	

Table 3. Number of earthquake in each of the zones defined by the latitude and longitude.

Longitude (E)	60·0		65·0		70·0		75·0		80·0		85·0		90·0		95·0		100·0		10
Latitude (N)																			
45·0	—	—	1	—	—	2	5	20	19	30	29	14	5	6	2	6	14	9	
	1	2	7	15	31	29	42	40	29	32	21	14	4	5	1	3	—	2	
41·0	8	33	6	34	144	146	91	97	5	3	1	6	6	—	9	4	—	5	
	3	2	16	125	364	197	54	13	6	1	8	5	12	3	14	13	17	8	
37·0	1	4	13	180	500	50	33	40	28	8	12	7	4	6	13	4	6	6	
	9	—	2	34	38	50	36	15	34	10	7	19	15	11	13	8	11	12	
33·0	8	2	10	26	22	18	42	30	10	19	22	26	17	26	21	7	12	28	
	5	3	29	85	36	3	1	33	67	20	18	17	21	21	39	22	23	23	
29·0	16	6	36	23	2	1	3	2	10	23	35	21	30	31	50	16	29	28	
	26	12	28	12	3	—	1	—	1	—	3	12	60	37	128	46	26	18	
25·0	3	21	11	12	9	—	—	3	2	—	1	1	23	142	61	16	17	16	
	5	1	1	1	—	1	1	2	1	1	2	2	5	95	20	16	29	5	
21·0	5	1	—	1	—	5	—	—	—	—	1	—	1	15	14	13	15	3	
	4	—	—	—	1	8	—	1	4	—	2	—	—	14	17	3	—	1	
17·0	—	—	—	—	—	—	—	—	—	—	—	—	—	—	1	—	—	—	

Table 4. Number of earthquakes in the magnitude ranges and time windows in the region defined by latitude 17·0°N to 45·0°N and longitude 60·0°E to 105·0°E. The numbers in the first column correspond to earthquakes with unknown magnitudes.

Year	Magnitude 0·0	1·0	2·0	3·0	4·0	5·0	6·0	7·0	8·0	9·0
1900	—	— — — — — — — — — — — 2 — — — — 1								
	3	— — — — — — — — — — — — 1 6 — 1 1								
1910	7	— — — — — — — — — — — 2 1 3 2 — 1								
	17	— — — — — — — — — — — 2 3 2 3 — —								
1920	56	— — — — — — — — — — 1 2 5 2 — 1 1								
	159	— — — — — — — — — — 7 7 8 2 — — —								
1930	128	— — — — — — — — — — 30 10 5 4 2 — —								
	146	— — — — — — — — — — 8 14 2 3 2 — —								
1940	60	— — — — — — — — — — 8 6 4 6 — — —								
	12	— — — — — — — — — — 1 2 2 — 5 — —								
1950	336	— — — — — — — — — — 1 10 4 3 — 1 1								
	184	— — — — — — — — — 6 4 13 6 3 1 — —								
1960	285	— — — — — — 2 9 37 32 15 13 8 2 — — —								
	238	— — — — — — 1 14 130 130 33 11 3 — — — —								
1970	226	— — — — — 2 7 26 134 137 30 10 3 — 1 — —								
	391	— — — — — 6 24 101 246 117 12 9 4 4 — — —								
1980	384	— — — — — — 14 101 347 91 15 7 6 1 — — —								
	279	— — — — — 1 9 99 185 36 7 3 2 — — — —								
1990	—	— — — — — — — — — — — — — — — — —								

5. Selection of M_0

Four earthquake with M greater than 8 and a larger number with magnitudes ranging between 7 and 8 have occurred during the past 100 years in the Himalayan region, which is the area chosen for the present study (table 4). Considering the 2400 km length of the Himalayan collision zone, an equal number of such earthquakes could possibly occur in the future in other segments of the Himalayan belt, particularly in the region flanked by the rupture zones of these 4 earthquakes. However, since about 1970, the region has been relatively quiet. During 1970–1987, only one earthquake of magnitude 7·0 or a little higher has taken place. One can, therefore, test algorithm M8 only for M_0 greater than or equal to 7. For larger M_0, only false alarms, but not the failure to predict, could be considered.

6. Diagnosis of TIPs

The area under study was spanned by 18 squares centred at points shown in figure 3. For $M_0 = 7$, the length (L) of the side of squares turns out to be 560 km, according to the formula stated earlier. The lower magnitude cut-off in the catalogue is, however, too high (5·0). Therefore, the average annual number of the main shocks is well below the required number 20. In some of the squares, this figure is as small as 3. Therefore, values of the threshold n had to be lowered. For the common values in all squares, we assumed $n_1 = 3$ and $n_2 = 1$, instead of 20 and 10, normally used in earlier studies. The other possible alternative of using $n_2 = 2$ was also tried.

The threshold values of G and H chosen for recognizing the instant of TIPs, were 4 and 6 respectively, the same as used in other parts of the world where M8 has been applied. Application of this algorithm to the Himalayan belt yeilded TIPs preceding strong earthquakes, in the square covering the India-Burma border region, as well as some false alarms in others. These results are shown in figure 3. They are reasonably acceptable and practically the same for both values of n_2. The TIPs occupy 18% of the total time-space, and precede the only strong earthquake ($M_b = 7{\cdot}1$) that occurred on 29 May 1976, in the India-Burma border region (24·53°N 98·71°E). A TIP is also recognized in the Quetta region preceeding a strong earthquake of magnitude 7·0 which occurred there (33·025°N, 66·315°E) on 3 October 1975. Some agencies reported this earthquake as having a magnitude of 6·7.

7. Discussion of results

In applying M8 to the present study, the criterion used for recognition of TIPs was the same as for other regions of the world. However, the parameters n_1 and n_2 were adjusted in the manner explained above for the purpose of defining magnitude

Table 5. Number of earthquakes in the magnitude ranges and time windows in the Quetta region defined by latitude 29·0°N to 31·0°N and longitude 61·0°E to 63·0°E. The numbers in the first column correspond to earthquakes with unknown magnitudes.

Year	Magnitude 0·0	1·0	2·0	3·0	4·0	5·0	6·0	7·0	8·0	9·0
1900	—	— — — — — — — — — — — — — — — — — — —								
	—	— — — — — — — — — — — — — 1 — — — — —								
1910	—	— — — — — — — — — — — — — — — — — — —								
	—	— — — — — — — — — — — — — — — — — — —								
1920	—	— — — — — — — — — — — — — — — — — — —								
	2	— — — — — — — — — — — 1 — — — — — — —								
1930	—	— — — — — — — — — — — — — 2 — — — — —								
	1	— — — — — — — — — — — — — — — — — — —								
1940	1	— — — — — — — — — — — — — — — — — — —								
	—	— — — — — — — — — — — — — — — — — — —								
1950	5	— — — — — — — — — — — — — — — — — — —								
	2	— — — — — — — — — — — 1 — — — — — — —								
1960	3	— — — — — — — — — 1 — — — — — — — — —								
	—	— — — — — — — — 4 3 1 1 — — — — — —								
1970	—	— — — — — — — 2 2 1 1 — — — — — — —								
	—	— — — — — — — 5 3 5 1 — — — — — — —								
1980	—	— — — — — — — 8 10 3 — — — — — — — —								
	—	— — — — — — — 2 4 — — — — — — — — —								
1990	—	— — — — — — — — — — — — — — — — — — —								

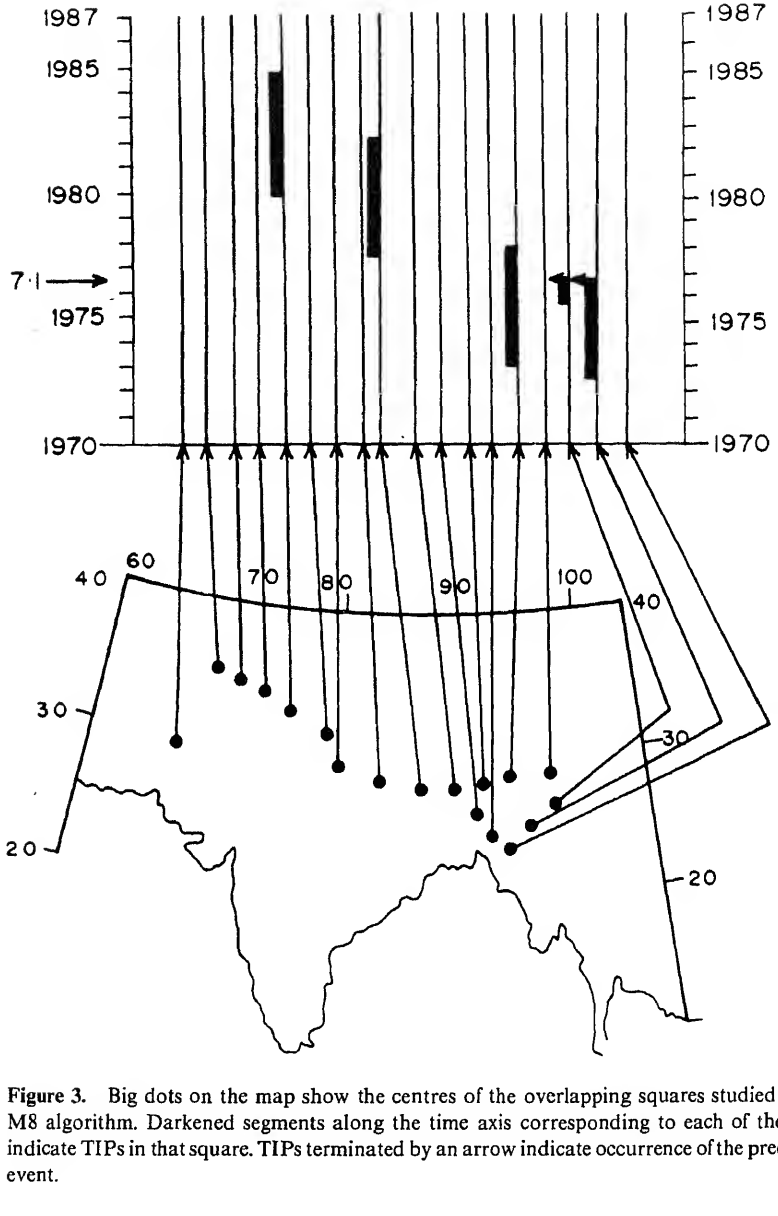

Figure 3. Big dots on the map show the centres of the overlapping squares studied u
M8 algorithm. Darkened segments along the time axis corresponding to each of the
indicate TIPs in that square. TIPs terminated by an arrow indicate occurrence of the pred
event.

thresholds. This enforced change in the values of n_1 and n_2, makes it difficul
directly support our results by those of earlier studies in other regions. On the o
hand, this change hardly made the diagnosis easier. When n is small, the ranc
variations of all functions are expected to increase, thereby increasing the err
However, our experience in carrying out this exercise on Himalayan data did
bring out such randomness. This, though contrary to expectation, is neverthe
encouraging. For, this may be the result of a higher cut-off for lower magnit
thresholds of detectability and a near completeness of the catalogue. The anal
was repeated by adopting 1967 as the cut-off data as the catalogue of lower magnit

earthquake that occurred after that date was expected to be more complete. This exercise however, yielded only marginally better results.

These results indicate that future monitoring of TIPs in the Himalayan region, using this algorithm may prove to be quite illuminating. It may however be necessary to develop region-specific parameter thresholds for various segments of the Himalayan belt. To do this, the available seismic data recorded by the national network of stations over the past half century need to be rigorously studied to produce a more representative and complete catalogue by including even such events which are not so well located.

Acknowledgements

This study was made within the framework of the joint project on earthquake prediction, established by the agreement on scientific cooperation between the Academy of Sciences, USSR and the Department of Science and Technology, India. We are greatly indebted to Prof M Chinnery of the World Data Center A, Boulder, Colorado, who most generously and promptly provided us the latest issue of the NOAA catalogue of earthquakes. Mrs M Murali Kumari provided valuable assistance right from the stage of data handling to the preparation of this paper.

References

Allen C, Hutton K, Keilis-Borok V I, Kuznetsov I V and Rotvain I M 1984 Dolgosrochni prognoz Zemletryaseni i avtomodelnost seismologicheskih predvestinikov. Kalifornia, (Long-term earthquakes' prediction and self-similarity of premonitory seismicity patterns. California, M$\rangle$/6·4, M$\rangle$/7, in Russian). In *Dostizheniya i problemi sovermennoi geofisici* (Computational Seismology issue 21) (Nauka: Moskva) pp. 152–165

Gabrielov A M, Dimitrieava O E, Keilis-Borok V I, Kosobokov V G, Kuznetsov I V, Levshina T A, Mirzoev K M, Molchan G M, Negmatullaev S Kh, Pisarenko V P, Prozeroff A G, Rinehart W, Rotvain I M, Shebalin P N, Shnirman M G and Schreider S Yu 1986 Algorithms of long term earthquakes' prediction; *Rev. Geofis.* (in press) Historia (Comision de Geofisica)

Gabrielov A M, Keilis-Borok V I, Levshina T A and Shaphoshinkov V A 1987 Block model of the dynamics of the lithosphere; in *Computational seismology* (New York: Allerton Press) issue 19 (translation from Russian)

Keilis-Borok V I and Kosobokov V G 1984 A set of premonitory seismicity patterns before strongest earthquakes of the world. In *Earthquakes and mitigation of natural hazards, XXVII International Geological Congress Colloquium 06.* (Nauka: Moskva) Vol. 61, 56–66

Keilis-Borok V I, Knopoff L, Rotvain I M and Sidorenko T M 1980 Bursts of seismicity as long-term precursors of strong earthquakes; *J. Geophys. Res.* **85** 803–811

Kosobokov V G 1982 Experience in transferring criteria of high seismicity (M$\rangle$/8·2) from the Circuve—Pacific belt to the Alpine belt; *Computational seismology* (New York: Allerton Press) issue 13 (translation from Russian)

Sadovsky M A, Bolchovitinov L G and Pisarenko V F 1982 On discreteness in solid earth material; Izvestiya Akademii Nauk USSR, Fizika Zemli N 12 pp 3–18

Proc. Indian Acad. Sci. (Earth Planet. Sci.), Vol. 98, No. 1, April 1989, pp. 125–132.

The importance of strong motion seismology in India

BRUCE A BOLT and JAMES N BRUNE*

Departments of Geology and Geophysics and Civil Engineering, University of California, Berkeley, California 94720, USA

*Seismological Laboratory, Department of Geological Sciences, Mackay School of Mines, University of Reno, Reno, Nevada 89557, USA

Abstract. The high seismicity of portions of the Indian peninsula, together with the high density of population and industrial growth, results in a significant seismic risk in many parts of the subcontinent. Large construction projects throughout the peninsula require an adequate basis for earthquake-resistant design. Thus, as well as strong scientific arguments, there are major practical reasons why a substantial programme to record strong seismic ground motion should be carried out in India. This paper first reviews the history of strong motion instrumental recording, beginning with the important accelerograms obtained in the Koyna earthquake of 11 December 1969 through the recent increase in strong motion instrumentation, particularly in association with construction of large dams. It is argued that there is a pressing need for further extension of strong motion accelerograph coverage of India, especially along the seismically active regional thrust faults of the Himalayan region. Such programme expansion should follow deliberate strategies of site selection, designed to optimize the scientific and practical returns, given the requirements of minimum costs, reliable maintenance and accessible data.

Keywords. Seismicity; strong motion seismology; strong motion instrumentation; ground motion recording.

. Introduction

There are three main reasons why a programme aimed at obtaining widespread ecordings of strong earthquakes in India is necessary. First, the large and growing opulation and rapid construction of major engineered structures demand mitigation of the high earthquake risk; secondly, such earthquake measurements contribute to he basic understanding of the complex tectonics of northern India; and thirdly, the nique continent–continent collision plate boundary of the Himalayas provides a aluable opportunity to further understanding of earthquake source physics and the eneration of strong ground motion by thrust faults.

The first two of these propositions have been discussed by Krishna (1981) who ointed out that because Peninsular India contains some of the most seismically ctive areas of the world there are both broad scientific and important social reasons or adequate measurements of strong ground motions. As illustrated in figure 1, India as had many strong earthquakes since the last century, six of them having a nagnitude greater than 8, and 55 with a magnitude between 6·5 and 8·0. Most but not ll of these damaging earthquakes have been from strain release in the Himalaya egion, extending from Assam in the east to Kashmir in the north, with most of the eismic energy taking place in northeast India. Overall there has been a considerable

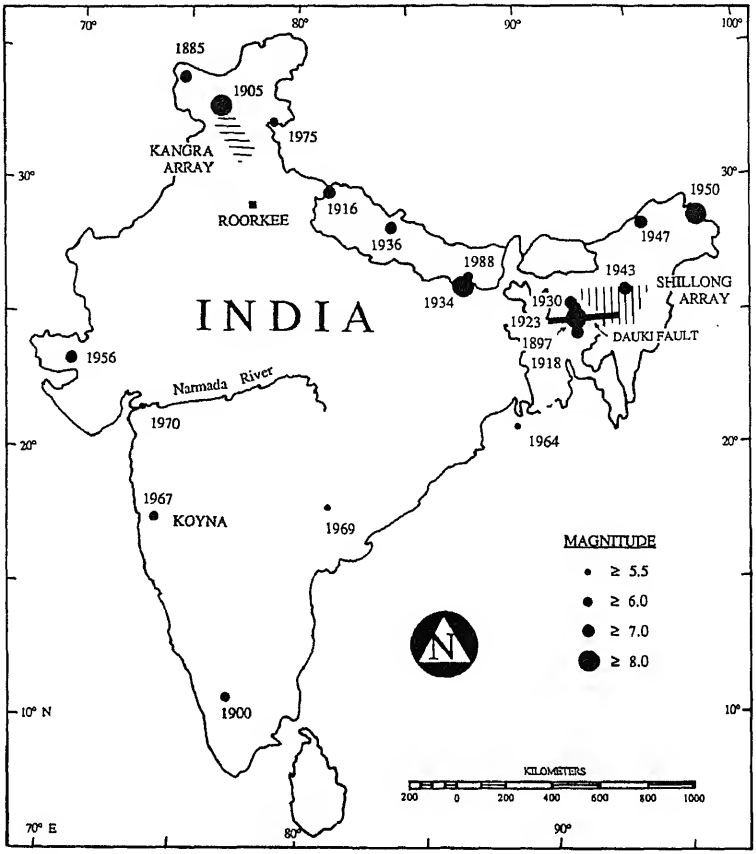

Figure 1. Plot of some historical India earthquakes (adopted from Kaila and Sarkar 19

bridges through unequal soil settlement. Because of population and construct increase, the next major earthquake could have even greater damage and loss of than any previous Indian earthquake. Yet, due to a lack of instrumental observati of strong ground motion in India to date, no suitable attenuation laws for la amplitude seismic waves are available (Khattri *et al* 1983) and no reliable estimates local site effects.

There are already available comprehensive earthquake catalogs (Bapat *et al* 19 and maps of earthquake epicenters (Rao and Rao 1984) as well as seismic inten zoning maps and seismic risk maps of India (Kaila and Sarkar 1978; Kaila and 1979). Some studies of major fault and seismicity patterns and relevant rec tectonics have also been published (e.g. Chandra 1977; Molnar and Pandey, Khattri *et al* all in this volume). This material provides a sound basis for planning extended strong motion instrument network with accompanying priorities probabilities of observational success.

2. Seismicity

Earthquakes occur in many parts of India with very variable recurrent rates (Rao

ao 1984; Gupta *et al* 1986). Along the Himalayan thrust belt and surrounding areas ey are felt almost daily. The high seismicity is exemplified by the twenty earthquakes ith magnitudes greater than 5·8 and ten with magnitudes greater than 6·5 that ccurred along the southern and eastern boundary of the Shillong Plateau, east of auki and north and northeast of Halflong during the last 70 years.

The Dauki-Halflong fault zone (see figure 1), along the straight east-west portion of e Assam-Bangladesh border, has shown medium local seismicity in the last 70 years, rming a seismic gap between adjacent regions with larger recent earthquakes. In rms of the usual frequency-magnitude relation, this fault zone gives an a value of 3·8 0-year period value) and a b value of 0·45. The low b-value suggests the existence of gh shear stress in the region.

In the meizoseismal area of the Great Assam earthquake of 1897, the probability in) years for ground accelerations greater than 0·2 ($M > 6{\cdot}5$) is very high with an timated value of about 0·8. For this reason, a strong motion earthquake array was roposed for this area at the International Workshop on Strong Motion Earthquake strument Arrays held in Honolulu, Hawaii in 1978 (Iwan 1978).

To the south, India is also subject to damaging earthquakes in some regions (see gure 1). The earlier view that most of the Peninsula is aseismic has had to be revised. dia differs in this respect from most other large shield areas which have low seismic sk. Examples of recent damaging earthquakes are Koyna (10 December 1967), hadrachalam (13 April 1969), Broach (23 March 1970), Hyderabad (30 June 1983) nd Dharamsala (26 April, 1986). One estimate of the b-value for Peninsula India is = 0·85 (with $a = 4{\cdot}4$), which is typical of moderate seismic region (Rao and Rao 1984). istorical earthquakes in the peninsula are concentrated (1) to the northwest from bout Koyna through Surat to Kutch; (2) to the eastern coastal zone from about adras to Nagaran, and (3) in the southernmost region from about Travancore to angalore.

Present strong motion instrument network

ne of the motivations for strong motion recorders in India was the construction of rge dams in India (Rau and Varma 1981). The first strong motion instruments of odern type were installed as early as 1963 at Koyna Dam in Maharashtra. Small rthquakes were located after the reservoir started filling in 1962. This part of India d been considered to be nearly non-seismic, and the occurrence of the damaging rthquake (magnitude 7) near Koyna Dam in 1967 was a surprise (Tandon and houdhury 1968; Chopra and Chakrabarti 1973).

This experience stimulated various plans for an India National Network consisting about 100 strong motion accelerographs to be placed in appropriate sites to cover e entire country. The concept included a supplementation of locally built celerometers called RESA by 500 simplified instruments (termed SSR and similar in sign to the U.S.G.S. seismoscope). As of August 1983, 20 RESAs and 200 SSRs had en installed in the field. These instruments were designed, fabricated and aintained by the Department of Earthquake Engineering at the University of orkee.

In addition, several river valley project sites in India have installed strong motion strumentation both in the free field and at various elevations in the engineered

Ramganga, Yamuna, Ukai, Kadana, Koyna and Iddiki (Rau and Varma 1981). In 1987, about 28 such accelerographs were reported operational at various dams (Chandrasekaran 1987).

In response to the 1978 recommendation from the Hawaii International Workshop, a joint Indian-U.S. project of 50 strong motion instrument stations, originally recommended as a large-scale strong motion array in the Assam region, was established in the Kangra region of the state of Himachal Pradesh (see figure 1). In 1906, this area experienced an 8 + magnitude earthquake. Forty-six accelerometers were installed by August 1983. The Kangra array is roughly in the form of a rectangular grid, with principal north-west to south-east axis, spanning 1·5° in latitude and 2° in longitude. The array covers the main fault trends in this region. The elevation varies between 500 and 2500 meters.

Somewhat later, a strong motion network at 45 sites called the Shillong strong motion array (see figure 1) began to be installed in Assam, also under the auspices of the University of Roorkee. This array covered the area between 25°N to 26°N latitude and 91°E to 93·5°E with station spacing about 30 km. This rather remote region presents considerable logistic difficulties in access and services. The installation and maintenance of the Shillong array reflects much credit and dedication on the sponsoring organizations.

Other groups in India are also active with research based on strong motion recording. For example, at the National Geophysical Research Institute at Hyderabad, digital accelerometers have been deployed in seismically active areas and appropriate digital data processing algorithms are being developed.

Parenthetically, we mention that the planned high-level bridge across the Jamuna (Brahmaputra) River in Bangladesh is being designed incorporating seismic resistance against substantial earthquakes. It is anticipated that part of the World Bank-funded project will be the installation of strong motion instruments in the East Bengal region.

4. Recordings of ground motion

Up to 1986, the only strong ground motions recorded by Indian accelerographs were those near the Koyna Dam 230 km southeast of Bombay on the Pre-Cambrian Shield, and no time histories of Himalayan earthquakes were available, although seismoscope records had been obtained for about 5 events in that region. The accelerograms recorded in the Koyna earthquake on December 11, 1967, with the peak horizontal acceleration of 0·63 g, represented an important class of recorded ground motions. These accelerations were the highest directly measured in the world up to that time.

The persistent interest of Indian earthquake engineers and seismologists began to bear fruit in 1986 with clear analog recordings of strong ground acceleration in earthquakes in the northern seismic region by a number of stations of the Kangra array. Figure 2 reproduces an accelerogram and velocity and displacement ground motions recorded in the Himachal Pradesh earthquake, April 26, 1986. The

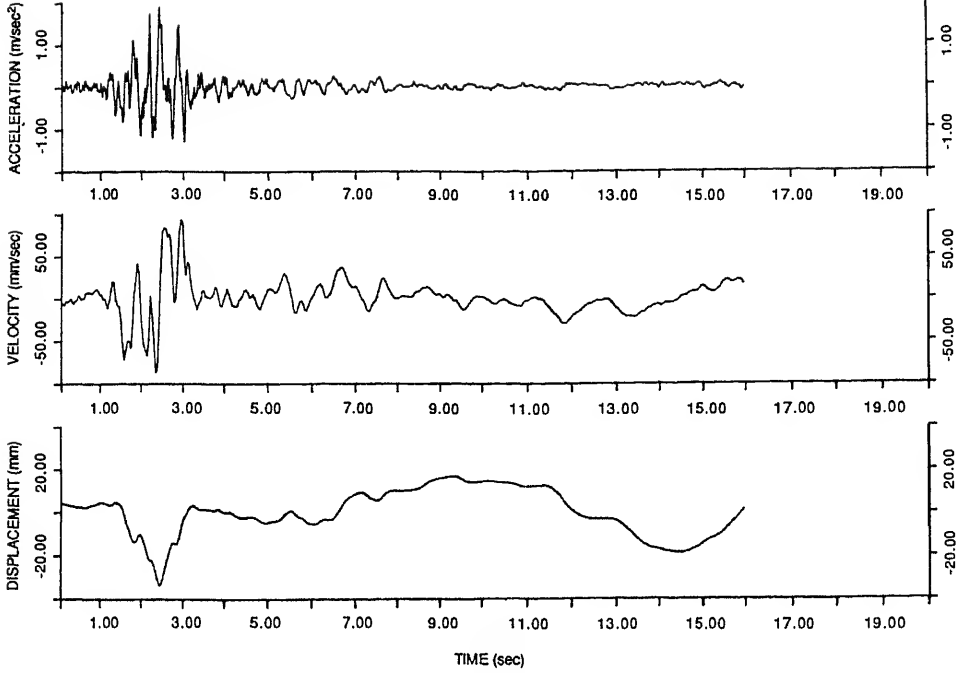

Figure 2. Recorded ground motions (N14E component) at the Dharamsala station in the Himachal Pradesh earthquake, April 26, 1986 (courtesy: A R Chandrasekaran). Epicentral distance about 5 km.

publication of the set of these records with peak accelerations in excess of 0·2 g will be a valuable addition to the strong motion data base of India.

On August 20, 1988, a major earthquake ($M_S = 6{\cdot}8$) occurred in the Bihar-Nepal region, in approximately the same place as the devastating earthquake of January 15, 1934 ($M_S = 8{\cdot}4$). The recent earthquake had high intensity over a substantial area (Richter 1958), with 800 loss of life from collapsed structures reported. It underscores the need for adequate strong motion instrumentation along the whole Himalaya region (Arya *et al* 1986).

5. Future developments

The Department of Science and Technology of the Government of India has reported an integrated project in Himalayan seismicity, particularly in the Himachal and Garhwal areas in the Eastern Himalayas covering Assam and Meghalaya. As well, monitoring of seismic activity is carried out by the India Meteorological Department and by other organizations such as the Department of Earthquake Engineering in Roorkee and the National Geophysical Research Institute.

Construction of large dams in various River Valley Projects in India has led to additional seismic surveillance in various parts of the country (Srivastava and Dube 1982). The minimum seismographic networks needed for engineering projects of various sizes have been discussed (Srivastava 1987), both of sensitive instruments for

The impounding of Shivaji Sagar Lake in 1962 by Koyna Dam led to much interest in reservoir-induced seismicity in India (Gupta, 1985). The continued occurrence of earthquakes in its vicinity (Rastogi and Talwani 1980) as well as the new major dams such as Navagam Dam in Gujarat provides ample justification for adequate future strong motion as well as sensitive seismic network around such facilities.

As mentioned in the introduction, the development of an enhanced all-India strong motion instrumentation network provides a singular opportunity to improve the basic knowledge of India earthquakes and to provide fundamental data for aseismic engineering design and seismic risk mitigation (Agbabian and Arya 1987). Continental-wide considerations and integration of both seismological and engineering needs (Bolt 1980) will help ensure that the observations of strong ground shaking are optimized and representative of various geological and soil conditions.

Because of the unique continent–continent collision tectonics of the Himalayan thrust, strong motion recordings in this region will also provide important information for fundamental studies of earthquake mechanisms, not only in India, but in similar geological conditions around the world. For example, recent research suggests that thrust type earthquakes produce higher accelerations than the normal and strike-slip earthquakes. This prediction depends on the friction-rupture relationships for faulting; other reasonable models might predict lower accelerations for thrust faults. Data from the unique conditions of the Himalayan thrust should provide important constraints on the parameters for modelling major earthquake ruptures.

Seismic gap theory should be given strong weight in consideration of the geographic strategy for deploying Indian strong motion arrays. It has now become clear from numerous successful predictions worldwide that seismic gaps usually represent regions of highest probability for very large earthquakes, although aftershock zones of earlier earthquakes often are the zones of highest short-term probability for smaller events. As the historic pattern of the occurrence of large events is now much better understood in relation to seismic gap theory (see other papers in this volume), it should play an important role in siting strategy.

It is hardly necessary to stress the need for a national plan aimed at standardizing the instrumentation and vital maintenance, developing rapid and validated recording, processing facilities, and establishing efficient data dissemination procedures. Valuable recommendations, objectives and resolutions relating to these questions are listed in the *Proceedings* of the 1987 Indo-U.S. Workshop on earthquake disaster mitigation research (Agbabian and Arya 1987).

Many decisions are required concerning the relative distribution of free-field instruments in relation to specific problems. Such instruments provide in time a sound physical basis for understanding the dynamics of faulting, the transmission of seismic waves through rocks and soils, possible nonlinear effects at soft-soil sites, topographic effects and the characteristic response of alluvial basins. Instrumentation of representative engineering structures such as buildings and dams is, of course, essential as well as installations to provide the seismic response of such "lifelines" as bridges and piping.

The major projects involving the Kangra and Shillong arrays are now providing

experience in India with large regional arrays of the type classified as "source mechanism and were propagation arrays" at the 1978 International Workshop report (Iwan 1978). These Indian arrays are well situated to measure ground motions from great earthquakes that may occur from fault slip along two segments of the major boundary thrust fault system. Consideration of the priorities for arrays of different classification (Bolt *et al* 1987) such as liquefaction and soil-structural arrays is now opportune.

Objectives and guidelines for the deployment of strong ground motion arrays require appropriate indigenous studies but, in general, two criteria can be recommended:

(i) Arrays should be sited with specific aims to measure well-defined aspects of strong seismic motion, and
(ii) Siting should follow studies that optimize the scientific and engineering returns, given knowledge of the local three-dimensional geologic environment and the distribution of earthquake sources.

In the last few years, considerable experience has been obtained in a number of countries, particularly the United States (California), Japan and Taiwan, with digitally recording instruments. The older analog instruments were thought (e.g. Iwan 1978) to provide more reliable and tested data acquisition in various harsh field conditions. The modern digital accelerometers, however, have proven to be comparable in reliability and because of their extended dynamic range and simplicity of data processing (now with regular PC tape or disc input), they must be seriously considered. A decision in each case depends on answering the questions: What is the expected maintenance of each system? And how will limitations on operational life affect the overall recording objectives in the region?

Because large earthquakes may not occur for several years, there are special organizational and funding problems in maintaining long-range programmes for instrument maintenance, data analysis, archiving, distribution and data use. The only solution is stable, continuous commitment of government agencies and organizations with vigorous support from professional groups of seismologists and earthquake engineers. It is sometimes possible, as in the current California Strong Motion Instrumentation Programme (SMIP) to obtain significant financial support from mandatory small fees from large-scale building owners that are assessed at the time of building permit approval. (Currently this fee in California is 17 cents per 100 dollars construction cost, or 0·017%).

It is crucial to pool strong motion data from every seismically active country of the world in a global effort to understand strong earthquake motions and mitigate seismic risk. An upgraded and integrated India strong motion network could contribute much to this international objective. The opportunity is particularly inviting following the recent creation of the Decade of Natural Disaster Reduction (1991–2000) by the United Nations. For a solution to the problems of earthquake hazard reduction, a key ingredient is more adequate sampling of strong seismic motions.

Acknowledgements

The authors would like to acknowledge the assistance of a number of colleagues in

the National Geophysical Research Institute. Dr A R Chandrasekaran at the University of Roorkee generously supplied the strong motion records in figure 2. Dr D Hudson of the California Institute of Technology kindly provided comments.

References

Agbabian M S and Arya A S 1987 Earthquake disaster mitigation research. In *Proc. Indo-US Workshop* Jan. 19–23, 1987, N. Delhi **2**

Agarwal P N 1978 Seismological instrumentation for local networks. In *Symp. on Earthquake Eng.* University of Roorkee, Vol. II, p. 10–13

Arya A S, Gupta S P, Lavania B V K and Kumar A 1986 Report on the Dharmsala, Himachal Pradesh earthquake, April 26, 1986, Dept. of Earthquake Engineering, University of Roorkee

Bapat A, Kulkarni R C and Guha S K 1983 *Catalogue of earthquakes in India and neighbourhood* (Roorkee: Indian Society of Earthquake Technology)

Bolt B A 1980 *US earthquake observatories: recommendations for a new national network* (Washington DC: Natl. Res. Council)

Bolt B A, Abrahamson N A, Darragh R B, Penzien J and Tsai Y B 1987 The SMART 1 accelerograph array (1980–1987): A review; *Earthquake Spectra* **3** Univ. of S. Calif. 1987

Chandra U 1977 Earthquakes of Peninsula India: A seismotectonic study; *Bull. Seismol. Soc. Am.* **65** 1387–1413

Chandrasekaran A R 1987 Measurement and analysis of strong earthquake ground motion; *Bull. Indian Soc. Earthquake Tech.* **24** 77–86

Gupta H K 1985 The present status of reservoir induced seismicity investigations with special emphasis on Koyna earthquakes; *Tectonophysics* **118** 257–279

Gupta H K, Rajendran K and Singh H N 1986 Seismicity of the northeast India region; *J. Geol. Soc. India* 343–406

Iwan W D 1978 Strong motion earthquake instrument arrays. In *Proc. Int. Workshop on strong motion arrays*, Calif. Inst. of Tech., Pasadena, USA Honolulu, Hawaii

Kaila K L and Sarkar D 1978 Atlas of isoseismal maps of major earthquakes in India; *Geophys. Res. Bull.* **16** 234–267

Kaila K L and Rao N M 1979 Seismic zoning maps of the Indian subcontinent; *Geophys. Res. Bull.* **17** 293–301

Khattri K N, Rogers A M and Perkins D M 1983 Estimates of seismic hazard in northeastern India and neighbourhood; *Bull. ISET* **20** 1–22

Krishna J 1981 Geotechnical and strong motion aspects of recent Indian earthquakes. In *Proc. Int. Conf. on Recent Advances in Geotechnical Earthquake Engineering and Soil Dynamics* St. Louis pp. 845–848

Rao B R and Rao P S 1984 Historical seismicity of Peninsula India; *Bull. Seismol. Soc. Am.* **74** 2519–2533

Rastogi B I and Talwani P 1980 Relocation of Koyna earthquakes; *Bull. Seismol. Soc. Am.* **70** 1849–1868

Rau S N and Varma R K 1981 Planning instrumentation monitoring in dams. In *Proc. Int. Conf. on Recent Advances in Geotechnical Earthquake Engineering and Soil Dynamics* University of Missouri-Rolla pp. 855–856

Richter C F 1958 *Elementary seismology* (San Francisco: W H Freeman)

Srivastava H N 1987 Seismological network in India for river valley projects; *Bull. Indian Soc. Earthquake Tech.* **24** 67–76

Srivastava H N and Dube R K 1982 Seismicity studies of some important dams in India. In *Proc. IV Int. Cong. Int. Assoc. Engl. Geol. India* **7** 219–227

Tandon A N and Choudhury H M 1968 Koyna earthquake of December 1967 India Meteorological Department Scientific Rept. No. 59

Vol. 98, No. 1, April

Proceedings of the Indian Academy of Sciences

Earth and Planetary Sciences

CONTENTS

Special issue on Seismology in India

Indexed in CURRENT CONTENTS

Edited and published by G Srinivasan for the Indian Academy of Sciences, Bangalore 560080. Ty
Thomson Press (I) Ltd., New Delhi 110001 and printed at Macmillan India Press, Madras 600 0